OZONE ABSORPTION OF ULTRAVIOLET RADIATION IN THE UPPER ATMOSPHERE

by

J.R. Catchpoole, B.Sc.

A Thesis

Presented for the Degree of

Master of Science

in the

University of Adelaide.

April, 1964

CONTENTS

Contents (Cont'd.) Page

Contents (Cont'd.) Page

Contents (Cont'd.) Page

LIST OF FIGURES

List of Figures (Cont'd.) Page

LIST OF TABLES

SUMMARY

This thesis outlines the preparation for an experiment to measure the vertical distribution of ozone in the upper atmosphere. The equipment built has been flown in a rocket to determine the intensity of certain solar ultraviolet radiation as a function of altitude. This determination was made at a wavelength within the region in which ozone absorption is considerable and in which that by any other atmospheric constituent is negligible. The ultraviolet attenuation is thus a measure of ozone distribution.

In Part A, a survey is made of atmospheric ozone and of the part it plays in the physics and photochemistry of the atmosphere. Variations in observed ozone content and distribution have important relations with the dynamics of the atmosphere and with several meteorological parameters. Established and suggested correlations with other geophysical phenomena are also noted. The review includes reference to the various methods of ozone measurement which have previously been used.

Part B gives some details of the preparations for the experiment. The method of measurement is explained and the several experimental units which have been built are described. Consideration is given to various factors relating to the expected response from the flight equipment, and there are some notes on the first rocket installation.

More detailed measurements of the characteristics of the different components of the units are given in part C. In particular, these include filter, phosphor and photocell measurements. The variations in filter transmission with angle of incident radiation, and temperature effects on filter and photocell are especially relevant to the experiment. A brief note on theoretical dissociation rates for molecular oxygen and ozone follows in part D; and part E includes some comments on the record obtained from the units flown in the first rocket experiment.

This thesis contains no material which has been accepted for the award of any other degree. Except where due reference is made in the text, it includes no material known to have been previously published or written by another person.

31/3/1964.

OZONE ABSORPTION OF ULTRAVIOLET RADIATION IN THE UPPER ATMOSPHERE

PART A : SUMMARY OF THE THEORY AND MEASUREMENT OF ATMOSPHERIC OZONE

The ultimate objective of this study has been the measurement of the absorption of ultraviolet radiation by the ozone of the upper atmosphere. Subsequent parts of this thesis deal with the experiments planned and give descriptions and measurements relating to the units which have been prepared for the project.

These details are prefaced in this first part by a general and very brief review of the theory of atmospheric ozone. The fairly well-established facts are summarised; and reference is made to some of the more recent investigations into the many other aspects of the subject which are not yet fully understood. Amongst these, especially, are numerous suggested correlations with other geophysical phenomena; and hence the correct integration of ozone theory into the whole physics of the atmosphere.

The present project is concerned mainly with conditions in the upper part of the ozonosphere and results from the experiment will perhaps best be first related to those aspects of the photochemical theory which are important at such altitudes. However, it is now recognised to be preferable to treat the atmosphere as a whole whenever possible; rather than considering phenomena of one altitude division as unrelated and separate from those of the others. It is accepted, for instance, that, for a full understanding of the processes involved, the circulation, along with other related

meteorological factors, needs to be considered throughout the depth of the atmosphere; not just within the troposphere alone. Similarly the ozone profile which should be obtained from the present experiments may well be viewed against the whole picture of atmospheric ozone which is outlined below.

1. INTRODUCTION AND GENERAL COMMENTS

Historically, the subject of ozone in the atmosphere begins with the observation that the spectrum of the sun, as observed on the earth's surface, ends quite abruptly at a wavelength of about 2900A. In 1879 it was first suggested by Cornu that this ultraviolet limit is due to the absorption of lower wavelengths by the constituent gases of the atmosphere. This has been shown to be the case and Figure 1 is a useful general diagram illustrating the effect (References 72 and 76, e.g.). The figure gives, as a function of wavelength, an indication of the depth of penetration of solar radiation into the earth's atmosphere before absorption reduces its intensity to a fraction $^1/_e$ of its incident value. It is seen that there are broadly three wavelength regions concerned and the gases mainly responsible for absorption in each are noted alongside the appropriate part of the curve. The shortest wavelengths (Region I) can be absorbed by all constituents. Hence absorption here is in fact due mainly to those constituents which are still present at the highest altitudes. In the vacuum ultraviolet region of 1000 - 2000 A (II), the primary absorber is

molecular oxygen; while between 2100 and 3000 A (III) absorption may well be attributed entirely to ozone.

The more complete statement of atmospheric photochemical theory (referred to below) includes the less significant but possible reactions and allows for these in calculations of the balance between production and destruction of each of the constituents involved. The general description of the main processes concerning ozone is, however, given in terms of the above considerations. Ozone is produced consequent to the molecular oxygen absorption of lower wavelengths of the incoming solar radiation. The resulting ozone itself absorbs the higher wavelengths but at a generally somewhat lower altitude.

Although it assumes such a very important role, there is relatively very little ozone in the atmosphere. The total ozone content is an important parameter, being the first figure obtained from spectrophotometer measurements. This is defined as the amount of ozone, expressed in cms. at S.T.P., which is contained in a vertical column of air extending from the ground to the top of the atmosphere. Its value varies from 0.15 cms. to 0.45 cms. with an average of about 0.25 cms. (8 Km. is the comparable reduced thickness for the whole atmosphere.) Paetzold (Ref.11) estimates that 10^{12} Kgm of ozone are destroyed annually throughout the atmosphere. Comparing this with the estimated total molecular oxygen content of 10^{18} Kgm., it can be supposed that this latter

would take a million years to all go through the ozonised state.

Figure 2 illustrates a typical vertical distribution of ozone in the atmosphere (Ref. 2). Appreciable quantities of the gas are present between 10 and 40 Km. Traces persist to considerably higher altitudes, although the details of the upper part of the curve are not very well known. The measurement of this higher ozone region is the aim of the present experiment. There is also a small but measurable quantity of ozone at ground level; this is the first apparent anomaly on the basis of a simple photochemical explanation of the distribution. (The average amount below 10 Km. is from 2 to 4.10^{-3} cms/Km. Ref. 11.)

Subsequent sections will illustrate further the importance of the study of atmospheric ozone in several respects. Some of these are briefly summarised here:

(1) Atmospheric ozone is of intrinsic interest, especially perhaps in the nature of its variations.

(2) Such intrinsic observations of the variations in content very soon lead, of course, to another important aspect of the study - the attempted correlations with numerous other geophysical phenomena. Ozone in this way forms an important link in atmospheric physics.

(3) The absorption by ozone provides part of the shield preventing the penetration of solar ultraviolet radiation; and so contributes to atmospheric photochemistry. In addition, ozone

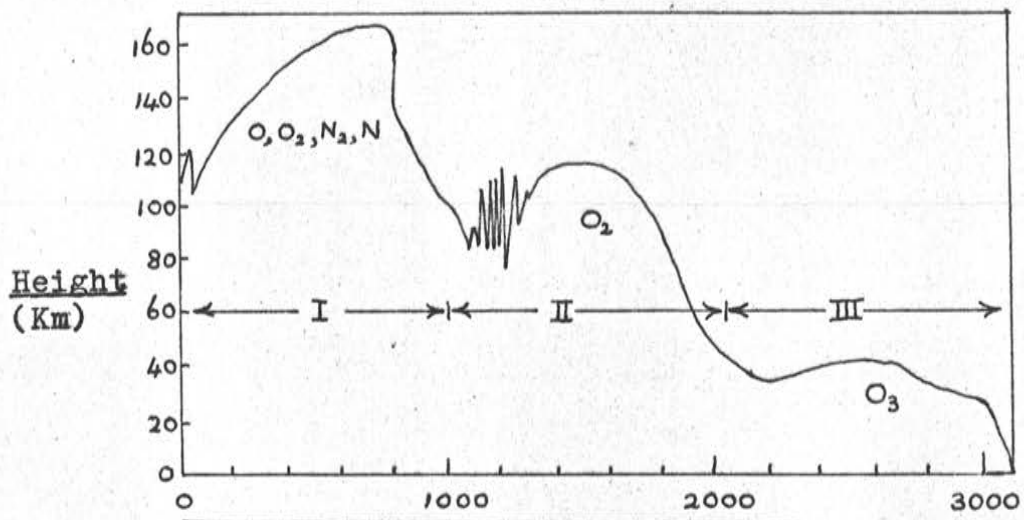

FIGURE I.

Penetration of the Atmosphere by Solar Radiation.

(Ref. 76)

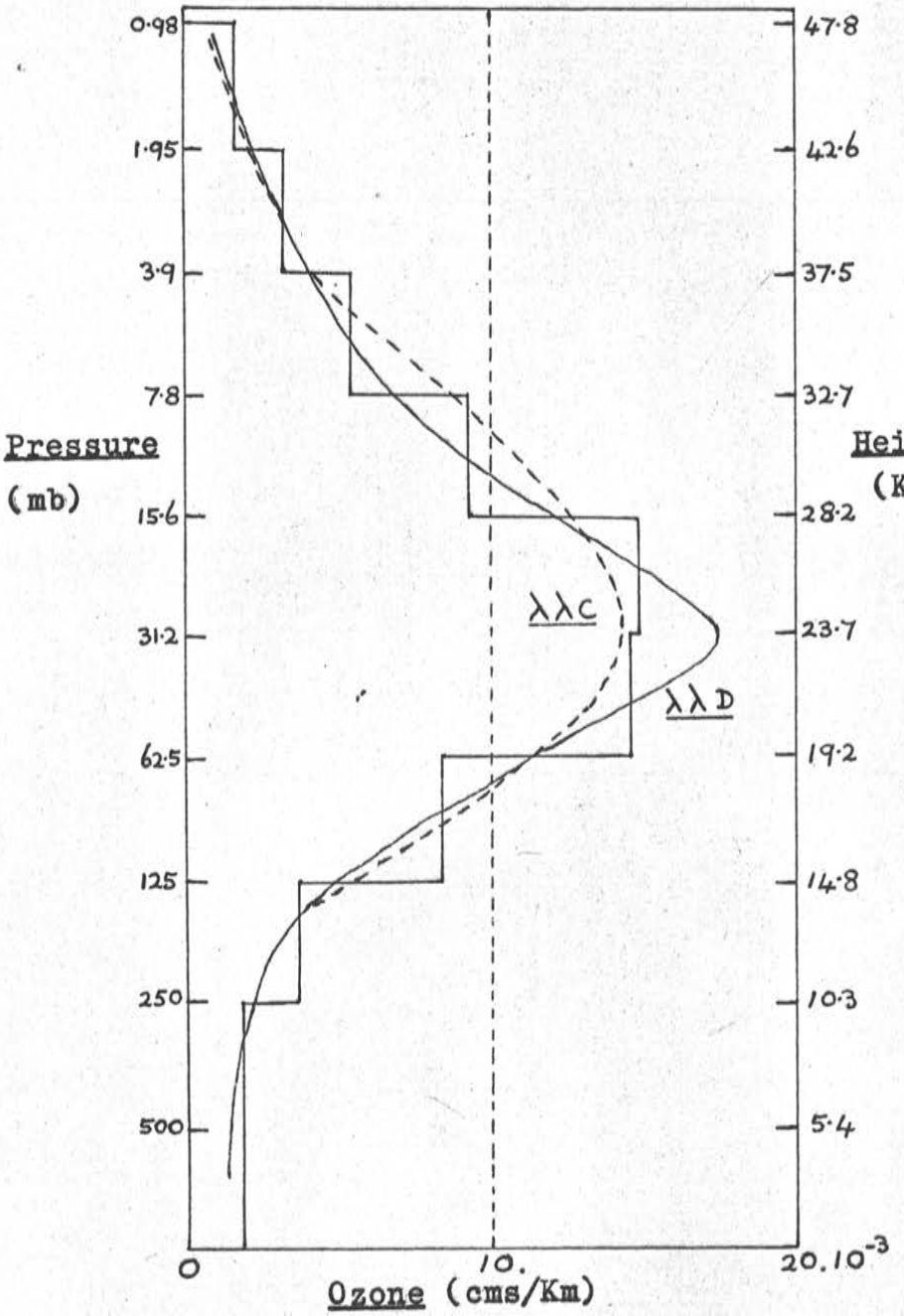

FIGURE 2.

Typical Ozone Profile.

(Ref. 2)

has a significant function in the transfer of radiative energy due to its infrared absorption which is of special relevance to outgoing radiation from the earth's surface (114). Hitschfeld and Houghton (32) demonstrate the importance of radiative transfer in the ozone band. Their calculations indicate heating rates of the magnitude of + 0.4 to - 0.4°C per day, which are of the same order as those due to carbon dioxide. Ozone absorption brings about the atmospheric heating responsible for the stratopause peak in the temperature profile (73, e.g.).

(4) Following on from this, there is the role of ozone in the general mechanism of energy transfer between the upper and lower parts of the atmosphere. This leads to consideration of the dynamics of the atmosphere, of circulation, of the nature of atmospheric energy sources and sinks, and to similar basic questions of meteorology.

(5) There are more specific and immediate relations between ozone and the weather - that is, relations to tropospheric conditions of pressure and temperature.

(6) Below about 30 Km., ozone is in a photochemically protected region and here it acts as a quasi-conservative property of a given air mass. It is in this way that it can be used as a tracer for large-scale atmospheric circulations; hence information on stratospheric winds is available. This importance as a tracer is quite distinct from its other more active roles.

2. OZONE ABSORPTION

There are several important regions of ozone absorption over quite a wide range of the spectrum.

In the visible region, bands of radiation between 4400 and about 8000 A are weakly absorbed by ozone. These are the Chappuis bands and they reach a maximum near a wavelength of 6000 A, where the decimal absorption coefficient has a value of about 10^{-1}. There are three main absorption bands in the infrared (65) and these are of significance in atmospheric energy considerations. Strong absorption is effected at a wavelength of 4.76 μ and somewhat weaker absorption at 14.1 μ. In both cases the corresponding spectral lines are difficult to identify in atmospheric studies because of the presence of overlapping lines due to water vapour and to carbon dioxide (and also, to a lesser extent, from CO). The third infrared absorption band of ozone is at 9.6μ, and this is an especially important one, not only because the absorption is very strong but also because it occurs in an otherwise transparent spectral region.

The most important ozone absorption in the upper atmosphere, however, is that of the ultraviolet region which plays an essential part in the photochemical reactions of these altitudes. Two ultraviolet absorption bands are recognised (Figure 3). By far the more important of these is the Hartley bands system. This covers the region from 3200 to 2100 A and consists first of a

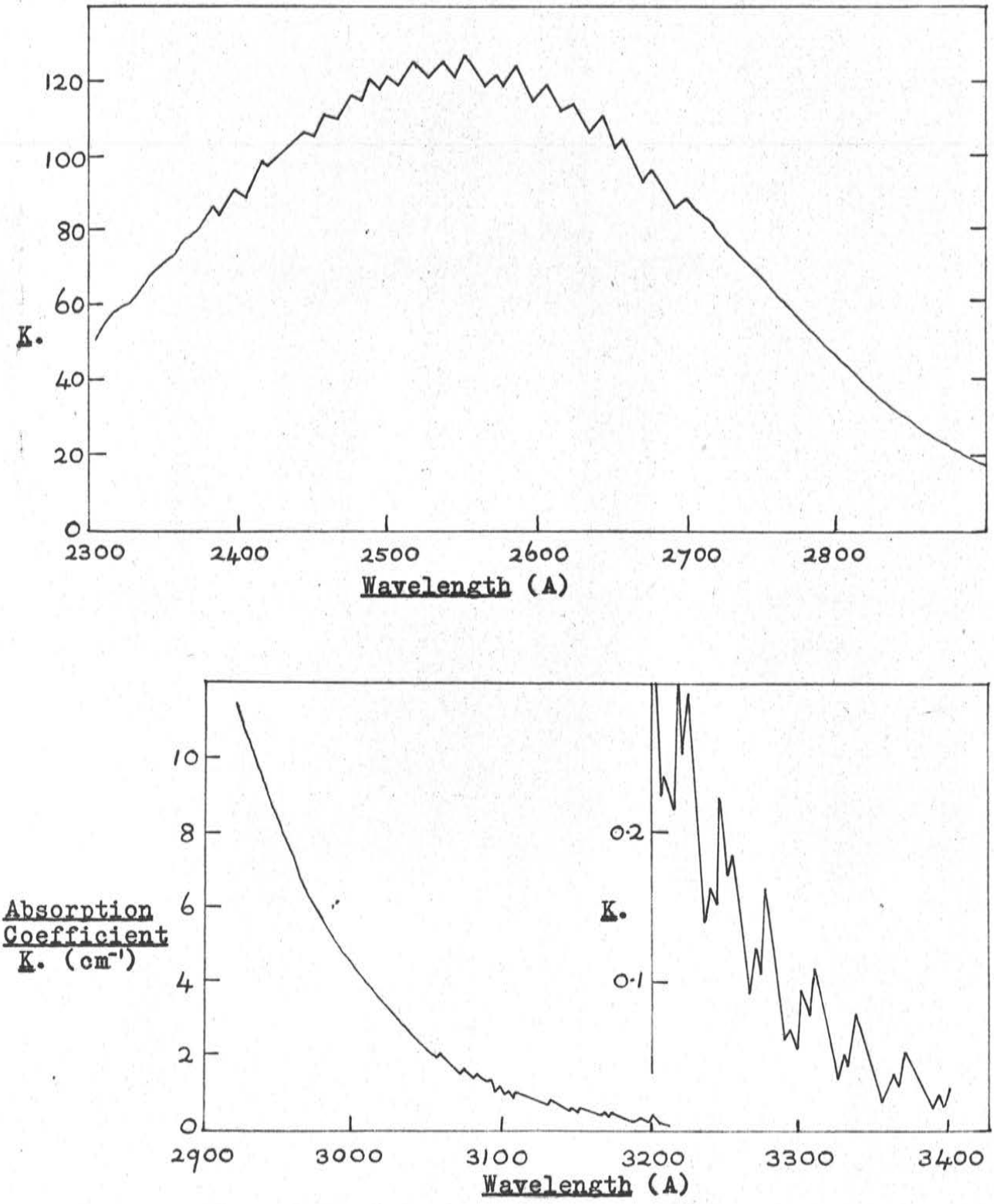

FIGURE 3. Ozone Absorption Coefficients. (18°C.) - Vigroux.

series of diffuse bands which extend down to a wavelength of 2340A, and then of a strong absorption continuum to the lower limit of 2100A. The greatest absorption is at 2550 A, where the coefficient is above 10^2. Solar flux at this wavelength is attenuated by a factor of 10^{40} in its passage through the full depth of the atmosphere. In addition there is weak absorption in the Huggins bands which extend from the upper limit of the Hartley system to about 3600 A.

This ultraviolet absorption (together with that in the visible) is due to electronic transitions in the ozone molecule. Vassey (68) has shown that the absorption is here independent of pressure; that is, Beer's Law is followed. However, there is a temperature effect, some indication of which is provided by the tabulated values of Vigroux (70). Both of these observations are relevant to applications to atmospheric conditions. In the infrared, on the other hand, absorption is due to vibrational-rotational modes of the molecule and is both temperature and pressure dependent. Strong and Watanabe (67) showed for instance that absorption in the 9.6 μ band varies as the fourth root of the pressure. This pressure sensitivity of the infrared absorption was subsequently used by Strong as a means of determining the average height of the gas in the atmosphere (61).

The ozone absorption coefficients measured by Ny and Choong were given in 1932 (66). These were used extensively for

calculations in early ozone work, including the important survey of ozone by Craig (53). However, they have since been shown to be 1.36 times too large, so resulting ozone amounts based on these coefficients are too small by the same factor. The latest determinations and the best now available were made by Vigroux in 1952. These are given in extensive tables in References 69 to 71, and some are plotted here in Figure 3. The values, which will be needed in the interpretation of trials results from the present project, are given as decimal absorption coefficients. These are the values K in the Lambert Law expression,

$$I = Io\ e^{-\alpha x} = Io\ 10^{-Kx} \qquad (1)$$

which relates the incident intensity Io of certain monochromatic radiation to the emergent intensity I after its passage along a path length x cms. through the absorbing gas. Vigroux' results also include measurements at different temperatures between $-92^{\circ}C$ and $+120^{\circ}C$. These indicate that the temperature effect is of relatively less importance in the region of highest absorption. Nevertheless across the atmospheric region of interest in the present experiments the changes could be of significance for accurate measurements. Temperature changes with altitude from the tropopause to the stratospheric inversion point can typically be from 200 to $330^{\circ}K$. The decrease from 50 Km. to the top of the ozonosphere can be of the same order.

3. ABSORPTION BY OXYGEN AND OTHER ATMOSPHERIC CONSTITUENTS

Apart from general considerations relating the various physical processes of the atmosphere one to another, there are two specific respects in which absorption by other constituents is here relevant to the theory of atmospheric ozone. First of all, the present experiment (as outlined in the next part) attributes the change in intensity of a particular monitored radiation wavelength entirely to absorption by ozone. It is important, therefore, that the wavelength chosen is one well away from regions of absorption by other gases. Secondly, other constituents play various parts in the general photochemical theory of the upper atmosphere. Nitrogen and hydrogen, for instance, may become of greater significance at higher altitudes by virtue of several possible reactions, both directly with ozone and indirectly with other constituents. In particular, however, absorption by molecular oxygen itself is basic to the whole photochemical theory of the production of atmospheric ozone.

Recent measurements of the absorption of molecular oxygen and of many other atmospheric gases (including ozone) are reported by Watanabe (72).

The dissociation of molecular oxygen corresponds to an energy quantum of wavelength 2400 A, and there are three major absorption bands below this. First, there are the weak Herzberg bands which converge near 2400 A. Much stronger absorption

results in the Schumann-Runge bands between 1925 and 1760 A, merging into the continuum which extends down to 1250 A. Further strong absorption takes place in the Hopfield bands of 1100 to 600 A. Above 80 Km. in the atmosphere, the dissociation of oxygen is predominantly due to absorption in the Schumann-Runge continuum. Measurements indicate, however, that it is the absorption in the Herzberg continuum (although in itself about a million times weaker) that becomes the principal source of oxygen atoms below this altitude (62). Herzberg continuum absorption is thus of great importance in the formation of the ozone layer.

In the present experiment, it is necessary to consider the neighbouring oxygen absorption in choosing a particular wavelength for monitoring within the ozone ultraviolet band. Below 2500 A, ozone absorption decreases (Figure 3), while the Herzberg region of molecular absorption is approached. For wavelengths greater than 2200 A, ozone is still the more effective absorber, especially in the upper part of the ozonosphere. Even well below this wavelength, the absolute value of the ozone coefficient remains appreciably larger. (At 1900 A, for example, the absorption cross sections are of the orders 10^{-21} for O_2 and 5.10^{-19} for O_3. c.f. (72)). However, the very much greater density of molecular oxygen, particularly below 30 Km., more than compensates for its small absorption, once wavelengths below 2200 A are considered. The result is, therefore, that at these altitudes the Herzberg continuum near its maximum absorbs more than does the lower

wavelength part of the ozone region. In this way the atmosphere remains opaque in what would otherwise be a window between strong O_2 and O_3 absorption regions.

4. METHODS OF MEASUREMENT OF ATMOSPHERIC OZONE AND OF ITS VERTICAL DISTRIBUTION

In this section, a summary is made of the important features of several methods which have been used to measure the ozone of the atmosphere; together with recent suggestions for future satellite determinations.

(a) The Dobson Spectrophotometer and the Umkehr Effect

The Dobson spectrophotometer is a quarz optical system consisting of a double spectroscope which separates two different wavelengths. By means of a system of slits and shutters, these two radiations are made to fall alternately onto a photomultiplier and optical wedges are then inserted into the more intense beam until the same current output is recorded for each. In terms of the calibration of the wedges, the relative intensities of the two wavelengths are found.

In the determination of ozone content, the relative intensities of two wavelengths of the sun's direct radiation are thus measured after they have passed through the atmosphere. The wavelengths isolated have very different absorption coefficients for ozone and four sets have been chosen for routine observations (1). An extension of Lambert's Law (equ^{n} (1)) now relates Io, the

intensity incident on the top of the atmosphere, to I, the intensity at the spectrophotometer in terms of the total ozone content (x cms.) :

$$\log I = \log Io - \alpha A x - \beta B. - \delta \sec z \qquad (2).$$

This refers to the one wavelength λ, for which perhaps there is moderate ozone absorption with coefficient α, while a similar expression holds for λ' which is only weakly absorbed (α'). β is a coefficient representing the scattering due to air molecules, and δ is another to allow for aerosol or particulate matter scattering (104, 105). z is the solar zenith angle.

An important extension of the above was made when Götz pointed out that not only the total content but also the vertical ozone profile could be derived from ground observations with the spectrophotometer. This is possible because of the peculiar altitude variation of ozone in initially increasing in density with height. The scattered light from a clear overhead sky is this time observed when the sun is at a much greater zenith angle. With increasing solar zenith angle, the intensity ratio (of strongly to weakly absorbed radiation) decreases to a minimum at about 86°. This is the Umkehr or Inversion effect and is due to the progressively greater absorption of the more and more oblique rays in their passage through the ozone layer. Finally, any radiation which still reaches the surface is that scattered from above the ozone layer. This has the minimum path length to traverse (the vertical

depth of the layer).

To get the profile, the Dobson spectrophotometer is used to take measurements for a large number of solar zenith distances between 40° and 90°. The lengthy procedures of calculation based on these are outlined in Reference 1 (also 15). One procedure (Method A - Walton) gives an approximate distribution, by dividing the ozonosphere into just five layers, by making certain assumptions about the ozone in the lowest and highest of these, and by considering primary scattering only (using the Rayleigh-Cabannes formula, together with the Cauchy expression for refractive index). In the second method (B - Ramanathan and Dave), the atmosphere is divided into layers 6 Km. in thickness and multiple scattering is taken into account. This introduces complications because the multiple scattering is itself dependent on the distribution with height of the primary scattered light. It is therefore different for the two wavelengths which are differentially absorbed by ozone. Walton estimates that the effect of correcting for secondary scattering is to lower the calculated centre of gravity of the ozone distribution by two or three kilometers.

The Dobson spectrophotometer has now been used for many years to make routine ozone measurements on a more or less world-wide basis. Most of the data which have been accumulated and on which the theory has been developed is still that derived from this instrument. Its one great advantage is in its being based on the ground.

(b) Instruments flown in Balloons, Rockets and Aircraft

A different technique is available, of course, in actually taking instruments up to higher parts of the ozonosphere. Measurements made in this way can be either of the content of a sample at a particular altitude, or else of the total ozone amount still present above the point of observation. These methods are advantageous in providing a more detailed profile of the distribution, especially at the higher altitudes of decreasing content. The uncertainties and analysis difficulties are perhaps less serious than in the case of the spectrophotometer means of profile determination.

The instruments flown may again use optical methods. There is the possibility of flying complete spectographs, as has been done for recording other parts of the solar spectrum. Less complicated apparatus in the form of suitable combinations of filters and photocells has been successfully used in ozone determinations, as in some of those by Paetzold at Weissenau (11). The intensity of a particular wavelength of solar radiation is measured and the ozone is calculated as the amount between the point of observation and the sun necessary to effect the observed intensity change. This is the method proposed for use in the present experiments. It is therefore considered in greater detail in the subsequent part of this report.

Chemical sondes of various descriptions have also been used. These are carried aloft by means of a balloon and the

measurement is made on the basis of the reaction of ozone with a potassium iodide solution:

$$2KI + H_2O + O_3 \longrightarrow 2KOH + O_2 + I_2 \quad (3)$$

(This reaction was used by Houzeau in 1858 when he first proved the existence of ozone in the air.) As the sonde rises through the atmosphere, the air (containing the unknown quantity of ozone) is pumped through the solution. In a method used by Regener, a known amount of sodium thiosulphate is also present and this reacts with the liberated iodine. A telemetry signal indicates when the thiosulphate is exhausted (by means of a depolarizing effect on a platinum cathode), and a new known quantity is added. In Brewer's method, the liberated iodine immediately depolarizes two electrodes and a constant telemetry signal indicates a current output which is proportional to the rate of ozone arrival.

R.H. Kay (6) describes a measurement by chemical means made from an aircraft flying to heights of 12 Km. His results gave the content in this region as 8.5% of the total. This is a useful determination as it makes computations for greater altitudes more reliable (as in the IGY method A referred to above) and also because this lowest region is the one in which both Umkehr and rocket determinations are least sensitive.

(c) <u>The Lunar Eclipse Method</u>

At the time of a lunar eclipse, a narrow greenish-coloured zone is observed in the vicinity of the earth's shadow.

This is due to the ozone absorption in the Chappuis bands of the solar radiation traversing the long tangential paths through the earth's atmosphere. An estimate of ozone content is thus possible by measuring, within these bands, the spectral distribution of light on the moon's surface. Mitra (58) considered that valuable information is available by this analysis because of the greatly different ozonosphere paths taken by radiation transmitted at different heights; that is, at different phases of the eclipse. Paetzold (who reports results of observations - 11) also pointed out that the method is potentially useful in determining the distribution at those latitudes where other observations are normally difficult. In addition to the extinction by scattering and absorption in the atmosphere, the optical refraction causes a 15-fold magnification at the lunar surface. This has made it a successful method in practice but there are severe limitations to its use, not the least of which are that there are only two or three total lunar eclipses a year and that recording of the reflected intensities are needed continuously throughout the several hours of the transit of the shadow.

The principles of this method of intensity measurement of radiation traversing long, oblique ozonosphere paths has, however, been extended to two other important methods for ozone determination. One is to make photometric measurements of and from artificial satellites, as considered in the next section (and in (16)). The other is the adaption of the method using other

screens, the position of which (unlike the moon) can be controlled experimentally. Pittock (17, 18) has used balloons for this purpose. Photometric measurements of the twilight reflection from the balloon have been made at wavelengths of 4400 and 6125 A, and the analysis allows for attenuation and scattering effects along both the sun-balloon and balloon-ground paths. This has proved a useful new method of determining ozone vertical distribution but is mainly sensitive to the lower stratosphere only; that is, to the region of maximum concentration.

These methods are restricted to clear sky observations, and, by their nature, give values for the vertical distribution which are smoothed out over considerable horizontal distances. That is, the actual distribution over a given point on the earth's surface at a given time is not obtained, and it is often this which provides the most valuable information and the best possibilities for correlation.

(d) Satellite Photometry

Two possible general means exist for the determination of ozone using artificial earth satellites. In the first place, measurements could be made from the satellite itself, looking down onto the earth's atmosphere and ozonosphere. These measurements would be of the appropriate solar ultraviolet radiation which is reflected and scattered back to the satellite, and hence of the absorption by the atmosphere on the way. The great advantage in such a proposed experiment is that simultaneous measurements of the

direct solar intensity could be made. That is, there could be continuous monitoring of the incident intensity, which figures in other methods as a far less certain quantity.

Then, secondly, there could be observation (as in the lunar case) of light reflected from the satellite to an observer on the ground. Here absorption is always present along the path of the reflected ray; to this may be added further long-path absorption as the satellite moves into the earth's shadow.

Singer and Wentworth (20) first suggested that satellite measurements of scattered light might be used for the determination of ozone. Such an earth satellite would be ideally suited for synoptic measurements of meteorological significance. A narrow spectral region with appreciable variation in atmospheric penetration was considered, and calculations made of the effective depth to which a suitable ultraviolet detector would actually "see" into the atmosphere by virtue of scattering. This depth is defined in terms of the point above which 90% of the contribution to the response is made. Their calculations are based on a reduced atmosphere, 8 Km. thick at S.T.P. For ozone considerations, this idealisation is valid since the Hartley band absorption is independent of pressure.

These ideas were further developed by Twomey (21). He considers a simple scattering atmosphere with a constituent such as ozone which absorbs to differing degrees at various wavelengths; then finds a relation for the dependence of the spectral

distribution of the reflected energy upon the shape of the vertical distribution of the absorbing constituent. It is shown that, for primary scattering only, the reflected spectral energy distribution (expressed as an explicit function of the absorption coefficient concerned) is a Laplace transform of the vertical distribution (this latter being expressed as a function relating pressure (height) and mass of absorbing constituent (above that height)).

The calculations of Singer and Wentworth are most applicable when the diffused radiation comes from that part of the atmosphere well above the ozone maximum. A more detailed analysis of the situation which prevails when a significant portion of the incident solar radiation penetrates to lower altitudes (i.e. when the effective scattering depth increases) is given by Sekera and Dave (19). The solar ultraviolet diffuse reflection is computed for a plane-parallel atmosphere of finite optical thickness which is divided into two layers relative to the problem and to the distinction of this more comprehensive treatment. The calculations are based on an analytical representation of a typical ozone profile and are made in terms of five components which ultimately contribute to the satellite detector response. The first of these is the diffuse reflection of the direct solar radiation by the upper layer (as before). The other four derive from the direct and the diffuse transmission by the upper layer of (outgoing) radiation diffusely reflected from the lower layer - this latter originating in one case from the attenuated direct solar radiation, and in the other from

diffuse transmission through the upper layer. This analysis assumes the earth's surface to be a perfect absorber and that there are no clouds in the lower layer. A more serious omission is that of aerosol scattering (105).

The second possibility referred to above (that of the extension of the lunar method) is considered by Venkateswaren, Moore and Krueger (22) who analyse the general case of reflection to the ground of radiation from a satellite which has already penetrated the atmosphere along its incident path. The theory they develop is used in the evaluation of results of the Echo I satellite of 1960. Elements of path length traversed (a i j) are specified by division of the atmosphere into spherical shells and an expression of the following form is derived:

$$\alpha\,(A)\ \{X\} = \{L^{(\Lambda)}\} \qquad (4)$$

Here (A) is an nxn matrix of the geometrical elements aij and $\alpha = \sigma(\lambda_2) - \sigma(\lambda_1)$ is the differential cross-section for the absorbing constituent x , ozone in the present application. $\{X\}$ is the column vector of the xj's, that is of the incremental ozone amounts in the various altitude elements. This, of course, is what is to be deduced from the observations, the aim being to determine xj as a function of j. These measurements are represented by $\{L^{(\Lambda)}\}$, the column vector of $Li^{(\Lambda)}$, where (Λ) refers to values at the satellite. Similar expressions are derived for ground measurements (which include the additional atmospheric penetration).

Also,

$$Li = \ln\left[Ri/Ro\right] \quad \text{where} \quad Ri = \frac{Ii\,(\lambda_1)}{Ii\,(\lambda_2)} \qquad (5)$$

This final ratio is that of the intensities recorded by a two-colour photometer. The theory is extended to cover more than one attenuating constituent in the atmosphere traversed. The authors suggest that a possible experiment of interest would be one in which two constituents are considered; the first, a minor one like ozone, attenuating the solar beam by absorption, while the other (neutral air) attenuates by molecular scattering.

5. VARIATIONS OF ATMOSPHERIC OZONE AND THEIR SIGNIFICANCE. CORRELATIONS WITH OTHER GEOPHYSICAL PHENOMENA.

The present experiment has as its aim the determination of the absolute amounts of ozone at the higher altitudes of the ozonosphere. Such results should add to the overall knowledge of ozone in the atmosphere. However, this overall picture is perhaps of greatest use in presenting not the absolute quantity of the gas at a particular point, but rather data to further the study of the variations in ozone amount, and hence of correlation of these with other atmospheric parameters.

Very generally, the amount of ozone occurring at a given time and place is a result both of photochemical production and destruction there and elsewhere, and also of atmospheric dynamics. Atmospheric transport of one form or another is the first and

principal explanation for differences and apparent anomalies between observed values and those predicted simply on the basis of a photochemical production locally. Other suggested sources and sinks for ozone need to be considered as well for a more detailed assessment of the quantity of the gas (see especially, Ref. 52). In addition, other variations are recorded which are also not immediately explicable in terms of the simplest photochemical concepts, and attempts to correlate such changes with numerous other parameters have been made. Usually, however, these other proposed factors, such as sunspot activity, are themselves possible indirect causes of change in the photochemical balance.

This section contains a summary of some of the ways in which atmospheric ozone content is observed to vary. Attempted correlations of such variations with other geophysical factors are noted; so also are some of the possible deductions from the variations concerning atmospheric and meteorological phenomina.

(a) Latitudinal and Seasonal Changes

The extensive data collected from observations up to 1950 have been considered in a comprehensive survey of atmospheric ozone by Craig (53). If for each of the stations involved, the recorded ozone amount is plotted against the time of year, and if these are then arranged in order of latitude, the following characteristics are apparent. First there is a quite definite one year period in the ozone amount with a maximum in the spring and a minimum in

autumn (and, of course, with the appropriate 6 months phase difference between hemispheres). Some stations show a secondary maximum in late summer. The amplitudes of these seasonal variations are least at the equator; and in general increase towards higher latitudes. The ozone amount is a minimum in the tropics, and the latitude gradient is appreciably greater in spring than in autumn.

The observed minimum at the equator and the maximum in late winter or spring (but not summer) are both contrary to what the theory of photochemical production would suggest. So the simple dependence of total ozone on solar zenith angle is quite insufficient to account for the observations. Instead, transfer of ozone within the atmosphere is suggested as an explanation, and three possibilities involving such motions of air masses have been considered. These involve, as their central features, vertical motion, horizontal advection and mixing. Dutsch envisaged a vertical motion of air masses resulting from a net sinking of the stratosphere in winter and a net rise in summer due to the sun's heating effect. A meridional circulation from summer to winter hemisphere is also supposed. Wulf and Craig consider a meridional circulation within each hemisphere which results in the equatorial stratosphere undergoing a steady subsidence with consequent horizontal divergence. Ozone is transported to higher latitudes from the equatorial regions where it is continuously replenished by photochemical production. Ramanathan and Kulkami

(13) develop this idea further and point to a link between the study of ozone problems and that of the time and space variations of the tropopause levels. Observed major discontinuities in these levels are especially relevant to meridional circulation. Newell (28) assesses the role of quasi-horizontal circulations in the ozone budget and also extends the hypothetical ozone transport path to where in higher latitudes and in the vicinity of the jet stream, it can be removed from the stratosphere to the troposphere. A combination of these two gives the third possible transfer mechanism in explanation of observed seasonal and latitudinal variations. This supposed that large scale mixing processes give additional ozone during periods of cyclonic activity by transporting ozone to lower levels. That is, there is a more immediate relation between season and ozone. Reed (30) has dealt with this, after estimating the relative importance of vertical motion and horizontal advection in producing day-to-day ozone changes and concluding that at most one third of the range can be directly attributable to the former.

A somewhat different approach to the question is made by Pressman who considers the way in which the actual absorption by ozone might vary with latitude and season (12).

(b) <u>Ozone Profile Variations</u>

Changes are observed in the height of the ozone centre of gravity such as would be expected from the above total ozone variations. Increase in content results in a higher concentration at lower levels with a corresponding fall in the centre of gravity.

This lowering is observed in spring and at higher latitudes.

Figure 2 shows a typical ozone profile but actual traces of the distribution can vary markedly from this. The peak of the concentration curve may be much broader or may in fact oscillate between two levels at different seasons. Such a result is reported from Umkehr observations over certain Canadian stations (9) where a peak at 27 Km. was found to be slightly more predominant in spring, summer and autumn, but another at 15 Km. much more so in winter. Multiple peaks at the one time are also observed and Paetzold classifies three types of ozone distribution from his measurements (11). In the first, there is just the one maximum at 23 Km. altitude. The second type has two maxima, that at 23 Km. together with one at either 15 or 5 Km. altitude. Finally all three may be present. The secondary maximum was shown to be caused by advection, there being an abrupt change in wind direction at that altitude. Different air supplies at various heights might also account for the tertiary maximum.

(c) Relations of Ozone Variations to the Weather, and also to Stratospheric Meteorological Parameters

A close relation is evident between day-to-day ozone variations at some particular station and the prevailing isobaric pattern of the surface weather map. Such variations, which are expressed as departures of ozone content from the monthly mean, are greatest in spring and at high latitudes; they often exceed the range of monthly means for the whole year. It is observed that

positive ozone departures are associated with the passage of low pressure systems at the surface; negative departures with high pressure. The highest deviations are slightly to the west of the centre of the system. Similarly, a warm front (which slopes forward with height) is generally preceded by a fall in ozone amount; a cold front (backward slope) followed by a rise. It is supposed that those frontal surfaces not accompanied by ozone changes do not extend up as far as the stratosphere. Other correlations between ozone and weather or low-level parameters have been made (31 e.g.). Occlusions, for instance, can be classified into three groups depending on the effect on ozone content (24). Meetham studied short-period ozone changes in terms of tropospheric pressures. Other tropospheric ozone variations are noted in a subsequent section.

This study is extended to the stratosphere where a greater ozone mixing ratio exists and where a relative change in content has a greater effect on the total ozone amount. This extension is especially relevant as the study and interest of meteorology itself is centered more in these higher altitudes. An investigation has been made by Ohring and Muench (29) to establish the relationships between ozone variations and pressure systems and other parameters in the lower stratosphere. The ozone-geopotential height correlation (100) is negative for both troposphere and stratosphere. Correlation with temperature which is negative in the troposphere, is found to be positive at higher altitudes. The correlation with

the height of the tropopause is negative. In addition, high ozone amounts in the lower stratosphere are found associated with southerly winds and cyclonic curvatures. Ohring and Muench define and estimate coefficients for these correlations. There is no regular seasonal variation of these coefficients, and evidence for only a small latitudinal variation for the 100 mb. level wind correlation. Lower stratospheric troughs appear as regions of relatively high ozone content - in contrast to other results published (23) which relate to the levels of the middle stratosphere above 100 mb.

As noted in a subsequent section, the study of ozone in this regard soon becomes closely associated with that of upper atmosphere meteorology, especially concerning motions of various air masses. The latter assumes a special significance in polar regions, so the study of ozone becomes important there as well. Polar ozone is a unique study in its own right, however, both because of an apparent reversal in latitudinal gradient (section (g)) and also because of its special situation (particularly in winter) with respect to photochemical production and low zenith (or shadowed) solar radiation. For these reasons, the extension of the above correlations to high latitudes is of interest. Johansen (26) considers results from Tromso.

(d) Tropospheric Ozone Variations

A mechanism (such as one of those considered above) for its transport to lower storage regions, together with stratospheric photochemical production and destruction from the basis of present

theories of atmospheric ozone. A complete account needs, however, to take into consideration the possible roles of the gas in the troposphere. Here its absolute amount is less, and its very presence (contrary to the initial photochemical prediction) could perhaps be attributed simply to exchange from the stratosphere (28). However, significant tropospheric contribution to the production of ozone has sometimes been suggested; and, even apart from this, its destruction at and near ground level is an essential part of the overall ozone cycle (57).

An extended theory (section (6)) postulates the photochemical production of ozone in an atmosphere containing small concentrations of nitrogen dioxide and hydrocarbons. This will be small compared with the oxygen production, but at lower altitudes, and especially in urban areas, its contribution may be more significant. Frenkiel (50) suggests the need to account for the measured ozone distribution in terms of the added effects of both stratospheric and tropospheric sources. He considers data on urban pollution which can give an accumulated ozone cloud under certain meteorological conditions; and concludes that this, together with other suggested tropospheric sources, could give an ozone amount of the order of that actually observed in the lower stratosphere (that is, without allowing for transport from above).

The probably most significant natural tropospheric source of ozone is in atmospheric electric discharge. Variations in ozone content during a thunderstorm were early recognised, with a rise on

the approach of the storm. This has previously been considered only a local variation and not of significance to the overall atmospheric theory. Paetzold and Regener have made calculations to this effect, concluding that the high altitude production was the only important source of ozone - that from lightning being less by a factor of 10^4. However, in a recent article (52), Kroening and Ney have arrived at the quite different conclusion that production by lightning is of a comparable order. This discrepancy arises because the latter use an energy efficiency factor (instead of a current factor) in the calculation of the ozone produced. The number of molecules of ozone is given by multiplying this efficiency factor by an average value of energy dissipated per lightning flash and by an estimate of the world-wide lightning frequency. An important aspect of lightning production, if proved to be of this magnitude, is in its being not uniformly distributed over the earth's surface. A more direct explanation of seasonal and latitudinal variations might be apparent; an additional factor would also be involved in ozone-circulation correlations. It is further suggested that this tropospheric source might account for the third (lowest) ozone maximum observed by Paetzold (section 5(b)).

In addition to methods mentioned before, tropospheric ozone determinations have been made from studies of infra-red emission spectra. Goody and Roach (51) give an analysis based on measurements of the 9.6 μ ozone band. Most of the emitted

radiation of this band comes from the lower atmosphere and so contains information on ozone distribution for these levels.

Another suggested factor which could make possible a somewhat more direct contribution to latitudinal and seasonal variations is contained in the study of the strength of the ozone sink at ground level. Kroening and Ney point out that adsorption and storage at the earth's surface (in addition to decomposition) should be considered in determining the sink strength; and hence that this latter might vary with both the substance and temperature of the surface. Especially at high latitudes, the low surface temperature (favourable for storage) may be important - and possibly a weak sink could more than compensate for decreased high altitude production in the explanation of high winter ozone values.

Various estimates of the vertical ozone flux in the troposphere (and higher) have been made and are summarised by Junge (Table 1 - Ref. 57). Only one has been measured directly and this at near ground location (60). The concepts of ozone rivers (Kroening and Ney) and of an ozone current (Paetzold) contrast with the ozone "holes" observed over the Alps (Fohnwaves - 11 and 100).

(e) Tropospheric - Stratospheric Relations

Nicolet (74) has made theoretical estimates of the rate at which ozone equilibrium is reached in the production by solar ultraviolet radiation. Supposing first the complete removal of ozone, he finds the times necessary to reach concentrations corresponding to 50% of photochemical equilibrium. For an overhead sun,

only 30 minutes are taken at 50 Km. altitude, 3 days at 30 Km, but 7 months at 20 Km. For the sun at the horizon, a somewhat longer time is taken at the higher altitudes; and a great deal longer (12 years) at 20 Km. It is apparent from figures such as these that the ozone concentration below about 30 Km. is not directly affected by the sun, either in production or destruction. That is, at these altitudes ozone acts as a conservative property of a given air mass and hence can be used as a tracer.

It is in this respect that ozone is most valuable in upper level meteorology and in global atmospheric dynamics. Partly on the basis of ozone data, various circulations have been postulated; as have certain ideas concerning transfer and energy exchange between stratosphere and troposphere. A few relevant references are noted here.

Calculations to derive a possible meridional circulation in the stratosphere and mesosphere have been made by Murgatroyd and Singleton (27). Amongst other meteorological data on which this is based is the heating effected by ozone absorption, and the cooling by long-wave radiation. The circulation calculated is supported by the tracing of ozone and other materials. It allows in general for air in the 25-35 Km. region (that is, the region of maximum ozone content), to be transported upwards in the summer (tending to destruction and decrease in content); and downwards in the winter (protected lower stratosphere (and therefore total) ozone increase).

Murgatroyd and Goody (33) make certain computations concerning sources and sinks of radiative energy between 30 and 90 Km. and conclude that there is in general a close approach to radiative equilibrium at all these levels - except over polar regions. The relevant bands of water vapour, carbon dioxide and ozone are considered (Ref.24, also). Here the dominant 9.6 μ ozone band only is included. (A more precise estimate would allow for the 14.1 μ band also.) Radiation and flux divergence tables for ozone are given by Elasser (98).

An especially rapid increase in total ozone takes place in the late winter and early spring of polar regions. Godson (25) has considered the close relation between this and the coincident sudden warming of the arctic stratosphere. The ozone maximum is dependent on the intensity of the final high level warming. This is preceded by temporary stratospheric warming at somewhat lower latitudes; and the final sudden warming is accompanied by a destruction of the arctic jet stream and the setting up of less intense stratospheric circulation.

After a review of available data on vertical ozone flux and of tropospheric concentrations, Junge (57) gives a quantitative analysis of the ozone budget. This is based first on an approximation for tropospheric ozone content of the form of a sine wave (including a phase term to allow for seasonal variations), on a similar sine relation for stratospheric injection

rate; and on an expression for destruction as proportional to content. From these are calculated various ozone parameters such as residence times for stratosphere and troposphere, average vertical flux and global rate of destruction.

A large fraction of the exchange between stratosphere and troposphere appears to occur near the tropopause break of middle latitudes and the associated jet stream. Newell (28) considers this in his assessment of the part played by quasi-horizontal circulations in the ozone budget, and so postulates a transport path for ozone in the exchange. He correlates various factors from IGY data, supposing ozone transport to be effected by a combination of three mechanisms - mean meridional motions, transient eddy processes, and standing eddy disturbances. (The last involve the ozone relation to large-scale troughs and ridges.)

(f) Ozone Variations and Solar Activity

No significant correlation has been found between total ozone content and the earth's magnetic activity (37). Such correlation might well be expected since both the solar wave radiation and corpuscular radiation (76) are known to disturb the earth's upper atmosphere. One suggested explanation of the lack of correlation is that the corpuscular radiation does not penetrate as far as the ozone layer. Another possibility is that any ozone variation which might occur has perhaps not been observed because the simultaneous variation in Lo has not been taken into account.

Lo (cf equ^{n} (2)), the extra-terrestrial constant, is the logarithm of the ratio of the incident intensities for the two wavelengths observed. Further measurements at Quetta (39) have in fact confirmed a negative correlation between Lo variations and sunspot activity. If these variations in Lo are not allowed for, errors of 10 to 15% can be made in the calculated ozone amount of low latitudes.

A basic ozone parameter which has been routinely observed is ERTOR - The Effective Radiation Temperature of the Ozone Region. This is a development of a method of determining the vertical distribution of ozone by the complementary use of surface observations of <u>both</u> the ultraviolet and the infra-red (54). In a preliminary comment on the statistical study of measurements of this temperature, Adel (35) reports a strong solar-terrestrial relationship - the maxima and minima of ERTOR closely following the summer and winter solstices respectively. In a subsequent report (36), power spectrum analysis (101) of this and other atmospheric ozone parameters is made, alongside a similar comparison of two parameters of solar activity. An attempt is thereby made to investigate the means by which lower regions of the atmosphere respond to fluctuations in solar output. A distinct spectral peak in ozone parameters occurs at a period of 2½ weeks; to this is added the suggestion of a 1½ week period variation at high atmospheric levels in summertime. The slight peaks found at corresponding times in

the spectrum of the solar parameter F are considered to be not statistically significant.

A direct relationship between total atmospheric ozone content and the cycle of sunspot activity has often been suggested. No proof of this has been provided, however, until a recent report by Willett (43). This gives the analysis of relevant measurements over a 27 year period, and concludes that there is a highly significant negative correlation between the relative sunspot number and the world-wide average of total atmospheric ozone. A phase lag of about two years in peak correlation of the sunspots relative to ozone is noted. A relation between the earth's atmospheric ozone and the mean solar sunspot latitude is also established, but with a phase difference which is both smaller and of the opposite sign; suggesting a greater ozone sensitivity to sunspot latitude than to the actual number. Reference of these findings to an earlier suggestion that the effective height of the ozone layer varies inversely with sunspot number is also made. All of these interesting results become doubtful, however, after a subsequent review of the analysis by London and Haurwitz (41). They contend that the results obtained could have arisen from the use of biased data with respect both to time and to station location, and conclude that they are without statistical significance.

(g) The Southern Hemisphere

Reference has already been made above to Craig's 1950 survey of the ozone data then available (53). At that time, the measurements for the southern hemisphere were not very extensive, and those that had been taken were for far fewer stations than in the northern hemisphere and mainly only for low and middle latitudes. It nevertheless seemed that ozone distribution in the south was quite similar to that in the north, and that, allowing for the six month phase difference, the patterns of latitudinal and seasonal variations were similar.

Although necessarily still traced far less closely than in the north, appreciably more data is now available relating to southern hemisphere ozone. It is thus apparent that there are distinct differences in the ozone of the two regions, especially with regard to high latitude content. Associated with this, meteorological studies are revealing a profound difference also in the general circulation, especially in the seasonal control of large circulations, again at the higher latitudes.

Perhaps the first significant indication of such hemisphere differences was provided by the meteorological observations made at Halley Bay. These are reported by MacDowall (8), and the results of ozone soundings compared with those of other IGY stations. The overall picture thus provided of latitudinal and seasonal variations confirms the close similarity between

hemispheres only up to about 55° latitude. For higher latitudes, completely new features become apparent in the south. This difference is especially evident in comparing late winter to spring values - that is, at the time of the ozone increase. The ozone content in the northern hemisphere then continues to increase very rapidly with latitude, apparently almost up to the pole (c.f. 30). In the southern hemisphere, however, a reversal of the normal latitudinal gradient takes place from about 55°S, the content decreasing to a minimum at the pole (an amount no more than or even less than that for equatorial regions). The reversal occurs at somewhat higher latitudes at other seasons but always a final fall towards the pole occurs. This "anomalous" variation observed at Halley Bay (76°S) is also apparent at Argentine Island (65°S), but not at Melbourne (38°S). MacDowall investigates the relations between total ozone and upper air temperature and pressure measurements made at Halley Bay, and compares these with similar data for the south-east of England. Whereas in the latter case both short (3 day-) and long (10 day running mean) periods are related, in the Antarctic measurements only short period fluctuations in ozone amounts are related to upper air measurements. This indicates that the variations of different periods are here influenced by different dynamic processes.

A further interesting comparison of variations and distribution between hemispheres is given by Kulkarni (7). On the

basis of Umkehr observations, he concludes that, over the middle latitudes, there is more ozone in the southern hemisphere than in the northern - except perhaps for the spring maximum which appears to be much the same in both cases. The fact that it is in the spring that near equal amounts are reached corresponds well with the observed continuous latitudinal increase in the northern hemisphere (contrary to the southern). These results are considered in relation to the proposed mean poleward circulation of subsiding equatorial air in the lower stratosphere (Dobson-Brewer model); and it is concluded that such circulation in the southern hemisphere is probably weaker (and certainly no stronger).

The results, whichare related to tropopause height and hence to stratospheric ozone-holding capacity, also suggest less destruction of ozone (except in spring) in the southern hemisphere. This is an interesting point in view of Kroening and Ney's suggestions (52, and above) concerning the likely effect on the ozone cycle of differing magnitudes for the ground level sink strength. On the other hand, however, Junge (57) concludes that the destruction rate over the larger relative ocean to land area of the southern hemisphere cannot be much different from that of the smaller northern hemisphere distribution.

Indications that day-to-day variations are considerably smaller and seasonal variations more regular in the southern hemisphere are reported by Funk and Garnham (3), who point out that this

is perhaps to be expected in view of the lower high altitude values and the possibility of more restricted meridional trajectories. They also report a 24-month ozone cycle and suggest a relation here to the stratospheric subsidence pattern. (A yearly change in prevailing stratospheric wind direction (that is, a 24-month cycle) has also been noted elsewhere.)

(h) Other Correlations

Relations between atmospheric ozone and other geophysical phenomena have been suggested. Two of these, the theory for which is being developed, are just briefly noted.

Assuming that the energy gained by ozone absorption in the ultraviolet and visible regions during solar irradiation is lost at a constant rate throughout the whole day by infra-red re-radiation, it has been shown that such ozone heating is alone capable of accounting satisfactorily for atmospheric tidal oscillations (38 and 42). Atmospheric resonance, the basis in some form or another of previous tidal theories, is not required.

A statistical relation between rainfall and the relative positions of the moon and the earth's orbit has recently been established (93). Following on from this, preliminary evidence for the influence of the moon on atmospheric ozone has been reported (34). The lunar effect in both hemispheres appears to be to increase the vernal equinox high ozone values, and to decrease the autumnal low values. One suggested possible mechanism for this effect is a lunar modulation of the amount of meteoric dust.

6. PHOTOCHEMICAL THEORY

(a) An Oxygen Atmosphere

Oxygen exists in the earth's atmosphere in the three forms, atomic oxygen, molecular oxygen and the triatomic ozone. The chemical and photochemical reactions between these constituents tend to bring them into an equilibrium with one another and with the radiation to which they are subjected. The (partly resulting) absolute constituent concentration, the intensity of the solar radiation of various wavelengths of importance and the different rate coefficients for the processes involved, all determine the nature of the equilibrium. Concentration and radiation intensity are functions of altitude, depending not only on these reactions themselves but also on other factors such as ozone transport to lower levels and radiation absorption by other atmospheric constituents. The rate coefficients, which in any case are perhaps the least well-known parameters of photo-chemical theory, are also altitude dependent in so far as they are temperature and pressure dependent.

The basic concepts of the photochemistry of atmospheric oxygen were first outlined by Chapman in 1930. (A later review is given in Reference 46.) It was an attempt to account for what he termed the abnormal forms of atmospheric oxygen; that is, atomic oxygen and ozone. Rocket measurements have since confirmed the general photochemical prediction of distribution of upper

atmosphere ozone (4 and 5). The several (exclusive) processes of this original theory are still acceptable as the basis of a first approximation photochemical theory, which assumes all other atmospheric constituents to be inert up to about 100 Km. These processes are:

$$O_2 + h\nu \longrightarrow O + O \qquad (J_2) \qquad (6)$$

$$O_3 + h\nu \longrightarrow O_2 + O \qquad (J_3) \qquad (7)$$

$$O + O + M \longrightarrow O_2 + M \qquad (k_1) \qquad (8)$$

$$O + O_2 + M \longrightarrow O_3 + M \qquad (k_2) \qquad (9)$$

$$O + O_3 \longrightarrow 2O_2 \qquad (k_3) \qquad (10)$$

$$O_3 + O_3 \longrightarrow 3O_2 \qquad (k_4) \qquad (11)$$

$$O_3 + O_2 \longrightarrow O + 2O_2 \qquad (k_5) \qquad (12)$$

The first of these reactions is the dissociation of oxygen into its atomic form which is brought about by energy corresponding to wavelengths less than 2400 A. The second, equation (7), represents the dissociation of ozone. Its instability is such that this can be effected by all radiation up to a wavelength of 11,800 A; but in the ozonosphere it is mainly Hartley band absorption which is of importance. J_2 and J_3 represent the rates of dissociation per unit concentration, or the dissociation quantum yield, for O_2 and O_3 respectively. Equation (8) shows the collision process of atomic oxygen recombination which requires also the presence of the third body M to conserve energy and momentum

across the reaction. This is neglected by Craig and others in deriving expressions for ozone content. Such a procedure is justified within the main ozone layer; but the reaction becomes important in the upper ozonosphere above about 50 Km. Here there is a great increase in the atomic oxygen content, so the relation and transition of predominance between this and the following reaction (equation (9)) becomes very important. Despite the increase in atomic oxygen, the high altitude decrease in the molecular form results in decreased ozone production by reaction (9). In addition, reaction (8) like other generally less important reactions, becomes significant in consideration of the secondary ozone layer which can form above the stratopause at night-time. The spectral states of the atoms and molecules together with the transitions involved in these various reactions are noted by Mitra (58) and by Watanabe (72); and are considered in some detail by Herzberg (64). The reaction of equation (11) is the thermal decomposition of ozone and is not important for the concentrations encountered. Together with reaction (12), this can usually be neglected. k_1 to k_5 are the rate coefficients (or collision coefficients) for the various recombination reactions.

On the basis, then, of these reactions and in terms of their coefficients, expressions can be written down for the time rate of change of the concentrations of the different constituents, represented $[O]$, $[O_2]$ and $[O_3]$. Neglecting (8), an

expression for the equilibrium atmospheric ozone concentration is thus obtained of the form (47) :

$$[O_3] = [O_2]^{3/2} \left[\left(\frac{J_2}{2J_3}\right) \left(\frac{f_2}{f_3}\right) k \rho \right]^{1/2} \qquad (13)$$

Here f_2 and f_3 are the numbers of quanta absorbed each second per molecule of O_2 and O_3 respectively. For a given altitude, these can alternatively be given in terms of absorption coefficients, of concentration of absorbing constituents along the atmospheric path involved, and of spectral distribution of radiation incident on the top of the atmosphere. ρ includes the ratio of concentrations of nitrogen to oxygen, and their relative effectiveness in acting as the third body M in reaction (9). k is equal to k_2/k_3 .

In photochemical calculations, four sets of data are thus required (besides a value for ρ). These are : (1) The ultraviolet solar emission spectrum which is incident on the top of the atmosphere; (2) the ratios of the rate coefficients, k and J_2/J_3 ; (3) the vertical distribution of molecular oxygen; and (4) the absorption spectra of oxygen and ozone. The last of these are quite well known; their main features are outlined above in sections (2) and (3). However, there is a serious lack of reliable data for the other three parameters. Nevertheless, a close agreement generally has been obtained between photochemical

calculations and experimental results from rocket flights (5, eg). From the stratopause (about the level where the omission of reaction (8) becomes acceptable) to about 35 Km., the ratio of f_2/f_3 remains fairly constant leading to the rapid increase in ozone content due to the molecular oxygen factor. Below 35 Km., however, f_2 falls off much more rapidly than f_3 (penetration effect - Fig. 1.), so that the ozone content gradient becomes more gradual to peak at about 25 Km., and thereafter it decreases rapidly below.

On the basis of his calculations, Craig (53) estimates that only a few seconds or minutes are required to establish photochemical equilibrium at altitudes above 50 Km.; several hours at 38 Km.; a day or so at 35 Km.; and a period of 3-9 days at 32 Km. Dutsch (47) gives an expression for the time of half-restoration - the period needed to reduce to half any existing deviation from equilibrium - and concludes that this is a year or more below the level of the ozone maximum. He also gives a modification to equation (13) which is more applicable to the mesosphere where reaction (8) can no longer be disregarded.

(b) <u>Possible Extensions to an Oxygen-Nitrogen-Hydrogen Atmosphere</u>

Paetzold (49) also considers this necessity of including reaction (8) in any photochemical analysis of the upper stratosphere. Again the choice of realistic values of reaction rates presents some

difficulty, but in trying two likely combinations of k_1 and k_2, one is found to give a high altitude profile which better than the other fits the observed pronounced nightly maximum and rapid sunrise destruction.

However, this is not the main complication in the photochemistry of the upper stratosphere. This is rather than the whole of the above theory based simply on a pure oxygen atmosphere may now no longer remain so valid. As already briefly indicated, other atmospheric constituents also effect important absorption of incoming radiation. In any case, their very presence in the atmosphere allows the possibility of chemical reaction with oxygen constituents. At lower levels, these additional reactions are negligible in their photochemical effect, at least as regards ozone conditions. At higher levels, they become increasingly important. In the first place, the ozone amount itself is here rapidly decreasing, so minor reactions affecting it are of significance. These reactions may be directly between ozone and one of the other constituents; or perhaps equally important may involve the now scarce molecular oxygen or the essential atomic form. Also one of the additional constituents, hydrogen, increases in abundance. Hydrogen, nitrogen and their oxygen compounds comprise these further reactants which need to be considered for the whole problem of photochemical (and therefore oxygen and ozone) balance at the higher altitudes. The following are the main reactions to be added to

those of equations (6) to (12) :

$O_3 + N_2 \longrightarrow N_2O + O_2$	(k_6)	(13)[a]
$O + N_2 + M \longrightarrow N_2O + M$	(k_7)	(14)
$H_2O + h\nu \longrightarrow OH + H$	(J_4)	(15)
$H + O_2 + M \longrightarrow HO_2 + M$	(k_8)	(16)
$OH + H + M \longrightarrow H_2O + M$	(k_9)	(17)
$H + O_3 \longrightarrow OH + O_2$	(k_{10})	(18)
$OH + O_3 \longrightarrow 2O_2 + H$	(k_{11})	(19)
$OH + O \longrightarrow O_2 + H$	(k_{12})	(20)
$NO_2 + h\nu \longrightarrow NO + O$	(J_5)	(21)
$NO + O_3 \longrightarrow NO_2 + O_2$	(k_{13})	(22)
$NO + O + M \longrightarrow NO_2 + M$	(k_{14})	(23)
$N + NO \longrightarrow N_2 + O$	(k_{15})	(24)
$N + NO_2 \longrightarrow N_2O + O$	(k_{16})	(25)
$NO_2 + O \longrightarrow NO + O_2$	(k_{17})	(26)
$OH + O \longrightarrow O_2 + H$	(k_{18})	(27)

Although these reactions are almost entirely of upper atmosphere interest, there is one aspect in which one or two are relevant much lower. This is in a finer investigation of the problem of possible tropospheric ozone sources. The production of atmospheric ozone is only possible in the presence of atomic oxygen, so the question arises as to what sources of tropospheric atomic oxygen might exist. The subsequent photolysis of the N_2O

produced by reactions (13)(a) and (14) is ruled out as a possibility because of the slow reaction rates k_6 and k_7. These reactions, in any case, use up odd oxygen atoms or ozone molecules themselves. A perhaps more likely possibility is provided by equation (21) which represents the dissociation of NO_2 by wavelengths below 3800 A. However, reaction rates and the subsequent role of the NO which is also formed both need to be carefully considered; since the NO in its fast reaction (22) could itself finally make the net ozone production very weak.

These and other three-body and bimolecular reactions are considered by Harteck and Reeves (48) who assess their importance to atmospheric photochemistry. The part played by ion reactions is also dealt with, both in pure charge transfer between constituents and in ion-neutral reactions. Except in the case of nitrogen compounds, chemical yields by ion reactions seem to make only a minor contribution compared with that of uncharged dissociation products. Barth (44) analyses ionic reactions in an account of sources of atomic nitrogen.

A few general comments can be made on the above reactions. The ozone produced by (9) is either transported elsewhere or is finally destroyed by (10) and (18). Reaction (24) is very fast and is important in that N and NO cannot coexist in the upper atmosphere in appreciable concentrations. That of NO is insufficient, therefore, for observation by absorption. The NO_2

concentration in turn becomes insignificant - especially in the presence of atomic oxygen, reaction (26) also having a large rate coefficient. Reaction (14) is the probable source of N_2O ; reaction (25) being slow and making only a minor contribution. The dissociation of water vapour by radiation of wavelength less than 2000 A, reaction (15), provides hydrogen atoms and the OH radical. The hydrogen atoms removed by the reaction with ozone (18) are regenerated by reaction (20).

The atomic reactions of nitrogen and oxygen are a principal concern of the study of the chemosphere. Barth (44) has carried out numerical calculations based on the nine such reactions considered dominant, and presents the results as a series of graphs showing particle densities over two one-hour reaction periods at various altitudes. Ozone density is included.

The solar radiation dissociation of water vapour results finally in the continuous escape of hydrogen atoms into interplanetary space, but in the liberated oxygen atoms remaining in the atmosphere. The photochemistry of atmospheric water vapour has been considered by Bates and Nicolet (45). Even when the less likely reactions have been eliminated, the hydrogen-oxygen atmosphere remains very complicated. The most energetic part of the night sky-glow is in the infra-red Meinel bands of the OH radical. It is believed that this emission originates in the altitude region from 70 to 95 Km. where the product of ozone and hydrogen densities

reaches a maximum, and that the radiation comes from the excited radical produced by their interaction :

$$\left.\begin{aligned} O_3 + H &\longrightarrow (OH)^* + O_2 \\ (OH)^* &\longrightarrow OH + h\nu \end{aligned}\right\} \qquad (28)$$

Kofsky (40) concludes from an analysis of the effect on the ozonosphere of nuclear detonations, that only negligible additional ultraviolet radiation is thereby transmitted through the main ozone layer, but that higher altitude ozone might remain destroyed for several hours. He points out that this provides a possible test of the above hypothesis. Recent measurements of the rate constant for the primary reaction in equation (28), together with investigations into the nature of the secondary reaction of the excited OH are reported by Phillips and Schiff (83).

(c) Photochemical Rate Coefficients

The principal difficulties in the extension and application of the photochemical theory are the lack of reliable measurements, first of upper atmosphere constituent concentrations and irradiation, and secondly of representative rate coefficients for the reactions involved. Even where coefficients for a given reaction have been measured, it is often difficult to simulate in a laboratory the conditions of that reaction in the atmosphere. The pressure at 100 Km. is only of the order of one micron which makes the chemosphere equivalent to a huge reaction volume. In a

similar laboratory experiment, the wall effects would predominate, and results would have to be extrapolated. Certain upper atmosphere processes, such as three-body collisions and those in which re-radiation is significant, cannot really be duplicated at all.

Typical of the uncertainties in rate coefficients is the value to be used for k in equation (13), that is the temperature dependent ratio of the rates of the three-body to the two-body reactions which is important in even the simple oxygen atmosphere. Values for k at the same temperature but measured in different experiments differ by a factor of twenty. As a result, relatively slight differences, for example, between observed and calculated vertical distributions of ozone cannot be treated as sufficiently significant to derive information on vertical motions.

For reference, however, typical and fairly accepted values for some of the above rate coefficients are here listed in Table 1; while Table 2 shows the altitude dependence of the important (and uncertain) ratio k. Low concentration rate constants for ozone reactions with oxides of nitrogen are given by Ford (80 and 81).

TABLE 1

Rate Coefficients at 300°K (cc/particle)^2 sec^{-1}

k_1 : 3.10^{-33}

k_2 : 5.10^{-34}

k_3 : 3.10^{-14} / 2.10^{-15}

k_8 : 2.10^{-25}

k_{10} : 10^{-11}

k_{12} : 10^{-12}

k_{13} : 5.10^{-14} / $1.7.10^{-14}$

k_{14} 6.10^{-32}

k_{15} : $1\text{-}6.10^{-13}$ / 8.10^{-11}

k_{16} : 3.10^{-14}

k_{17} : $1\text{-}3.10^{-12}$ / 8.10^{-11}

k_{18} : 10^{-12}

TABLE 2

Values of $k = k_2/k_3$ in the Sunlit Ozonosphere

Altitude (Km).	k_o (per cc)
80	$5.4\ 10^{-18}$
70	$9.0\ 10^{-19}$
60	$7.0\ 10^{-20}$
50	$3.1\ 10^{-20}$
40	$5.6\ 10^{-20}$
30	$4.5\ 10^{-19}$

(d) Chemical Physics of Ozone

Measurements such as those above relating to rates of various reactions involving ozone lead to the study of mechanisms by which thermal or vibrational dissociation of the ozone and similar triatomic molecules might take place (113 and 108). Reference is here briefly made to a few reports of recent investigations in this field.

Benson and Axworthy (77) experimentally studied the thermal decomposition of ozone, and concluded that most of the data could be quantitatively explained in terms of the relevant reactions above. These may be generalised:

$$\left.\begin{aligned} M + O_3 &\rightleftharpoons M + O_2 + O \\ O + O_3 &\rightarrow 2O_2 \end{aligned}\right\} \qquad (29)$$

where M may be any one of a number of molecules or atoms such as O_2, CO_2, N_2 and He - besides ozone itself. They determined rate constants for this latter case of $M = O_3$; and also the efficiencies of the other molecules in activating ozone (relative to that for a second ozone molecule itself). They consider the possible effects on the rates observed of temperature gradients within the system, of direct bimolecular reaction, and of secondary activation of ozone by the activated oxygen molecules formed in the second part of equation (29). Any important effect of secondary activation (or energy chains) is supposed to be nearly temperature

independent, which is contrary to the present results. This is discussed in relation to the previous acceptance of energy chains as an explanation of high quantum yields in the ultraviolet; and an alternative explanation is considered.

Such studies of the thermal decomposition of ozone are very difficult in view of the extreme sensitivity of the reaction to trace analysis. However, Benson (78) concludes that there is no evidence for an energy chain. If such activation does occur, it is attributed to excited states of atomic oxygen. On the other hand, Schumacher (84) discussing results of photochemical ozone decomposition by both red light and ultraviolet light, considers that there is no reason to doubt the existence of such energy chains; nor to suppose that the excited oxygen atoms will not react with the ozone in a simpler way than in the scheme proposed by Benson.

Bunker has given results of computations of the dissociation rates of various triatomic molecules. Six hypothetical models of the molecules O_3 and N_2O are considered in Reference 79. They are supposed non-rotating and described in terms of bond lengths and bond angles. The object of the study was to isolate as many mechanical properties as possible which had any effect on the rates of dissociation of the molecule. Amongst other results, it was concluded that the usual normal-mode description is very poor for the models studied; and that theories of unimolecular

dissociation based on the assumption of harmonic molecules failed, except at high pressures. (Concepts of unimolecular reactions are given in Ref. 111.)

Results of another investigation of the vibration and decomposition of the ozone molecule and the exact manner in which it becomes energised are given by Gill and Laidler (82). The principal difference between the two main types of theory is that in the (original) Hinshelwood concept it is supposed that energy can flow freely between the various modes; whereas in Slater's treatment this is not possible. In the latter case, the dissociation occurs not when the necessary energy gets into a particular mode but rather when the vibrations come suitably into phase sufficiently to extend some critical co-ordinate. The results quoted agree much better with the former concept in the cases of nitrous oxide and hydrogen peroxide. In the case of ozone, however, it appears that there may not be a flow of energy between normal modes.

PART B : THE EXPERIMENT

1. THE AIM OF THE EXPERIMENT

The aim of the experiment is the determination of the ozone content and distribution in the upper atmosphere. As a function of altitude, measurements will be made of the intensity of certain relevant wavelengths in the ultra-violet region of the solar radiation. That is, the extent of the penetration into the atmosphere will be found; and, as the wavelengths chosen are within the region of high ozone absorption alone, the attenuation can be attributed to the quantity of that gas which is present between the point of observation and the top of the earth's atmosphere.

The altitude range in which measurements will be made is that above the ozone peak at about 30 Km. It is of particular interest to determine content and distribution at 50 Km. and higher. The expected density has by then again fallen to low values of the order of those recorded at ground level, but at such altitudes its presence is of photochemical importance. Measurement at the highest altitudes of the then negligibly small quantities of ozone would first require an extension of the present technique to a greater degree of accuracy. These radiation measurements from which atmospheric ozone content is to be deduced will be made from a rocket, and much of the work reported here concerns the development of units suitable for use during flight.

There is still very little experimental knowledge concerning high altitude ozone, and this is the main reason for the present study. Proposed satellite observations (16) should provide results along a considerable path length through the upper atmosphere; while chemical sondes and other balloon measurements have given data for lower altitudes. It is hoped that the present experiments will fill in the altitude gap between these other two. The results obtained will, further, provide distribution at a given geographical location, rather than the integrated content over a long path available from the satellite experiment.

The exact vertical distribution of ozone is not known very well above its maximum. This includes the region where the constitution of the atmosphere and the absorption of incoming solar radiation are directly accounted for in terms of the many possible reactions of photochemical theory (cf. part A). The most useful photochemical results would be derived from simultaneous measurements of atomic and molecular oxygen content, along with that of ozone.

2. BASIC CONCEPT OF EQUIPMENT AND PROPOSED METHOD OF MEASUREMENT

The intensity of a certain solar ultraviolet radiation, appreciably absorbed by ozone, is to be measured at various heights in the atmosphere. Knowing the appropriate ozone absorption coefficient, changes in the amount of ozone along the path from the

point of observation to the sun can be determined from the observed changes in intensity. The effect of scattering due to air molecules and to particulate matter needs to be taken into account (1).

Basically, the equipment consists of a combination of filter and photocell. The filter chosen must transmit a selected narrow wavelength range of ultraviolet radiation within the region of ozone absorption, and as far as possible must reject all other wavelengths. The radiation transmitted falls onto the sensitive area of a photocell. The resulting telemetry signal is thus a measure of the intensity of the ultraviolet radiation monitored, and hence of ozone amount.

The particular relation between incident ultraviolet intensity and telemetry input is determined by the filter characteristics, by a phosphor transfer efficiency, by the dimensions and geometry of the assembled unit and any slit system or aperture included, by the photocell spectral sensitivity and by the gain of the amplifier used. With the unit mounted in a rocket, it is also apparent that its output will depend on the attitude of the rocket at any instant. Rocket aspect is thus an essential piece of information required in interpreting experimental results from the equipment in flight.

The rockets used should carry the equipment well above the ozonosphere. It is the upper part of this region which in any case is of interest in the experiment. Besides this, it will be a

definite advantage to have the trajectory pass for a time through a high altitude region which can be supposed free of ozone. In this way, a signal from the unit above the ozonosphere could be used in the analysis as a reference point corresponding to zero ozone path.

The method of measurement is dependent on the rocket having a suitable roll rate. This must be such that it will bring the sensors used into a satisfactory orientation with respect to the sun often enough to give readings at sufficiently close height intervals. Trajectory information must be available to determine the height at which a particular intensity is recorded. The height range over which the experiment is carried out can be adjusted in selecting a suitable overall sensitivity by including apertures of appropriate sizes.

3. CALCULATIONS OF EXPECTED INTENSITIES AND EQUIPMENT RESPONSES

Comparison of relative intensities at different altitudes will alone provide useful information; and if a reliable reference point above the ozonosphere is obtained as well, intensities relative to this should yield the absolute ozone profile required. However, it is very desirable to have separate calibrations of the various stages of the equipment and to have a clear indication before flight of the response expected. This is essential, of course, for any attempted estimate of absolute radiation intensity and for selection by suitable aperture size of some particular

height interval to be monitored. Part (C) includes such calibrations of component parts. In this section, consideration is given to some more general factors relating to expected experiment response.

(a) Relative Intensities due to Ozone Absorption

Lambert's Law gives the relation between an incident intensity Io and the intensity I to which it is reduced by transmission through a thickness x of absorbing material. $I = Ioe^{-\alpha x} = Io\ 10^{-kx}$. Using the values for the ozone decimal absorption coefficient k given by Vigroux (69, and plotted in Figure 3) and a vertical distribution based on that of Figure 2, relative intensities have been calculated over a near ultraviolet wavelength region both as a function of altitude and of solar zenith angle. The intensities are referred to that at 80 Km., supposed unattenuated. The small corrections to the absorption coefficients as a result of temperature variations with height in the atmosphere have not been taken into account. Figure 2 shows the vertical ozone distribution given by Dutsch, on the basis of Umkehr wavelength D results, in an article on the comparison of various methods of ozone profile determination (2). For the present purposes, average densities are taken over the twelve height intervals indicated in Figure 2; and others represent a linear decrease from 50 to 80 Km. These values with the corresponding ozone paths through each layer for various zenith angles are shown in Table 3. The results for four zenith angles are plotted in Figures 4 to 7.

TABLE 3

Ozone Layers and Slant Paths

			$\chi = 0^\circ$		$\chi = 50^\circ$		$\chi = 70^\circ$		$\chi = 90^\circ$	
	Altitude Range (Km)	O_3 Density (cms 10^3/Km)	Slant Path (Km)	O_3 Path (cms 10^3)	Slant Path (Km)	O_3 Path (cms 10^3)	Slant Path (Km)	O_3 Path (cms 10^3)	Slant Path (Km)	O_3 Path (cms 10^3)
1	80 -70	0.15	10	1.5	15.1	2.3	26.8	4.0	65.1	9.8
2	70 -60	0.5	10	5.0	15.5	7.8	27.6	13.8	67.9	34.0
3	60 -47.8	0.8	12.2	9.8	19.2	15.4	33.5	26.8	94.5	75.6
4	47.8-42.6	1.6	5.2	8.3	7.8	12.4	14.4	23.0	43.8	70.0
5	42.6-37.5	3.2	5.1	16.3	7.8	24.9	14.1	45.2	45.8	146.5
6	37.5-32.7	5.4	4.8	25.9	7.4	39.7	13.5	72.8	45.9	247.8
7	32.7-28.2	9.3	4.5	41.8	6.9	64.6	12.8	119.3	46.2	429.5
8	28.2-23.7	14.7	4.5	66.1	7.4	108.2	12.4	182.3	50.0	735.3
9	23.7-19.2	14.6	4.5	65.7	6.9	101.5	13.3	193.7	55.0	803.3
10	19.2-14.8	8.4	4.4	37.0	6.1	51.5	12.4	104.2	60.4	507.6
11	14.8-10.3	3.8	4.5	17.1	7.8	29.5	13.3	50.4	72.0	273.7
12	10.3- 0	1.9	10.3	19.6	15.5	29.5	29.8	56.6	362.1	688.0

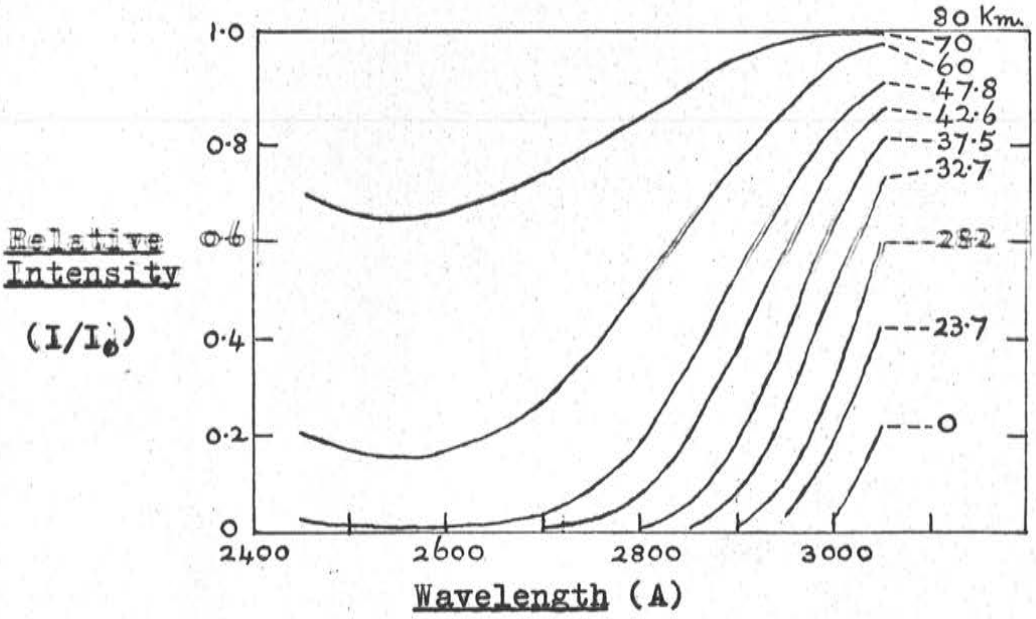

FIGURE 4. Penetration of Solar Ultraviolet Radiation into the Ozonosphere. $\chi = 0°$.

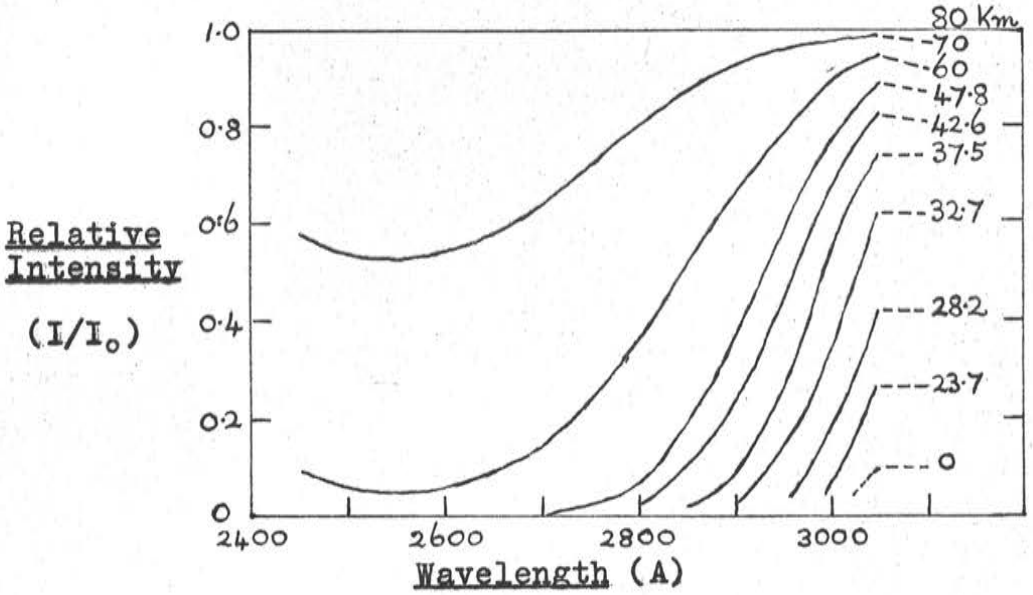

FIGURE 5. Penetration of Solar Ultraviolet Radiation into the Ozonosphere. $\chi = 50°$.

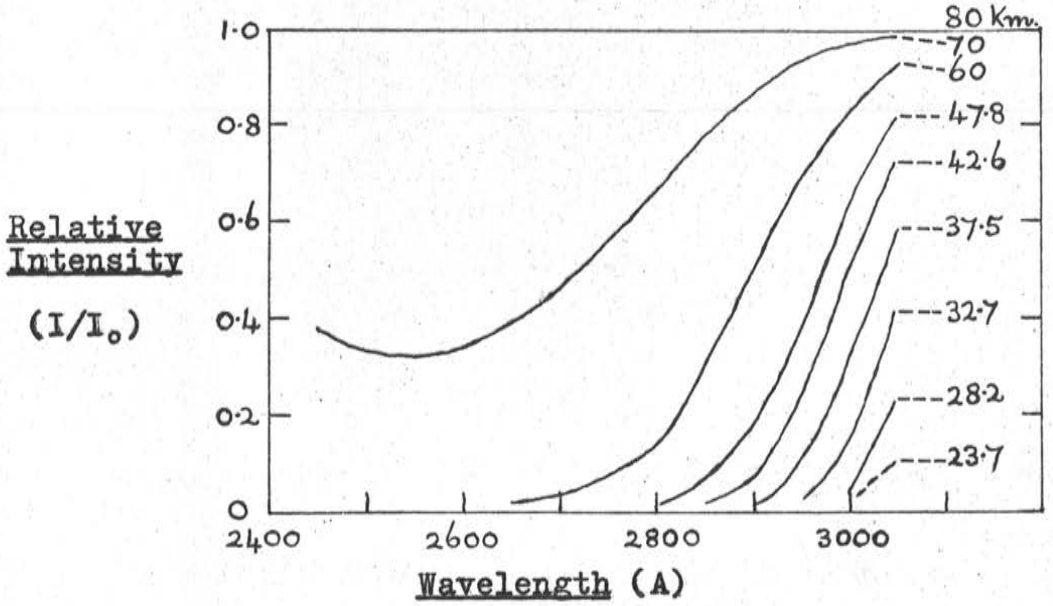

FIGURE 6. Penetration of Solar Ultraviolet Radiation into the Ozonosphere. $\chi = 70°$.

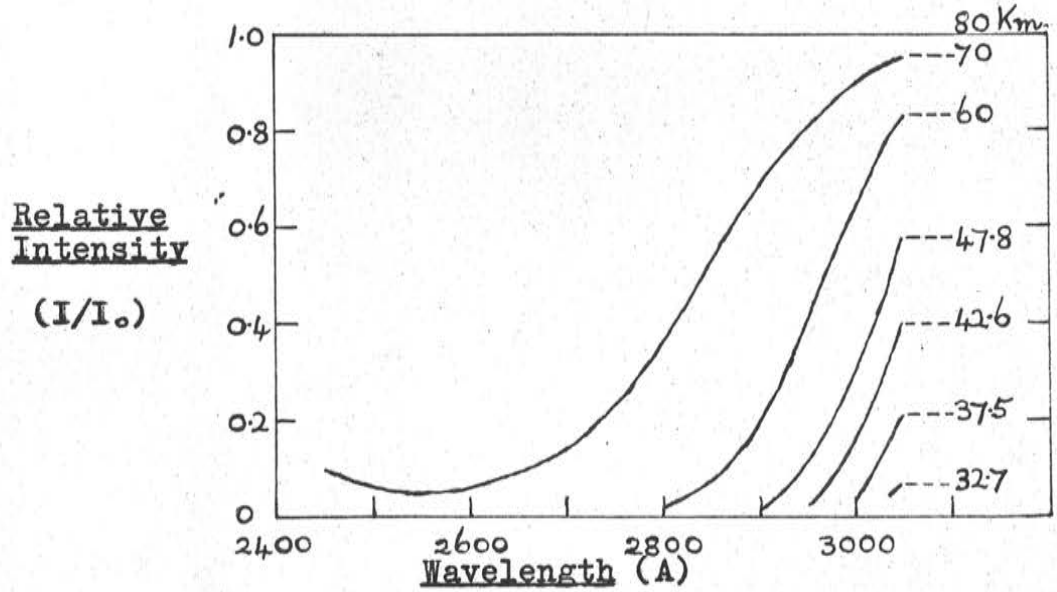

FIGURE 7. Penetration of Solar Ultraviolet Radiation into the Ozonosphere. $\chi = 90°$.

It is seen that the set of curves is progressively displaced towards lower wavelengths the higher the sun rises above the horizon. The intensity at 2900 A, for instance, is attenuated to much less than a tenth of its initial value in penetrating the atmosphere from 80 Km. to 50 Km. when the sun's rays are tangential to the atmosphere. With the sun overhead the corresponding reduction is only to about 0.6 of the incident value; and penetration to 30 Km. is possible before the previous decrease in intensity again results.

(b) Effective Filter Transmission

Ideally, a measurement such as planned in this experiment would be most accurate if made as nearly as possible at one wavelength only, for which the one value of absorption coefficient would be appropriate. However, in view of the finite width of the transmission region of a practical filter, it is necessary to consider also the variation in absorption over that range. The characteristic of the filter (U701) chosen for the first measurement is shown in Figure 17. If this is compared with Figure 3 it is seen that the filter covers an appreciable part of the higher wavelength side of the ozone band, and in this context is a wide band filter.

The object of the calculations noted in this section is to determine the contributions to the overall filter transmission from radiation at the various wavelengths; and to illustrate the way in which the relative magnitude of such contributions can be

expected to change at different altitudes of measurement in the atmosphere. That is, if a certain response is recorded at a given altitude, to what radiation distribution of the filtered region is this to be attributed - and hence what are the appropriate absorption coefficients to be used in calculation of the ozone amount?

Division of the ozonosphere was as in the preceding section (Table 3). Values for the unattenuated (or 80 Km) solar radiation intensity from 2900 A to 2630 A are taken from an article by Wilson et al (115). The few lower wavelength values used are those of Detwiler et al (95). Average values were taken over wavelength intervals of 10 A from 2630 $\pm$ 5 A to 2900 $\pm$ 5A ; also for the intervals 2550 $\pm$ 25 A and 2600 $\pm$ 25 A .

Figures 8 to 11 show the relative contribution from each of the wavelength intervals to the total response at a given height and zenith angle. The total transmission noted alongside each curve is referred to a value of unity at 80 Km. The curves illustrate the gradual decrease in relative transmission of lower wavelengths (because of the decrease in relative penetration of these) and the consequent shift in the effective peak transmission wavelength of the filter. The change is more rapid with altitude at higher solar zenith angles. The influence of the magnitude of the incident solar radiation is also reflected in the results. Especially apparent is the minimum in the effective transmission near 2800 A which corresponds with a low value of 0.8 μW cm^{-2} A^{-1} for this interval.

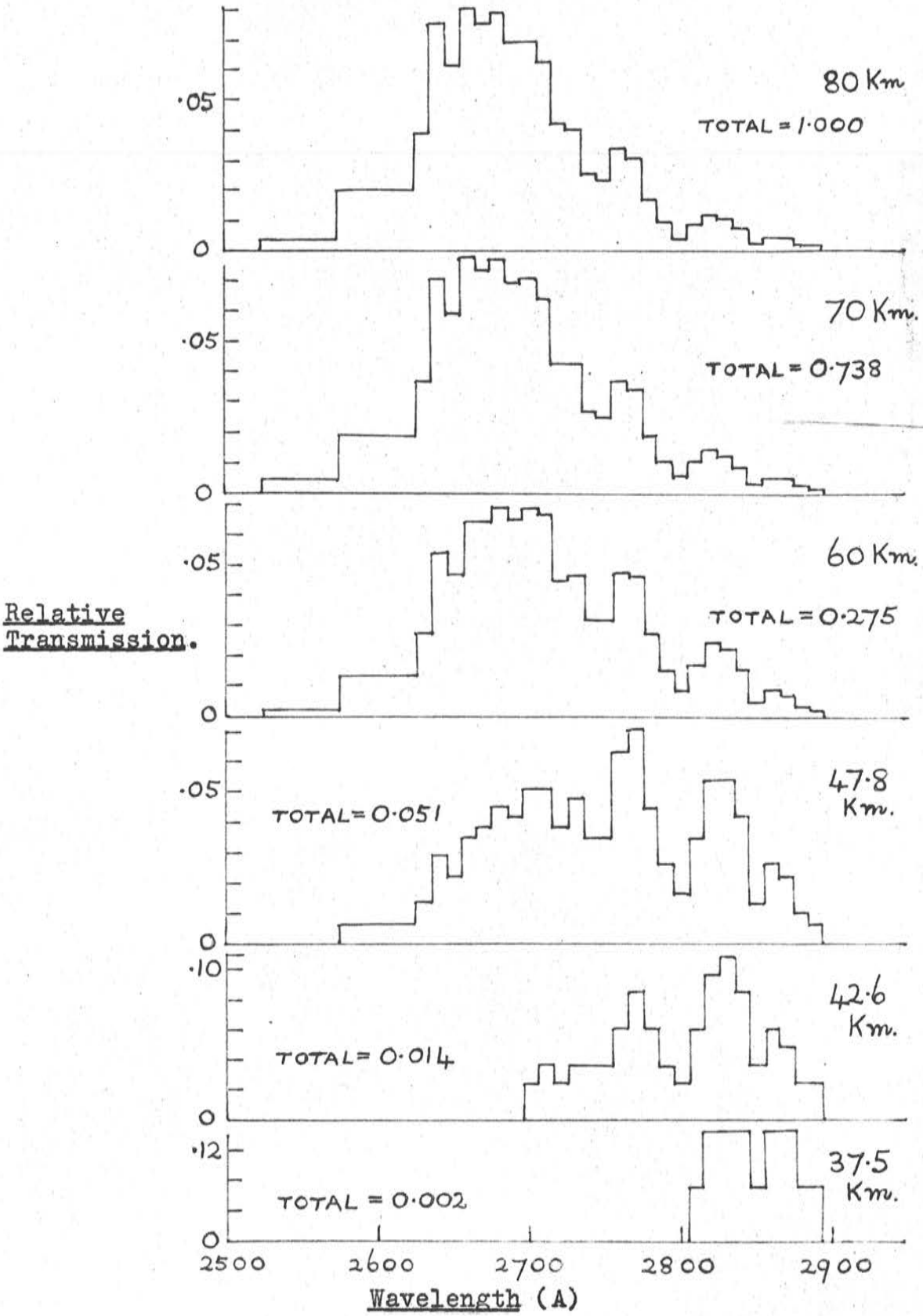

FIGURE 8. Relative Filter Transmission at Different Wavelengths. $\chi = 0°$.

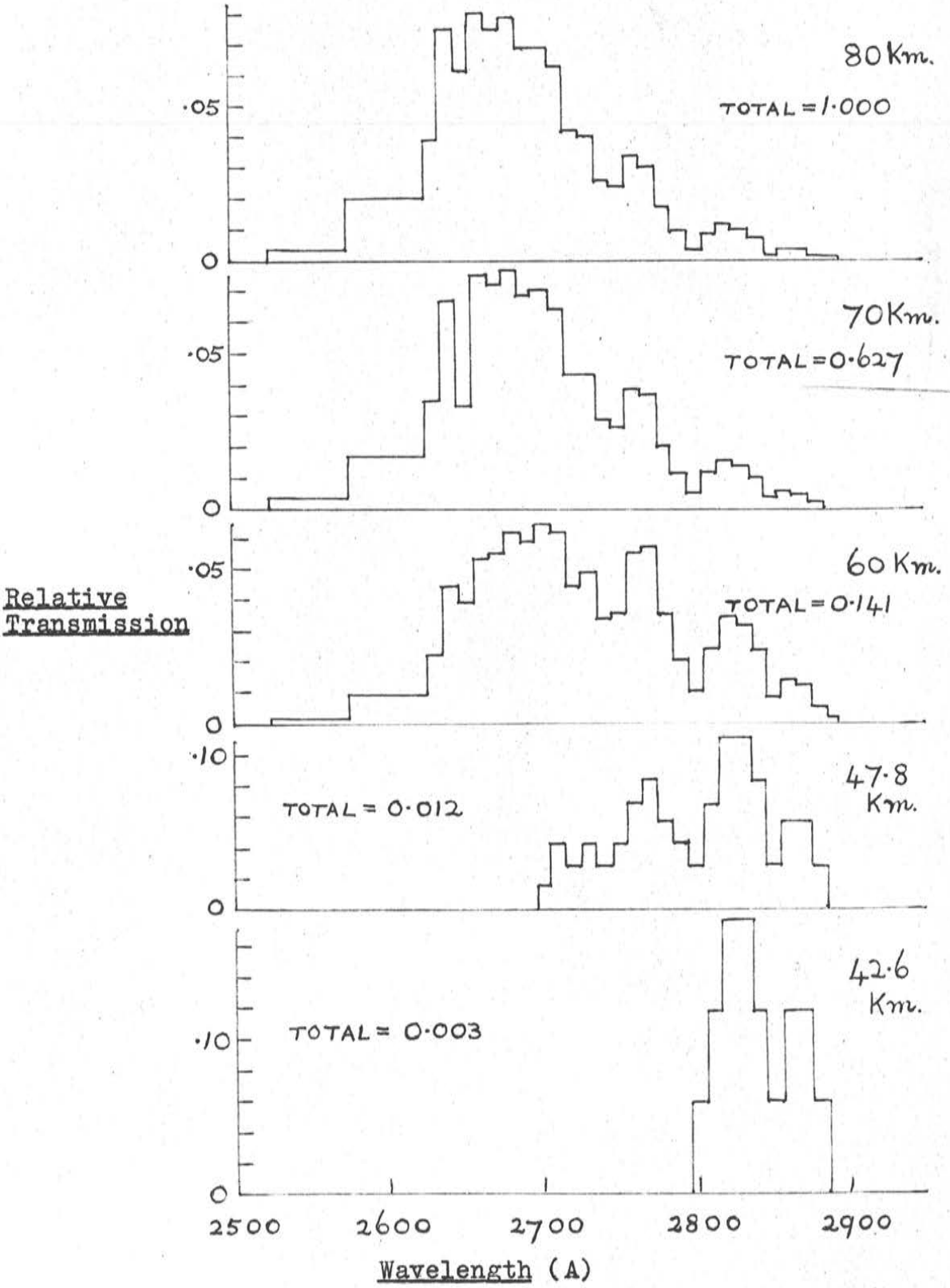

FIGURE 9. Relative Filter Transmission at Different Wavelengths. $\chi = 50°$.

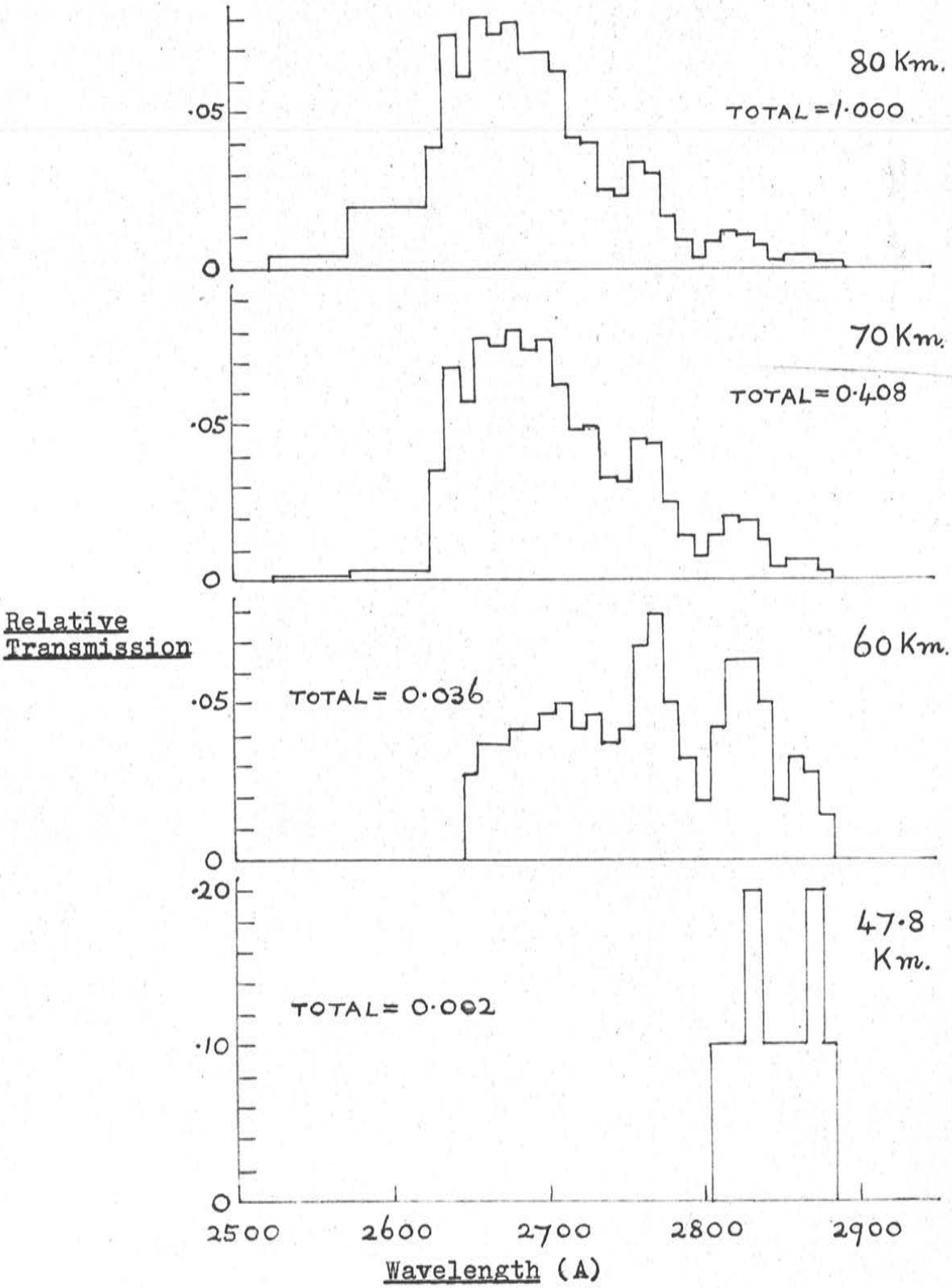

FIGURE 10. Relative Filter Transmission at Different Wavelengths. $\chi = 70°$.

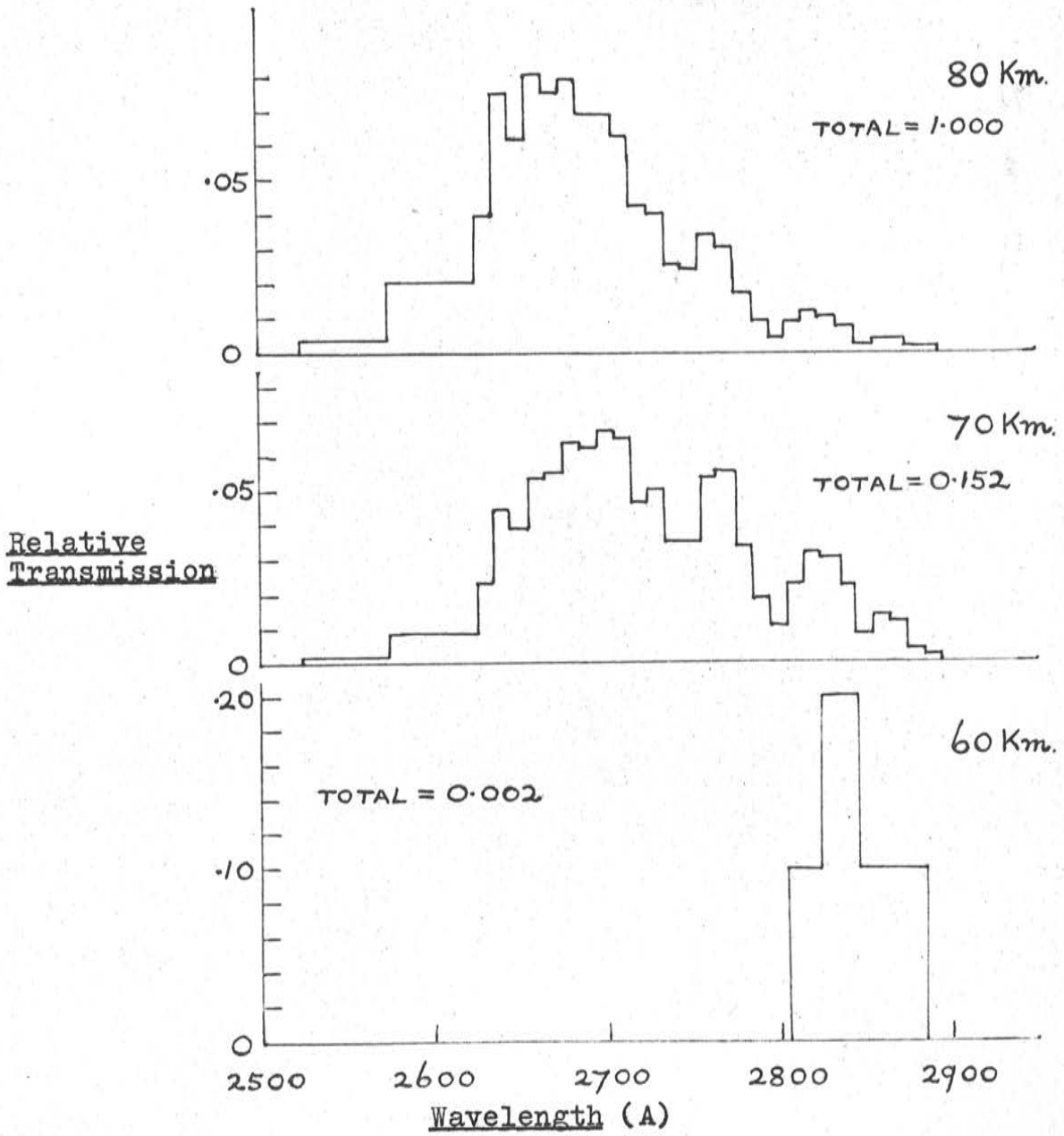

FIGURE II. Relative Filter Transmission at Different Wavelengths. $\chi = 90°$.

(c) General Photocell Characteristics

Early consideration was given to properties of photosensitive devices and the relations involved applied to the particular photocell chosen for the experiment. The total signal obtained from a photoelectric cell results from the sum of the various responses for each wavelength to the incident flux at that wavelength. Thus the resulting current is

$$Ip = c \int g_\lambda \, E_\lambda \, d\lambda \qquad (30)$$

The integral is taken over all wavelengths for which g_λ , the relative spectral response of the device, and E_λ , the light source spectral emission, have values other than zero. The quoted sensitivity of the photocell used, s , is expressed in milliamps per lumen; this being measured against an incandescent lamp of colour temperature T , emitting $680 \int v_\lambda \, E_{t\lambda} \, d\lambda$ lumens. (v_λ is the international luminosity factor.)

The photocell current resulting from an arbitrary light source is thus expressed as

$$Ip = \frac{680 \int v_\lambda \, E_{t\lambda} \, d\lambda}{\int g_\lambda \, E_{t\lambda} \, d\lambda} \quad \int g_\lambda \, E_\lambda \, d\lambda \qquad (31)$$

Calibrating source — Source to be measured

This integral was evaluated by taking average values over 500 A intervals for both g_λ and v_λ ; and by using the Planck

Radiation function to determine values of $E_{T\lambda}$ at the quoted calibrating colour temperature.

The relation finally derived for the expected current from the photocell considered is

$$Ip = 5.01.\ 10^{-3}.\ k.\ x.\ A\ (\mu A) \qquad (32)$$

Here A is the area of the photocell sensitive area illuminated; and the integrated energy transmitted by the particular filter used is x ergs cm^{-2} sec^{-1}. k is a measure of the energy transfer efficiency of a phosphor used (this is considered further in a subsequent section).

(d) Maximum Energy Transmission by Three Ideal Filters

As a further step in the estimation of the current to be expected on the basis of the relations of the preceding section, the solar energy transmitted by each of three ideal filters was calculated. Filter 1 transmits radiation between 2600 and 2700 A ; filter 2 between 2900 and 3100 A ; and filter 3 between 3600 and 4000 A . Transmission is supposed to be 100% within these regions and zero elsewhere. (Factors affecting a final choice of filter characteristics are noted in section e.) When the filters for use in the equipment were chosen and calibrated, more detailed consideration was given to their total transmission (Part c).

On the basis of Planck Black Body radiation, the transmission by each of the above filters was determined, supposing an

incident solar spectral distribution of a 6000°K black body at longer wavelengths, and 5000°K for shorter wavelengths of the far ultraviolet. The tables of Planck's Radiation functions given by Lowen and Blanch proved very useful in this (106). Amongst other factors, the ratio $E_{0-\lambda} / E_{0-\infty}$ is tabulated against λT. From this ratio of the energy contained in all radiation up to a wavelength λ to the total energy, the fraction in a given spectral band is found. Lists were prepared for 100 A wide bands over the whole region of filter interest.

For the above filters, these fractions of the total energy are:

Filter 1 :	6000°K	.00862
	5000°K	.00282
Filter 2 :	6000°K	.01426
Filter 3 :	6000°K	.04685

The total energy is given by $E_{0-\infty} = 6.493939\ c\ (T/c_2)^4$

For 1000°K, $E_{0-\infty} = 5.699 \times 10^7$ ergs cm^{-2} sec^{-1}

5000°K, $E_{0-\infty} = 3.561 \times 10^{10}$ "

6000°K, $E_{0-\infty} = 7.386 \times 10^{10}$ "

(e) Wavelengths to be Monitored

In deciding which wavelengths should be selected for intensity measurements during flight, reference is made to Fig. 3

of Part A and to Fig. 6 of Reference 72, which show the absorption of ozone and of molecular oxygen. Figs. 4 to 7 above are also relevant in determining altitude and zenith angle relations. It was decided to monitor radiation on the upper wavelength side of the Hartley Band of ozone absorption somewhere between 2500 and 3000 A. Higher wavelengths than this are unsatisfactory because of the low ozone absorption, while the lower wavelengths side of the ozone band was rejected in order to avoid getting too close to the region in which molecular oxygen absorption could possibly have some effect (cf. part A). In addition, filters for the somewhat longer ultraviolet wavelengths were more readily available and the choice of this region simplified calibration and the provisions of suitable light sources. Narrowing the choice still further, it is seen that the lower wavelengths (around 2500 A) are in the region of high absorption and are suitable for expanding the sensitivity of the equipment in high altitude regions. On the other hand, the higher wavelengths are nearer to the region of the proposed monitor unit operation.

Monitor Unit. Along with the ozone measuring assembly, an additional unit is included to measure radiation in a nearby band just outside the region of ozone absorption. Results of intensity measurements from this unit will enable corrections to be made to those from the ozone units themselves, so allowing for scattering effects and attenuation due to factors other than simple absorption

(cf equation 2). The filter for the monitor unit selects radiation above 3600 A where there is no absorption by ozone. From now on, this unit is called the "monitor unit"; while the main unit, which is, in fact, monitoring the intensity in the ozone region, is referred to as the "ozone unit".

4. EQUIPMENT AND UNITS IN MORE DETAIL

(a) Filters

In designing the equipment, it was first necessary to consider which filters were to be used. As mentioned above, it was decided that the ozone region radiation to be measured should be within the upper wavelength half of the Hartley Band between 2500 and 3000 A. In addition, a monitor unit would be sensitive to some band above 3600 A. There is some difficulty in deciding how wide a band to use with the ozone sensor. Because of the considerations of section 3(b) above and because the ozone absorption coefficients can vary markedly over even a small wavelength range (e.g. by a factor of 5 from 3200 to 3300 A), the radiation band transmitted to the ozone sensor should perhaps be as narrow as possible. However, a reasonable width is necessary to transmit sufficient intensity. In fact, the characteristics of the available filters at present resolve the question in favour of a rather too-wide band.

An investigation was made to determine what filters were

available and the following are some of the possibilities considered.

(1) Glass Filters. Information was obtained concerning glass filters, supplied by a number of manufacturers. These prepared by Chance-Pilkington Optical Works cover a wide and useful range, and include the filters used by the Meteorological Office in their ozone experiment in Skylark. A selection of these glass filters was obtained and it was the early intention to use them for both ozone and monitor units. The first units built (Type 1) were designed to take these glasses which are 1 mm. in thickness. However, although a combination of such filters is quite suitable for the monitoring function (and is, in fact, retained in the latest (Type III) unit); the filters extending into the ultraviolet were too wide and other types offered better possibilities. The Chance filter, Type OX7, for instance, transmits the whole of the 2500-3000 Å region and was initially considered for use in the ozone unit. However, the transmission curve for this glass also extends a good deal further on the high wavelength side (up to 3800 A).

(2) Interference Filters. One filter of this type (centered at 2500 A) was early obtained for possible use in laboratory calibration. It was finally decided however, that interference filters were needed in the actual flight units as well in order to obtain a reasonably narrow band in the ultraviolet. Six such filters were obtained from Barr and Stroud Ltd., two each with peak wavelengths at 2500 A, 2700 A and 2900 A. These are one inch in

diameter and the interfering surface is located between two filter glasses giving an overall thickness of 0.15". Subsequent calibration (Part C) proved these filters satisfactory for the experiment, and together with the photocell they determine the basic design of the latest (Type III) unit.

(3) Metal on Glass Films. A number of "spectrosil" silica plates (1" x 1" x 2 mm) were obtained for use in the optical experiments. The possibility of depositing thin layers of metal films on such transparent plates to form suitable filters was investigated. Various degrees of transmission can be obtained by varying the thickness of the coating of a metal such as silver or aluminium. Chemical methods of depositing silver are outlined in Reference 110. In the present experiments, however, films were made by evaporating silver on to the microslides. Two such films were prepared and their filter characteristics determined, as summarised in Part C. As seen from these results, about 50% transmission at 3250 A as a central wavelength resulted. However, such films were considered unsuitable for use in rocket-borne equipment. They are easily scratched and damaged and require careful preparation. Indeed the films prepared were found to be already tarnished after completing the spectrophotometer calibration.

(4) Other Special Materials. The possibility of chemically preparing other special materials was also briefly considered. Dunkleman gives curves of optical density for several materials which

have useful transmission bands in the ultraviolet. (Fig. 2 of 97.) A 2 mm. thick crystal of KCl: KBr doped with 0.05% of lead is reported to have an absorption band about 400 A wide with a peak at 2600 A. A 6 mm. thick crystal of nickel sulphate - nexahydrate has a very wide absorption region from below 2000 A to 3600 A, besides a second at higher wavelengths. A third interesting material referred to is Cation X (94). Enquiries revealed that these special materials were not commercially available, and no information could be obtained locally on possible methods of preparation. Just as a matter of interest the transmission of a Nickel sulphate solution contained in a silicon cell was measured (Figure 19).

(b) The 92 AV Photocell

The experiment consisting basically of a radiation intensity measurement, the photosensitive device used is the essential component of the equipment. As the ozone radiation of interest is in the ultraviolet, it is very desirable that the photocell used be directly sensitive to these wavelengths. At the time of the design of the present equipment however, such an ultraviolet sensitive cell was not available. In its place, the 92AV vacuum photocell has been used. This has a caesium-antimony cathode which is particularly sensitive to daylight and to bluish light. However, its sensitivity falls to zero below 3000 A, so its use in the present application necessitates the inclusion of a phosphor.

The latter is sensitive to ultraviolet and re-radiates energy in a region in which the photocell does respond.

The 92AV has a projected cathode area of 2.1 sq. cms. and its sensitivity (as defined above) is 45 μA/lumen. Its peak spectral response is at 4070 A, and this falls again to zero at 7000 A on the high wavelength side.

(c) Sodium Salycylate Phosphor

The primary detector of ultraviolet radiation used in this experiment is the phosphor sodium salycylate. The incident radiation excites the salycylate to fluorescence, re-radiating energy at wavelengths centred on 4300 A (89).

Such a use for a fluorescent substance was first suggested by J. and J.F. Thovert (91), and sodium salycylate was studied by Chevallier and Duboulez (85). The latter's results indicate that the composition of the fluorescent radiation remains independent over a considerable spectral range of the exciting radiation; also that the intensities of the two radiations vary closely in the same ratio. Assuming that the incident radiation is entirely absorbed by the phosphor, Dejardin and Schwegler (86) consider the variations of the salycylate yield as a function of wavelength and conclude that a linear law is valid from 2200 to 3400 A.

Subsequent measurements by later investigators suggest that the quantum sensitivity may well be uniform over quite a large wavelength region. The threshold for exciting radiation is

set at about 3400 A. F.S. Johnson et al (88) found the sensitivity to be nearly constant from 900 to 2300 A. Watanabe and Inn (92) measured the efficiency from 850 to 3000 A confirming that the curve was flat; and also at 584 A where the efficiency is down by about 15%. They also demonstrated the proportionality between fluorescence and intensity of exciting radiation over a range of a factor of 50. The characteristics of the coating were found to remain stable for months. Hammann (87) confirms the independence of the emission spectrum and finds the yield constant within about 3%. E. Krokowski (89) has made efficiency measurements in the X-ray region.

Over the relatively small wavelength ranges used in the present ozone experiment, it seems quite justified therefore to take the fluorescent intensity as directly proportional to the incident ultraviolet intensity; and to suppose that a given salycylate coating will maintain this proportionality throughout the flight.

Preparation of Phosphor Coatings. In the final units, the phosphor layer is applied to the back of the filters used. This requires a coating of less than a square inch and other coatings used for various calibrations have also been of about this size. The following technique has been used to prepare these phosphor layers. The salycylate is dissolved in methanol to give a saturated solution at room temperatures. The solution is then sprayed onto

the filter or silica glass surface from a distance of about two feet. The spray is very fine and only a small amount is deposited on the surface at a time. During the operation a jet of warm air is also directed continuously against the surface from a drier below. The fine droplets from the spray are in this way evaporated almost at once, to leave the small quantity of salycylate in solid form on the filter. Allowing the surface to dry thoroughly between each application from the spray the process is continued until a uniform layer of suitable thickness is built up.

(d) Monitor and Aspect Unit

Reference has already been made above to the concept of a "monitor unit", the purpose of which is to enable corrections to be made to final results because of intensity variations due to factors other than the ozone absorption. It was also mentioned earlier that accurate information on the aspect of the rocket during flight was required. An original proposal was to combine both the monitoring function and the aspect measurements in the one unit. Mainly because of geometrical limitations to the photocell used, this method cannot at present give the quite accurate aspect information needed; instead, aspect information is derived independently from a photo-transistor in a separate unit.

(i) The first possibility considered for use as an aspect device was a V-shaped slit to direct the incident radiation onto the photocell. The photocell would in general then be illuminated twice

as the rocket rolled through a complete revolution; once for each time each arm of the V-slit was in line with the sun. If the rocket were then instrumented to telemeter roll rate, the time between the two peaks of photocell output would provide a measure of the particular width of the V traversed and hence of the aspect. (A rapid telemetry sampling rate would be necessary to locate these peaks accurately, especially in the event of high roll rate.) Calculations were made to indicate the expected relative outputs from such a device for various roll angles and different zenith angles.

(ii) The combined monitor-aspect units which were finally built use instead just two narrow rectangular slits. These are set vertically above the photocell sensitive area which is thus illuminated only once per roll revolution. Information on the aspect of the rocket would, by this method, have been obtained by the use of two such units together. These would be mounted end to end along the direction of the rocket's longitudinal axis, and their construction and characteristics would be as far as possible identical, except for the position of the upper slit relative to the inner or lower one. On one unit the upper slit is displaced slightly forward and in the other slightly backwards. The output from each is telemetered and the difference is a function of the geometry of the slit system and the direction of illumination, or aspect. Pre-flight calibration determines the ratio of outputs

as a function of aspect. Theoretical estimates were made of the ratio of outputs for given geometry of slits. This was followed by numerous calibrations of actual assembled units, with various modifications to the design and in conjunction with both germanium and silicon transistor amplifiers.

The method provides aspect information for both positive and negative values of aspect angle. That is, the sun may be in either the forward or backward direction relative to the rocket, or for both ascent and descent along an ideal rocket trajectory. Measurements at the peak response give the required aspect information irrespective of rocket yaw motion.

However, the actual calibrations show a rather severe limitation to the magnitude of the value which the aspect angle can assume and still be measured accurately. Plotting typical results obtained for amplifier outputs against angle, it is apparent that a unique aspect reading is only really possible within a solar direction of $\pm 15^{\circ}$ from the normal to the unit (supposed set into the rocket skin). If this direction is steadily increased from within this range, some indication of angle might be possible up to 30°. This is basically a geometrical limitation set by the photocell construction. The exact effective distance of the photosensitive area from the envelope (and hence from the slits) cannot be well determined and this makes a more accurately engineered slit system not worthwhile. Also the photocell cathode

being set at an appreciable distance below the envelope precludes the possibility of using the method for large zenith angles.

(e) The Units

In this section an outline is given of the design and construction of those units which were finally built and which were used in calibrations in preparation for the ozone experiment. Three main types are involved and the progress from one to the next has been determined mainly by ideas on what filters would be used, together with the above change in philosophy concerning the use of a combined monitor-aspect unit. All were built with their development finally into flight models in mind, and this has also affected design changes, especially in trying to make the final unit as compact as possible.

Type I This is the combined monitor-aspect unit considered in the preceding section. During the course of calibrations, several modifications to the original design have been made, especially in slit dimension and geometry. Figure 12 illustrates the construction of these units and gives the final slit sizes used. The unit consists essentially of a box with a lid. The photocell is contained in the box, while the lid includes the slit system.

The photocell is held in a B7G valve base mounted on the cross piece of an H-shaped bracket. The valve base is so oriented that the photocell sensitive area faces upwards towards the lid of the box. In a final flight version, it was envisaged that bracket

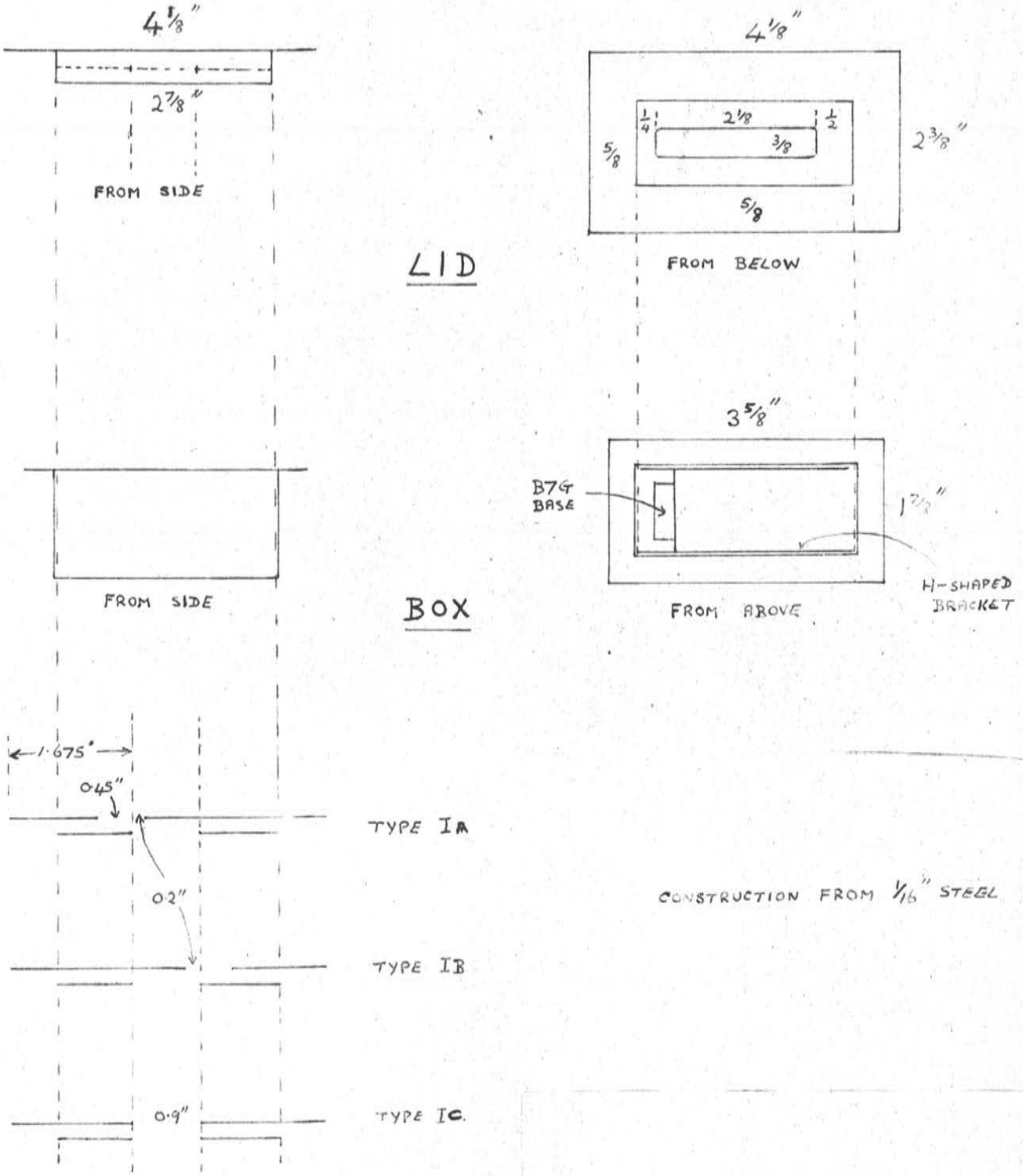

FIGURE I2. Type I Unit.

and photocell could be held securely in position by potting the lower part of the assembly into place. During the calibrations this has been achieved simply by packing with sponge rubber and by securing the lid which presses firmly down on to the top of the bracket.

Below the top surface of the lid there are two other parallel and accurately spaced surfaces, the whole built together as shown into the one lid unit. Except for the forward (in flight) end of the lower part (or the right hand side as drawn), the sides of these are all enclosed to form, in effect, two other shallow boxes. The two slits are cut into the upper two of these three faces. The position of the top slit is varied for the aspect units while the lower one retains the same position relative to the photocell and the rest of the unit. The lowest face has a larger rectangular section cut out as shown, just leaving a ledge around the sides. Above this, that is into the lower compartment, the glass filters are fitted, sliding in horizontally from the open forward end. The depth of this section allows for two Chance glass filters to be used in combination. The filters are secured into position by bakelite strips during calibration and in the proposed final version by a thin coating of araldite around the edges.

The very first proposal for flight equipment was that three such units as these should be used, mounted end to end in

the direction of the rocket longitudinal axis. Two, with slit systems, would be used (as above) as monitor-aspect units. Chance filters OX1 and OX10 would be included in these. The third unit (Type 1C) would have an upper slit the same as the lower and directly above it. With an OX7 filter (coated with salycylate) this would comprise the ozone unit.

Type II Figure 13 shows the second type of ozone unit built. As with Type I, this provides for the use of rectangular glass filters, but is otherwise quite different. The photocell is made more secure for flight and its position is better defined by mounting it in a cylindrical hole drilled in a solid block of cast aluminium alloy. A grommett at the top and a piece of rubber sheet are used to hold the photocell firmly into place. In addition, a piece of perspex is secured to the end of the unit and overlaps the valve base used so further preventing any movement.

The cylindrical hole is drilled from one end. From the top face a rectangular hole is cut to a depth of 5/16". The inner section of this is continued as shown to meet the cylindrical hole. Glass filters are fitted into the upper part of the rectangular aperture, held in place by the ledge below and above by a plate which is screwed into the top face of the unit.

Fitted with the appropriate filters, units of this type have been set up and calibrated as monitor units. An attempt was also made to use the unit for aspect measurements as in Type I, by

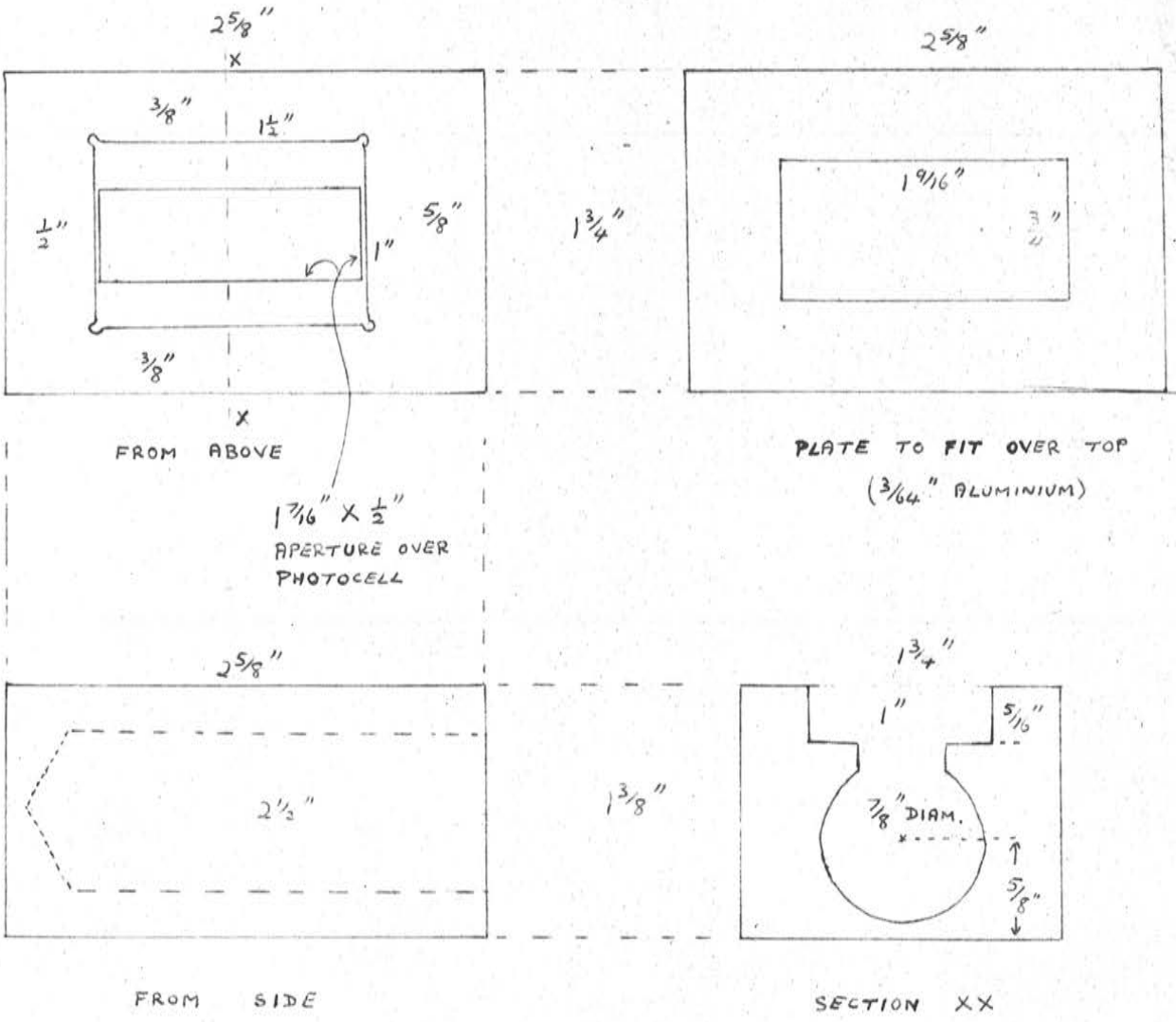

CONSTRUCTION FROM
BLOCK
$2\frac{5}{8}" \times 1\frac{3}{4}" \times 1\frac{3}{8}"$
OF LM8 CAST ALUMINIUM
ALLOY, HEAT TREATED.

FIGURE 13. Type II Unit.

including between the filter glasses slits which were cut from metal foil. The method was not very successful however, mainly because of uncertainty as to the exact positions of the slits relative to the photocell. The foil between the ledge and the lower glass especially was liable to distortion during assembly. Besides this, the design does not allow for the changes in slit position in a longitudinal direction which is required of the aspect unit.

Type III The preceding design is here adapted to take the circular interference filters which were finally chosen for use in the ozone units. To make the flight unit compact, the overall dimensions of the aluminium block were reduced considerably (Fig. 14). A further modification is that the top face of the unit is shaped to a radius of curvature of 4.9". This is the radius of the rocket which at the time was supposed most likely for the initial flights. The photocell mounting is similar to that of Type II, but a reduced clearance enables a standard valve base to be secured directly to the side of the block. The filter mounting is here a circular hole of diameter $1\frac{1}{16}$" to accommodate the Barr & Stroud filters. This is drilled in for 0.4" from the face of the unit, and then continued (at a smaller diameter as shown to meet the photocell mounting position.) The 0.4" is provided with a thread to enable the circular ring shown to be screwed down on to the filters. The depth provided allows for the thickness of the filters, of the ring and of thin washers, together with

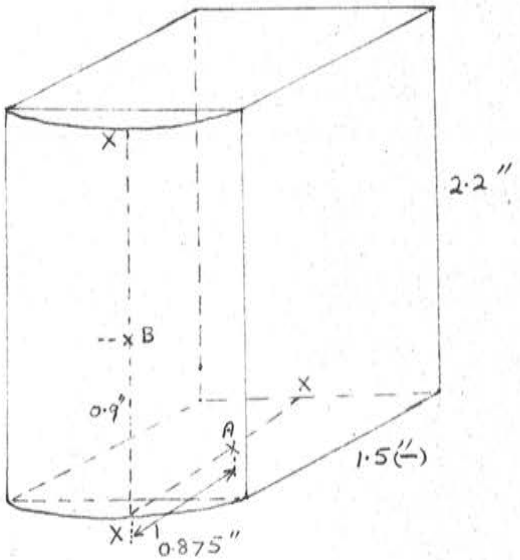

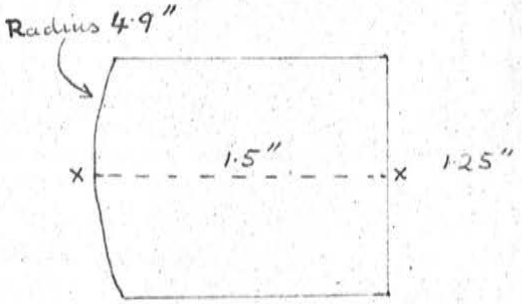

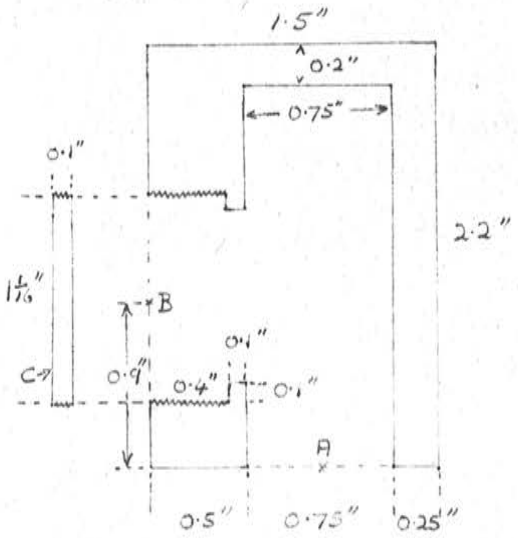

Section XXX

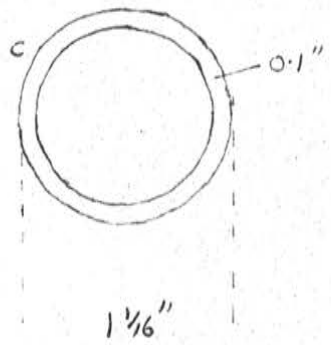

Ring to secure filters

ALUMINIUM LM8 ALLOY

BLOCK – MAX. OVERALL DIMENSIONS
1·5" x 1·25" x 2·2"

FIGURE I4. Type III Unit. (Circular Filter mounting).

a metal foil aperture if required. The ring is provided with slots to enable tightening.

The Ozone Unit and the Simple Monitor Unit Type III is designed purely as an ozone unit, without any thought of incorporating aspect measurements. Now that the latter purpose has also been separated from the monitor units, however, Type III units can also be used as monitors, circular pieces of the appropriate Chance filters being cut to size. The latest proposal, therefore, is for the use of this one type of mounting for both the ozone unit and the monitor unit; with aspect information derived from quite separate equipment.

(f) Associated Amplifiers

The radiation incident on the photocell causes a proportional current to flow through the detector. The current (or resulting voltage) must be amplified before being applied to the telemetry input. Two categories of amplifiers have been used with experimental units.

(1) Simple transistor amplifiers have been used with monitor and monitor-aspect units. Various circuits have been tried with modifications to the values of collector resistor and parallel photocell cathode resistor. The first amplifiers used the germanium 2N1308 transistor. Potted amplifiers were secured to the box of Type I units to form a complete assembly and many calibrations against direct sunlight were made. However,

temperature effect tests proved the germanium transistor amplifiers unsatisfactory for use in rocket flight during the course of which high skin temperatures can be expected. An initial 3 volt output decreased to 0.8 volt with increasing oven temperature to 35°C over a period of 15 minutes.

The units were therefore replaced by similar amplifiers using the OC203 transistor. The output now remained constant with temperature increase to 70°C and with heating continued over a period of 30 minutes. Numerous calibrations were made in conjunction with photocells and the standard light sources. Amplifier characteristics of the unit included in the first round were measured at 25°C and 50°C.

(2) An amplifier with greater gain is needed for the smaller response from the ozone unit. A calculation to find the expected relative responses from ozone and monitor units at the top of the atmosphere indicated a ratio of 1/500 for equal areas illuminated. An electrometer amplifier is used with the ozone unit. This is a modification of a circuit developed by the Physics Department, University College, London. A0-0.25 volt input gives a 0-5 volt output.

5. THE ROCKET

The first flight of the equipment was in a W.R.E. HAD rocket. A performance survey is available giving expected height, range, velocity and trajectory angle for various times during flight, and for Q.E's of 85, 80 and 70°. Firing specifications required a peak altitude range between 100 and 140 Km., together with information to enable determination of the trajectory to within ± 1.5 Km. The roll rate required is between one and 15 revs/sec. The lower limit assures ozone measurements at sufficiently close height intervals.

The design of the Type III unit has been adapted to the casting of the instrument section of the round. The photocells are mounted parallel to the rocket longitudinal axis with base connections potted in silastic. The filters are fitted into apertures in the rocket skin with an angle of 36° between the normals to ozone and monitor units. A cover surrounds this section of the round for the first part of the flight.

Battery power supplies include 45 volts for the photocell, 6 volts for the OC203 transistor amplifier, and -16 and -20 volts for the electrometer amplifier. A calibration unit provides suitable input steps for the calibration of the latter amplifier during flight. Monitor and ozone unit signals, together with those of other experiments and of rocket instrumentation, are sampled by a 24-position, 80 c/sec switch. A W.R.E. type

VLI (Mk III) modulator, operating from 130 to 180 Kc/sec frequency modulates the 465 Mc/sec signal from a W.R.E. Medium Power Oscillator.

As noted before, trajectory and rocket aspect information are essential for the interpretation of experimental results. Wreroc and Wreciss cameras were mounted in the round to provide this information. In addition, an Ackaid oscillator tracking system was used. The rocket instrumentation included sun slits which, through the response of a photo-transistor, give aspect information providing the rocket motion is essentially one of spin only. Thermistors monitored temperatures at different points in the round. One, close to the photocell, gives important information for the ozone experiment (cf. section 3(13) of part C).

PART C : CALIBRATIONS AND OTHER MEASUREMENTS

In this part more detailed reference is made to various measurements on the equipment components already mentioned in part B.

1. EQUIPMENT FOR USE IN CALIBRATION

The instruments which have been assembled and prepared for use in the pre-flight calibration of units for the ozone experiment are listed here. Spectrophotometers used are noted separately in the subsequent section on filter calibration.

(a) The Optical Bench

An optical bench has been constructed from a previous lathe bed. The overall length is 4'7" and the parallel sides are 5" apart to their outer edges. The levelling screws (two at one end, one at the other) have been fixed to metal plates welded underneath the original structure. Stands have also been made to hold the various pieces of equipment in place on the bench. These are based on rectangular metal blocks (3" x $5^{5}/16$") which fit over the parallel edges. A vertical cylindrical section of the stand is provided with a screw by which the lamps and other equipment are secured into place at the appropriate height. Filters, ozone units and other components can be held on the bench by means of small clamps forming an integral part of a rod which also fits into the stand assembly. The stands are tightened into place by means of a

screw and plate underneath the bench itself.

(b) Hilger-Watts Monochromator

This has a calibrated range extending from the infra-red down to 2000 A. It has been used in measurements of the source spectra, of phosphor and filter characteristics, and, in the early stages of the work, for the actual filter calibrations as well. It is used in conjunction with other equipment set up on the optical bench, the monochromator itself being lined up at the left-hand end of the bench. The entrance and exit slits give jaw spacing widths from 0.002 mm. to 2 mm. There is also provision for varying the effective height of the input aperture.

(c) Photomultiplier

The detector used to record the monochromator output, and similar low intensity radiation in other measurements is a photomultiplier. The E.M.I. phototube 6097B is used, and this, together with the associated resistor chain to supply the necessary voltages for the different stages, is built into a cylindrical unit with a cover 2.3" in diameter. An aluminium cap which fits over the phototube itself brings the overall length of the unit to 9". A circular hole was cut into the top of this cap to allow the mounting of glasses and filters in the early experiments; in later measurements this arrangement has usually been retained, using the $1\frac{1}{2}$" diameter hole as the input aperture to the photomultiplier. There are two leads provided at the back of the unit - onethe output,

the other the E.H.T. supply.

The front end of this aluminium photomultiplier unit is mounted into a black box for use with the monochromator. The box is secured to the monochromator by bolting it to an attachment provided at the exit slit. Pieces of felt prevent stray light reaching the photomultiplier, either through the junction with the slit assembly or at the point where the cylindrical cover enters the box. The lid of the box is fitted with a control by means of which a clamp can swing a filter or other glass into and out of the light path immediately in front of the photomultiplier.

The 6097B is an 11-stage photomultiplier of the Venetian blind type (Ref. 99). It has a caesium-antimony cathode with a spectral response similar to that for the 92AV photocell. Hence, it is not directly responsive to ultraviolet radiation below 3000 A. Its quoted sensitivity is 30 to 50 μA per lumen; and its cathode diameter (adjacent to the front envelope) is 44 mm. in diameter.

1100 or 1200 volts have been applied to the photomultiplier. This has been provided from a Model 412A Fluke, High Voltage D.C. Supply unit. The output is measured on a Hewlett-Packard microammeter.

(d) Sources of Ultraviolet Radiation

Three lamps have been used as sources of ultraviolet radiation. In the earlier work, usual mercury lamp sources were

used; one a high-pressure, the other a low-pressure discharge lamp. The main UV source now used is a mercury-zinc-cadmium lamp made by Philips (Type 93146E). Providing the radiation spectra of all three of these elements, this gives a more intense source extending much further towards lower wavelengths. Its relative intensity spectrum has been determined and is shown in Figure 22. Covers for all these lamps have been made for their convenient use on the optical bench.

(e) The Standard Tungsten Lamp

Several tungsten filament lamps were obtained, and one of these was calibrated as a sub-standard (Ref. 109). The type used are "Osram" 12 volt, 24 watt single axial filament lamps; and calibration was against a similar standard kept by the S.A. Institute of Technology. A photocell was used as the detector and its current measured when irradiation was first from the lamp, then from the standard. The lamps are set up with the filament in a horizontal position, and are allowed to operate for five minutes before taking an intensity reading. The current in each instance was adjusted to 1.70 amps. At this current (corresponding to a colour temperature of about 2600°K), the irradiance of the standard lamp (identification No. PT 13200) is $1.156. 10^{-4}$ Watts/cm^2 at a distance of one metre.

The calibration gives an intensity for the sub-standards of $1.425. 10^{-4}$ Watts/cm^2 (at one metre).

2. FILTER CALIBRATIONS

The filters which have been considered and selected for use in the project are noted in section (4) of part B. The Schimadzu spectrophotometer was used in early calibrations of the first filters available. One interesting effect noted in the calibration of the Chance glass OX1 with this instrument was that the curve obtained depended to some extent on the speed at which the radiation wavelength was scanned. This effect has not been noticed on other calibrations and has not been investigated further. However, if it is really due to the glass characteristics themselves, it could be important in rocket flight conditions where the illumination period is dependent on roll rate.

Other calibrations have been made on the Optica spectrophotometer. Scan speeds of 4, 8 and 16 A per second are available and most responses have been measured at the fastest of these speeds. In all cases, the corresponding hydrogen or tungsten lamp spectrum has also been recorded at the same time, without the filter but with the same instrument settings. Chart deflections have then been corrected in terms of these to give actual filter transmission.

Of the numerous calibrations recorded, the following examples are illustrated here. Figure 15 shows the transmission of the combination of glass filters OX1 and OY10 intended for the monitor unit. The curve for an OX7 filter which in the early

stages was considered for the ozone unit is given in Figure 16. The 2700 A interference filter calibrations are shown in Figure 17; while Figures 18 and 19 show the characteristics of one of the silver films prepared, and of a solution of nickel sulphate.

3. MEASUREMENTS OF CHARACTERISTICS OF THE UNITS, AND OF THEIR COMPONENTS

Included in the following are several series of measurements of various characteristics of the components of the proposed flight equipment. The units used are referred to in terms of the following nomenclature:

TABLE 4

Units Assembled

Type	Unit	Components and comments
I	A	Symmetrical slit system (IA). Originally planned for ozone unit (Part B - section 4).
	B	Monitor-aspect units
	C	0X1 + 0Y10 filters. 0C203 transistor amplifiers.
II	H	0X1 + 0Y10 filters. Calibrated as monitor unit
	J	-----
III	D	U703 (2900 A) filter.
	E	U701 (2700 A) filter. Proposed for first flight ozone unit.
	F	U753 (2500 A) filter. Subjected to accel.^{n}, vibration tests.
	G	Fitted with circular monitor filters, 0X1 + 0Y10. Proposed for first flight monitor unit
	K	-----

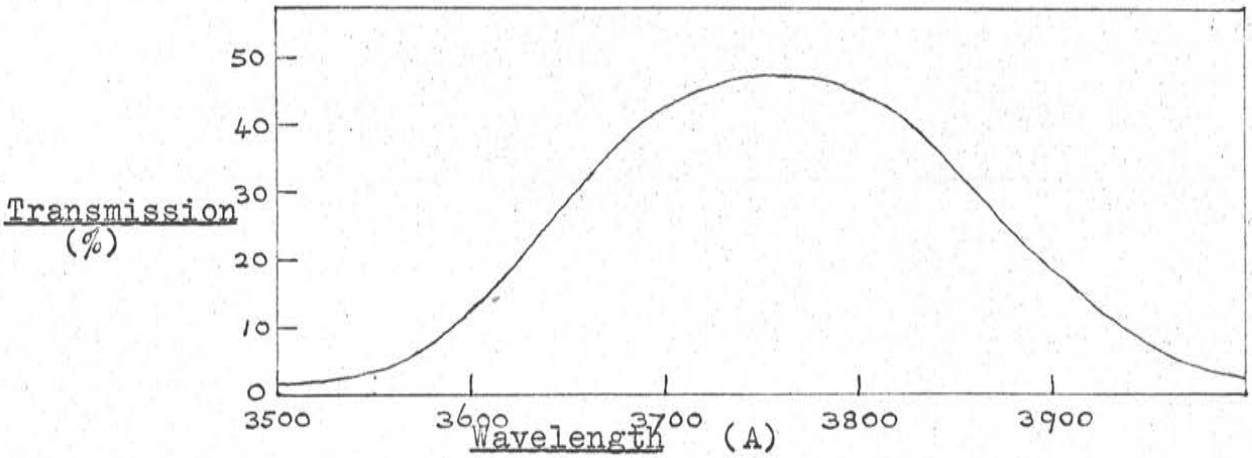

FIGURE I5. Calibration of combination of filters 0XI and 0YI0.

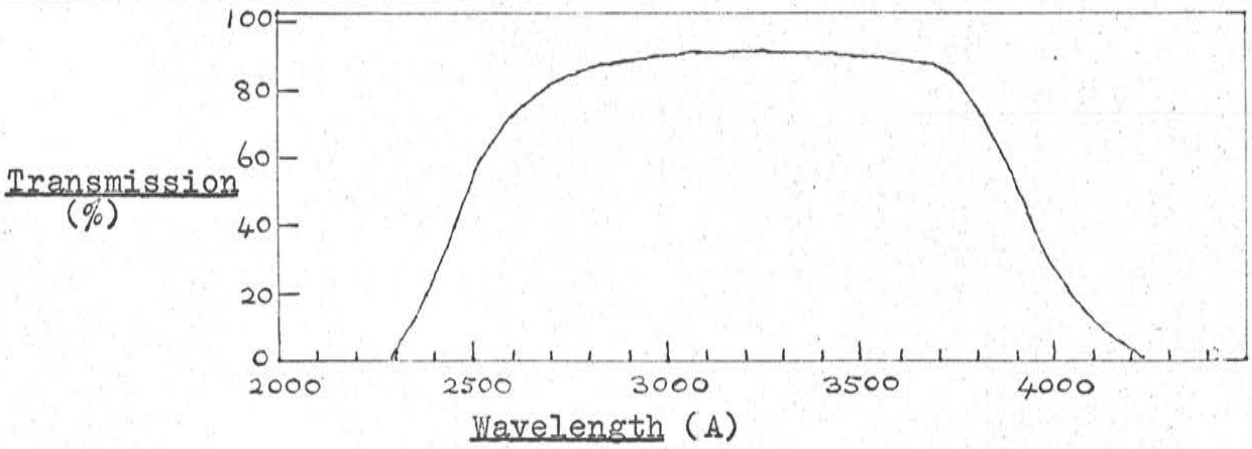

FIGURE I6. Calibration of filter 0X7.

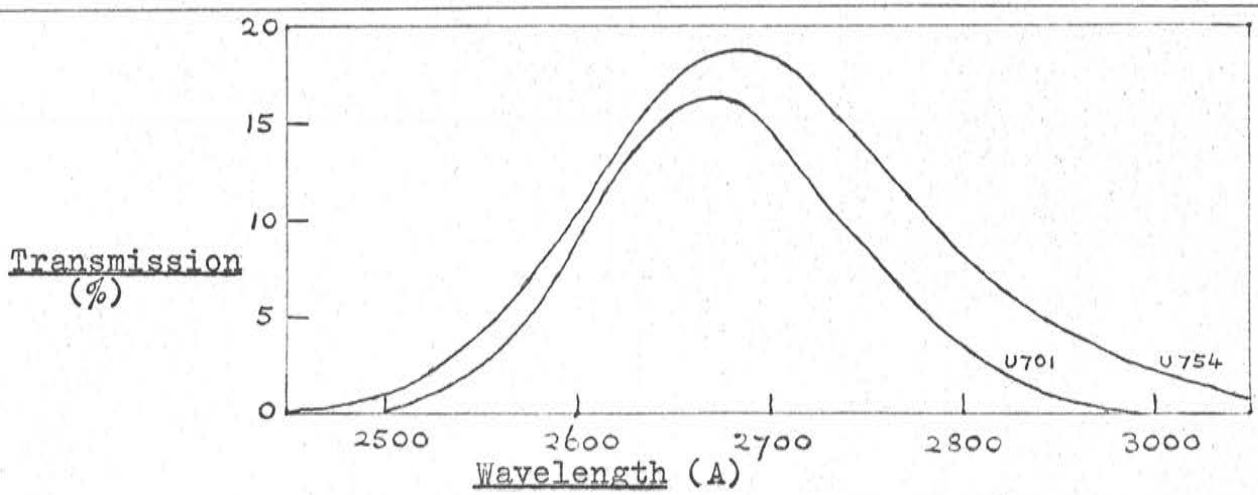

FIGURE I7. Calibration of 2700A interference filters U70I and U754.

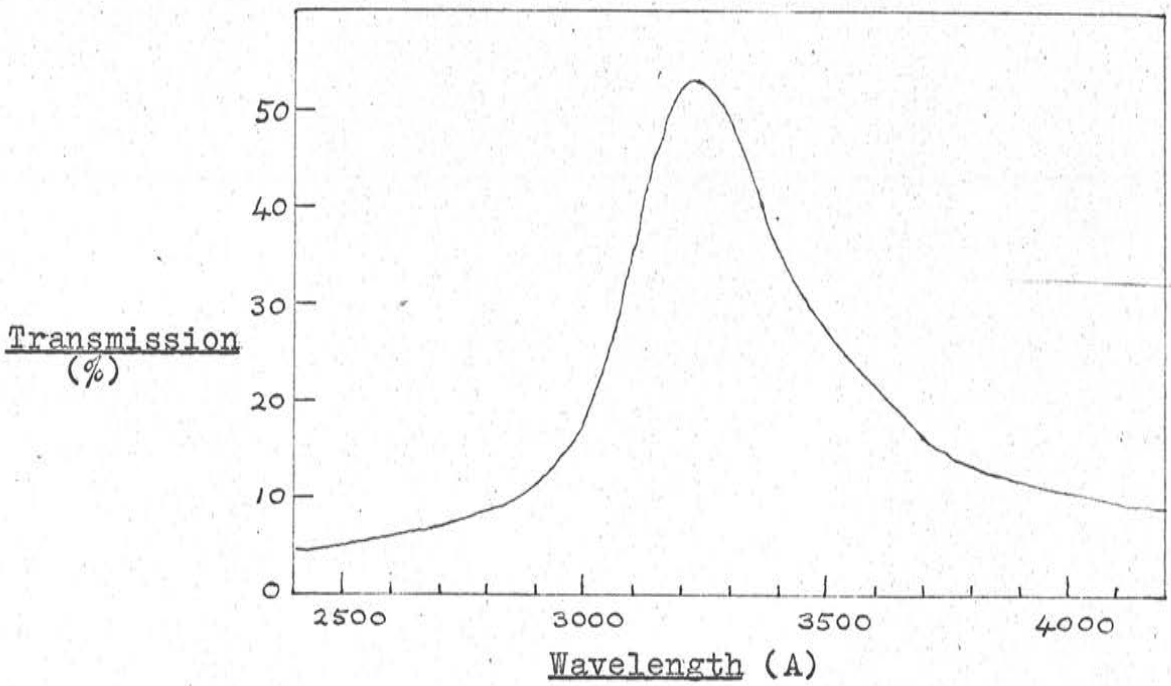

FIGURE I8. Silver Coating "A" Transmission.

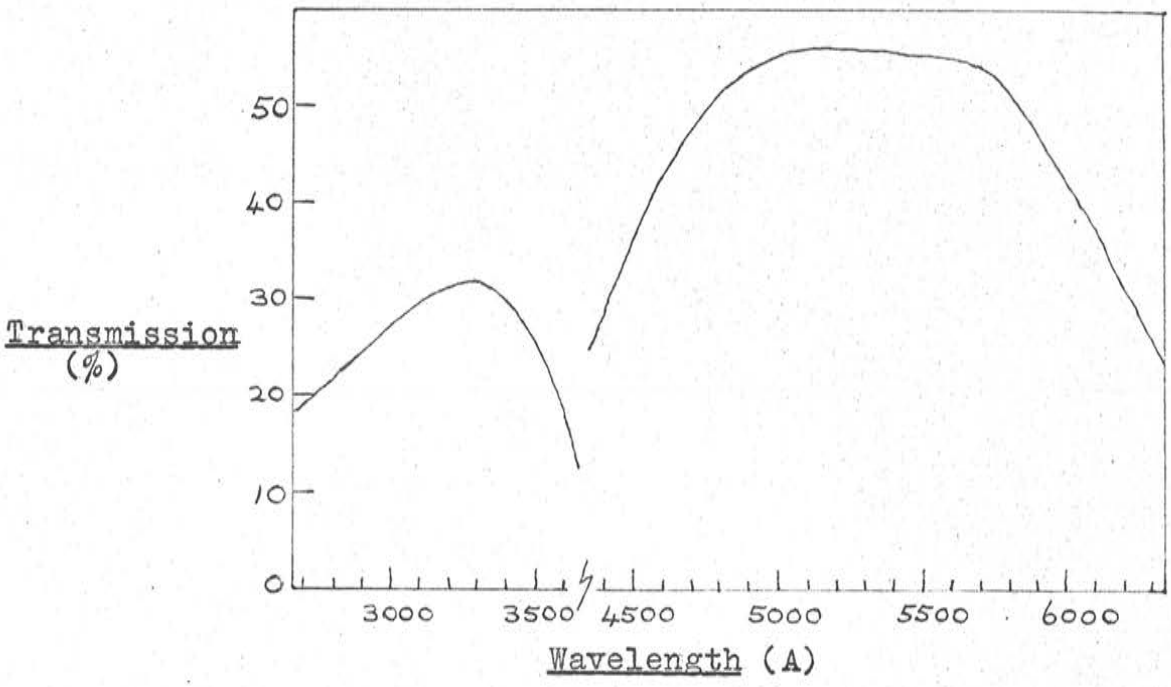

FIGURE I9. Nickel-sulphate Solution Transmission.

(1) Calibration of Photocell against Standard Tungsten Lamp

Calibrations of several photocells have been made to determine the currents produced by illumination from the standard tungsten filament lamp. In some cases, the output voltage of the amplifier for the corresponding unit was recorded at the same time. As an illustration, one of the earlier calibrations was that of the detector intended for use in unit A. The lamp was set up at measured distances between its filament and the photocathode, and the resulting current noted. The incident energy is found from the lamp distance and its known intensity at 100 cms. (cf. section 1). The slope of the resulting nearly straight line graph is 4.3 microamps for 3.10^{-3} watts per square cm. of total incident energy - or for $6.2\ 10^{-3}$ watts over the whole photocathode projected area. Using the tables of Lowan and Blanch (106) for the quoted lamp colour temperature of 2600°K, the fraction of the total energy in the 3000-7000°K range is .042, and in the 3000-6000°K range is .017. Therefore if the 92AV photocell is considered sensitive up to 6000°K, its sensitivity from the present measurement is 59 μA/lumen. For radiation up to 7000°K, it is 24 μA/lumen. (The quoted figure in the photocell specification is 45 μA/lumen.)

Other 92AV photocells give similar results. The sensitivity is maintained as the lamp is brought very close to the photocell, and as the current is so increased well beyond its recommended maximum value of 25 m μA/mm^2.

(2) Photocell Response with Time

A series of measurements was made over a period of several days to check whether there was any variation with time in the photocell response to given incident radiation. The current was again measured for various distances from standard lamp filament to photocathode. The distance was increased until the current fell to a low value, then several readings were repeated as the lamp was again brought near the photocell.

The results (Figure 20) indicate that there is little significant change in response so long as the photocell current is kept below its maximum recommended value of about 5μ A. For higher currents there is perhaps more scatter but this is on the steep part of the curve where the accurate measurement of distance becomes critical.

(3) Effect of Thickness of Salycylate Coating

Figure 21 shows measurements to determine the effect on total transmission of varying the thickness of the coating of phosphor applied to a filter. Various coatings of sodium salycylate were here applied to the far surface of a piece of OX7 filter glass illuminated by the Hg-Zn-Cd lamp. The transmitted and re-radiated energy was detected by the photomultiplier, the envelope of which was at 5.2 cms from the phosphor. The results show the photomultiplier current for four different values of applied H.T. and for different thicknesses of phosphor. The first coating used

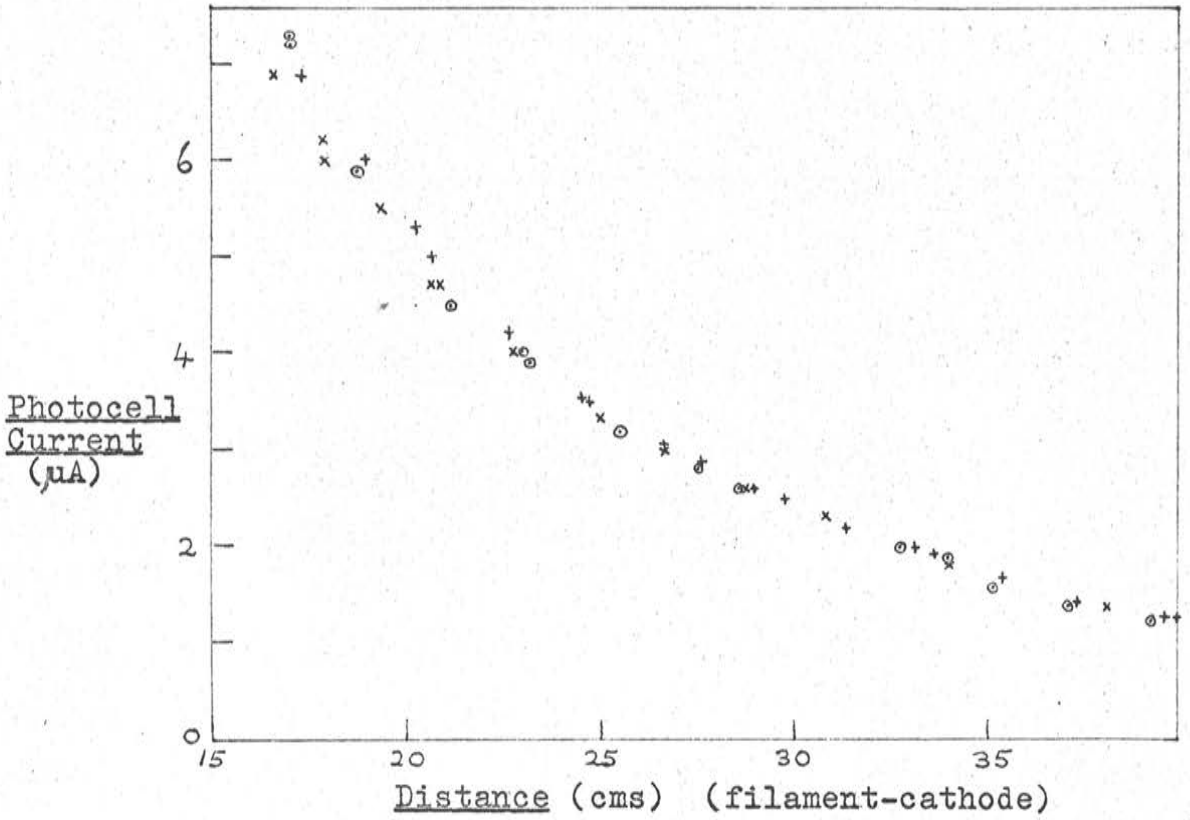

FIGURE 20. Photocell Response with Time.

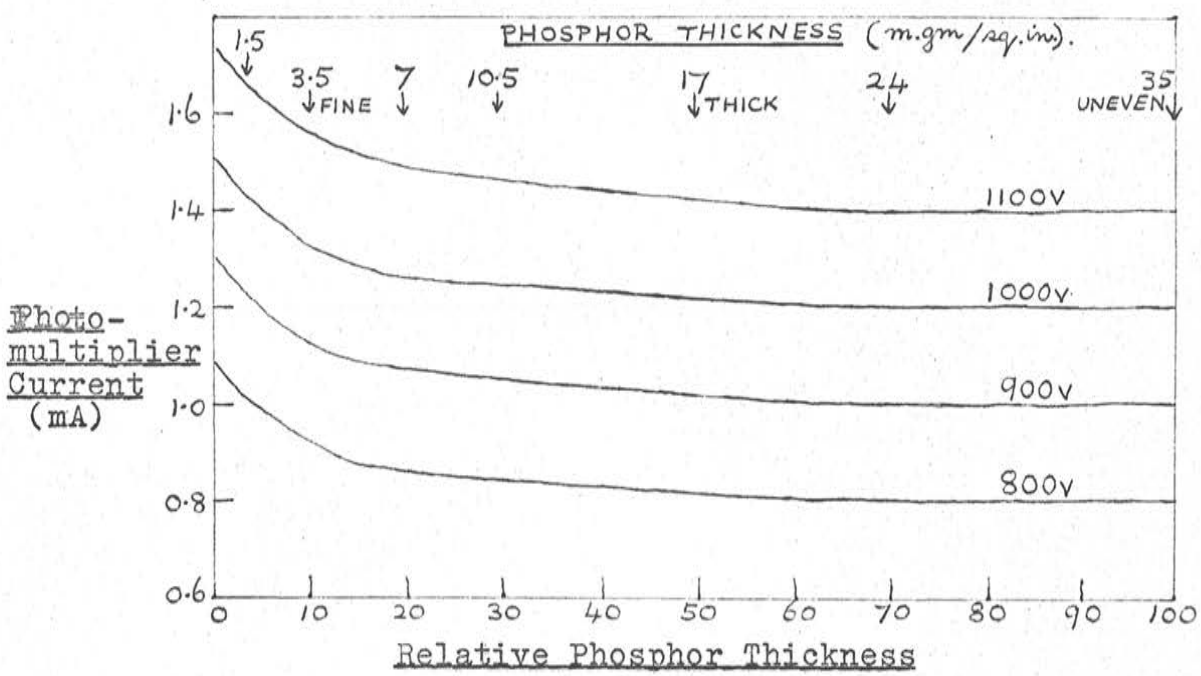

FIGURE 21. Phosphor Thickness.

was almost the finest perceptible; while the final one was far too thick for use, the phosphor being caked on the filter and very uneven. The graphs show that the gradual application of the salycylate at first reduces the total energy transmitted, but that the current finally reaches a steady value, presumably when the decrease in direct transmission is balanced by the increased re-radiation of the phosphor.

In subsequent measurements in which a phosphor coating has been used, the application has generally been such that the thickness aimed for is that designated (arbitrarily) by a value 20 in Figure 21 (about 7 mgm per square inch).

(4) Relative Spectral Distribution of Hg-Zn-Cd Lamp Source

Figure 22 gives the relative intensities of the radiation of the mercury-zinc-cadmium lamp from 2000 to 6600 A.

The lamp radiation was first analysed with the monochromator to the wavelength limit of the photomultiplier sensitivity. The output from the monochromator was detected by the photomultiplier and the resulting current recorded on the microammeter. These readings were corrected to allow for the corresponding photomultiplier spectral response, and then plotted as a measure of lamp intensity.

A second set of measurements was taken from 4500 down to 2000 A, this time with a phosphor coating in front of the photomultiplier envelope. Below about 3000 A, however, this did not

provide a sensitive means of tracing the spectrum. Instead, the intensity scale of a previously recorded trace of the lamp from a McPherson monochromator was adjusted to enable the 2000-3000 A range to be added. This was done by comparing notable peaks in the overlapping 3000-3150 A region.

The relative lamp intensities in 100 A wavelength intervals are listed in the following table.

TABLE 5

Hg-Zn-Cd Lamp Relative Intensities

Wavelength Interval	Energy (arb. units)	Wavelength Interval	Energy (arb. units)
2000-2100	7	4400-4500	6.5
21 -22	14	45 -46	30
22 -23	31	46 -47	87.5
23 -24	38	47 -48	72.5
24 -25	24	48 -49	57.5
25 -26	44	49 -50	6
26 -27	26	5000-5100	163.5
27 -28	14	51 -52	90
28 -29	27	52 -53	10
29 -30	31	53 -54	30
3000-3100	122	54 -55	175
31 -32	139	55 -56	77.5
32 -33	76	56 -57	16.5
33 -34	105.5	57 -58	70
34 -35	75.5	58 -59	45
35 -36	9	59 -60	12.5
36 -37	170.5	6000-6100	15.5
37 -38	8.5	61 -62	17.5
38 -39	3	62 -63	27
39 -40	3	63 -64	65
4000-4100	77	64 -65	100
41 -42	6	65 -66	129
42 -43	5		
43 -44	112		

(5) Response of Ozone Units D and E with Angle of Incident Radiation

Expected trials records will give the rocket altitude and the ozone unit response at given times during the flight. It is necessary, therefore, to have a calibration to provide an aspect correction for the ozone unit signal; that is, to provide some factor (dependent on angle) by which the actual recorded output is multiplied in order to give the equivalent response for normally incident radiation. The decrease in the output from the unit as the rocket motion takes the normal to the filter away from the solar direction is dependent both on filter and photocell characteristics themselves (see later) and also on the geometry of the sensor, especially on the extent to which the filter and photocathode are set below the level of the rocket skin.

Measurements of this effect were made on the completely assembled units D and E. The photocell current was monitored as the sensors as a whole were rotated relative to incident radiation from the Hg-Zn-Cd lamp. Rotation was first about the unit longitudinal axis; then about the transverse axis along the filter diameter. At normal incidence the whole filter area was illuminated. Figure 23 shows the responses relative to that for normally incident radiation for unit E. The curves are fairly symmetrical and much the same for the two axes.

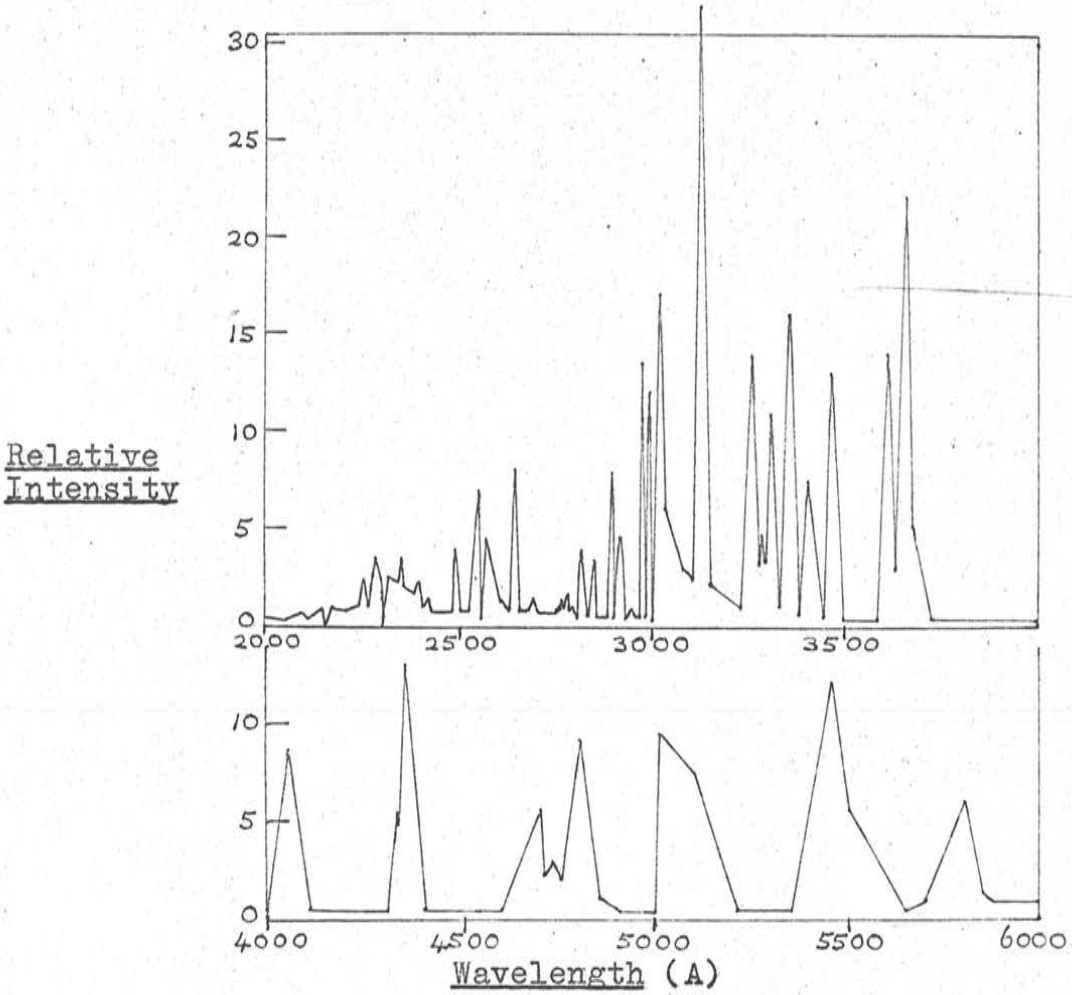

FIGURE 22. Hg-Zn-Cd Lamp Spectrum.

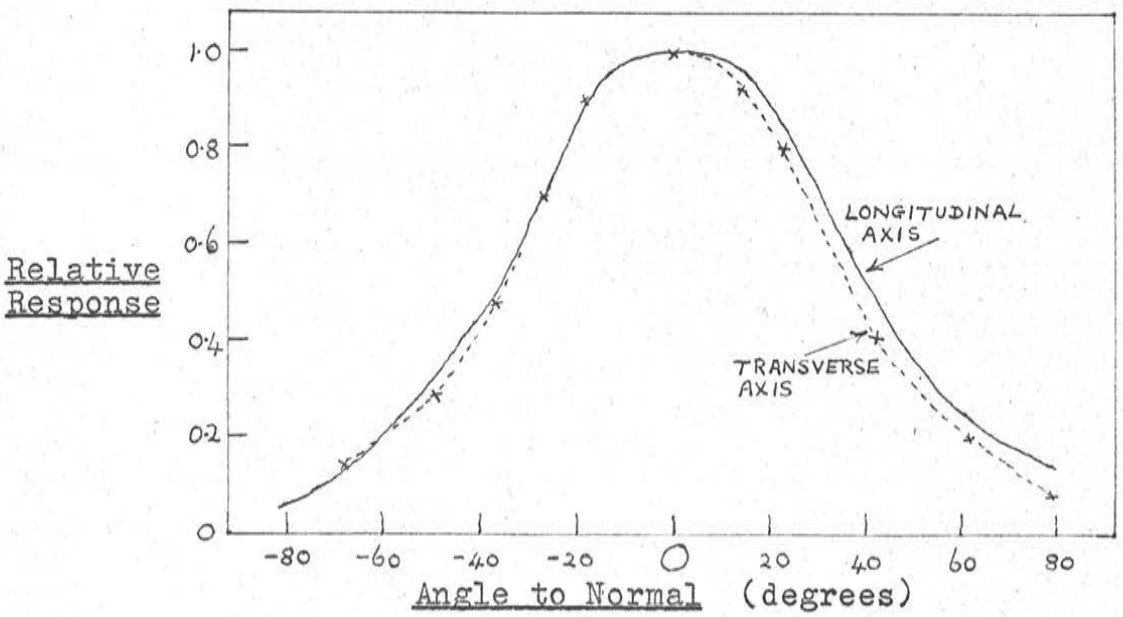

FIGURE 23. Unit E Aspect Correction.

(6) Aperture Effect in Monitor Unit Calibration against Direct Sunlight

Units G and H were fitted with monitor filters and with OC203 transistor amplifiers. The angular response of unit G against direct sunlight at ground level was determined and the amplifier output voltage plotted as a function of the relative solar direction. Various curves were obtained for illumination of the full filter diameter (1") and for the cases of apertures of different diameters. Brass foil, 4/100" thick and with centrally located circular apertures, was fitted between the two glasses of the monitor filter. With a 5/16" diameter aperture, for example, and an actual solar zenith angle of 40°, the amplifier output falls from 5 volts to a minimum of 2.6 volts at a relatively normal solar direction. When fitted with a 7/16" aperture, the output falls to zero at a solar direction of 20°. All curves are symmetrical about the position normal to the unit.

(7) Incident Angle Dependence of Interference Filter Responses

Spectrophotometer calibrations of the interference filters are referred to above. Measurements have also been made to determine any dependence between the relative response for different wavelengths within these bands and the angle of the incident radiation. Such a relation would be important in the accurate analysis of records from a rolling rocket. The filter

to be measured was set up on the optical bench 2.7 cms from a 0.5 cms diameter aperture in front of the Hg-Zn-Cd lamp. The intensity of the radiation which was transmitted in the same direction as the incident beam was measured with the monochromator, the input slit of which was 10.5 cms from the centre of the filter face. The angle θ between the normal to the filter and this lamp-monochromator line was varied in steps up to 60°. The monochromator input and output slits were adjusted to give a suitable photomultiplier output for a complete set of results.

The results are plotted in Figures 24 to 27. The relative intensity is that of the transmitted intensity at the indicated filter angle to that at the same wavelength when the radiation is normal to the filter. For different angles and for the three filters concerned, it is plotted as a function of wavelength in the first three figures. Figure 27 gives the same results as Figure 24 but with curves of a given wavelength plotted against angle. In the case of all these filters, relatively more radiation of lower wavelength and relatively less of higher is transmitted (in the same incident direction) up to filter angles of about 50°. (At 60°, generally less is transmitted for all wavelengths of the band.) The variation is least for the 2700 A filter. As the angle is increased, the maximum relative intensity tends to move towards lower wavelengths.

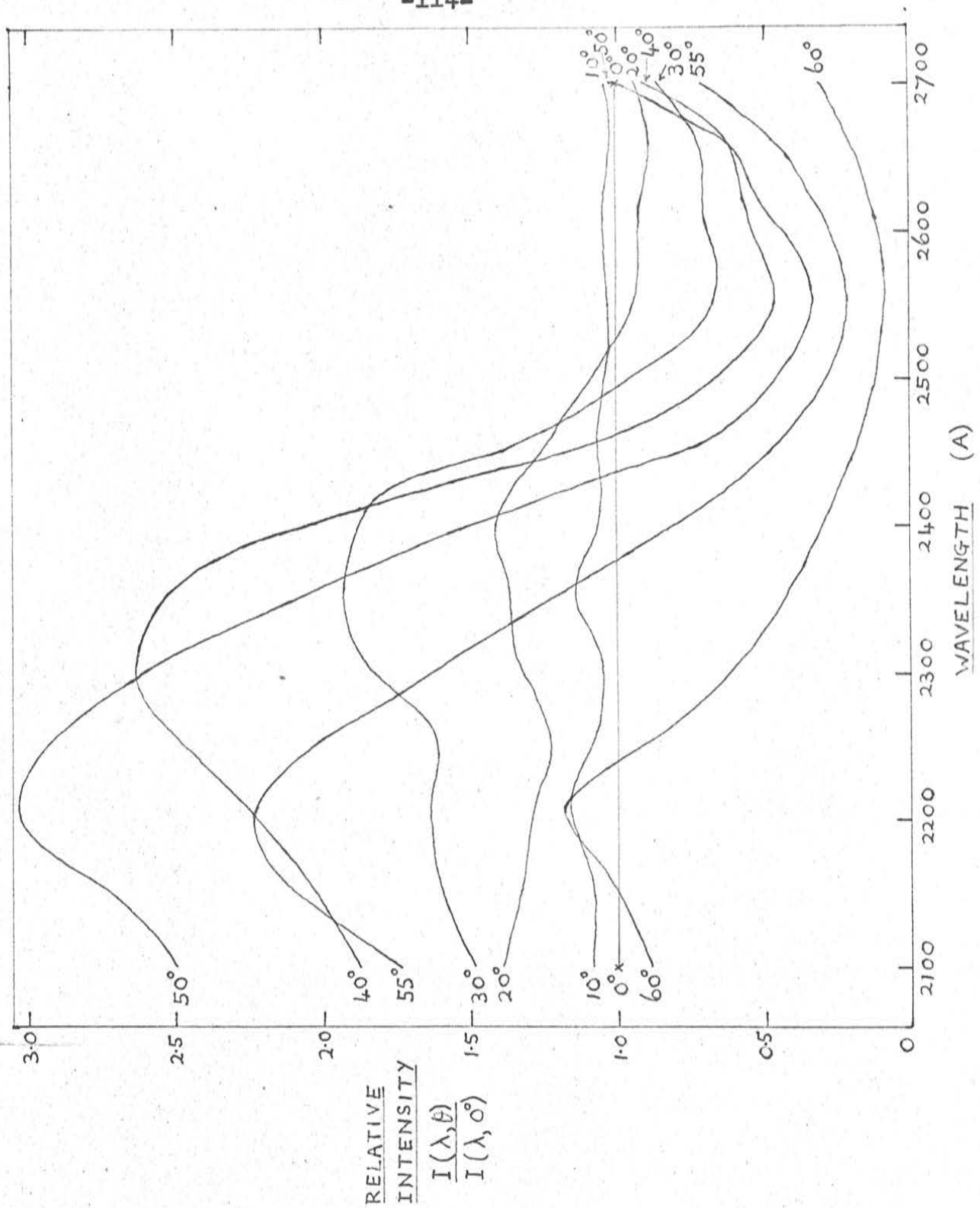

FIGURE 24. Incident Angle dependence - 2500A Filter (I).

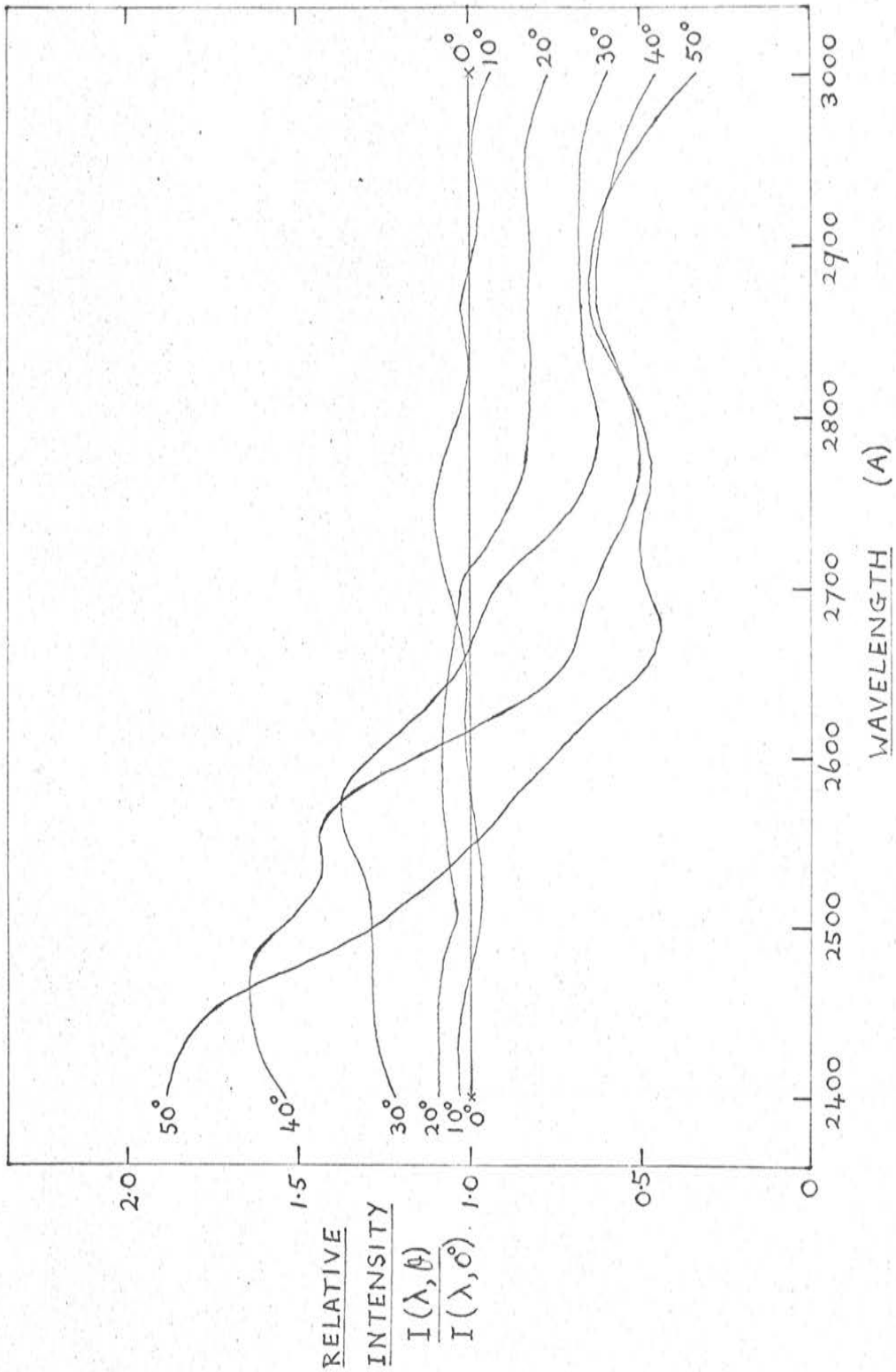

FIGURE 25. Incident Angle dependence - 2700A Filter.

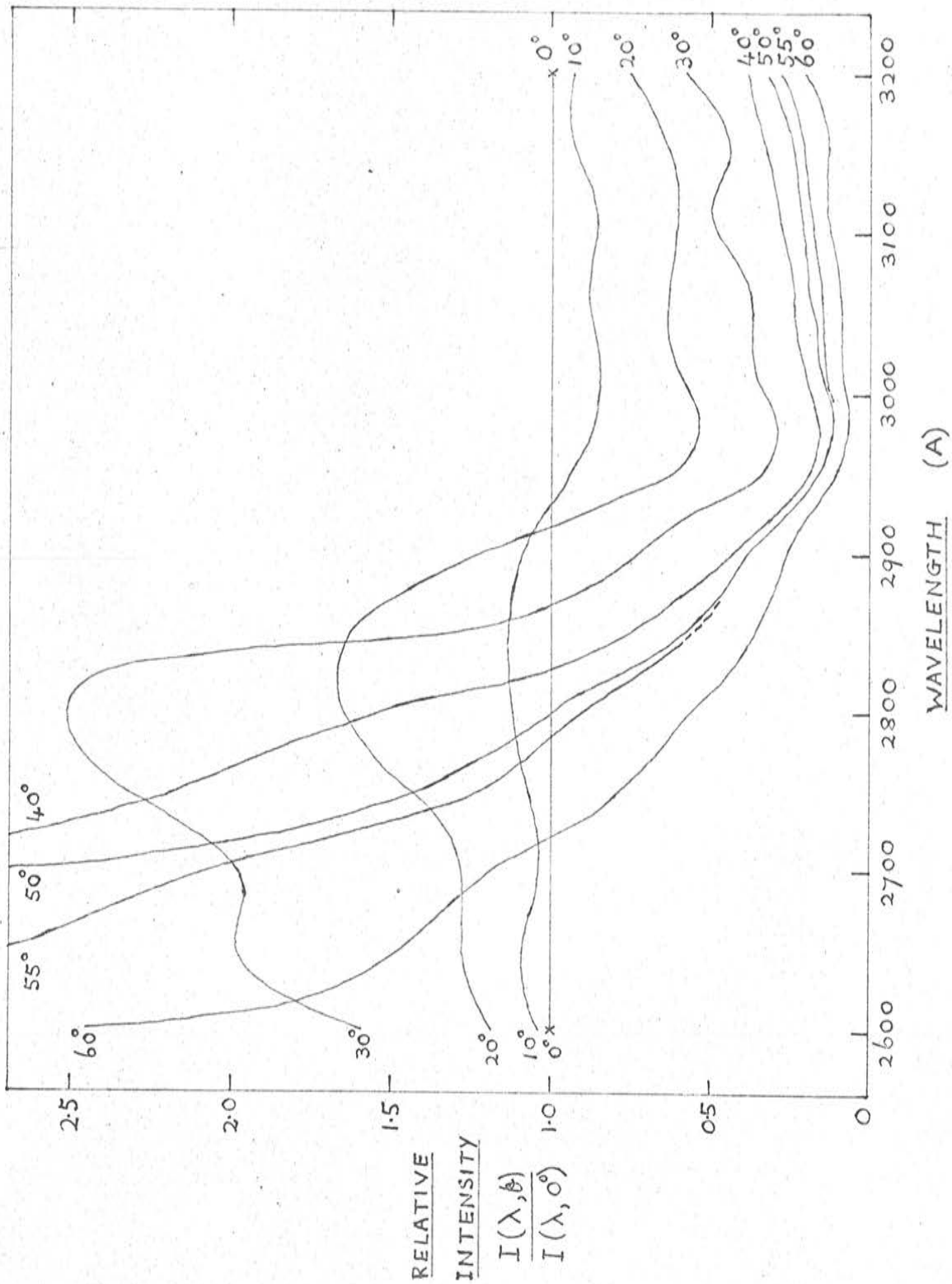

FIGURE 26. Incident Angle dependence - 2900A Filter.

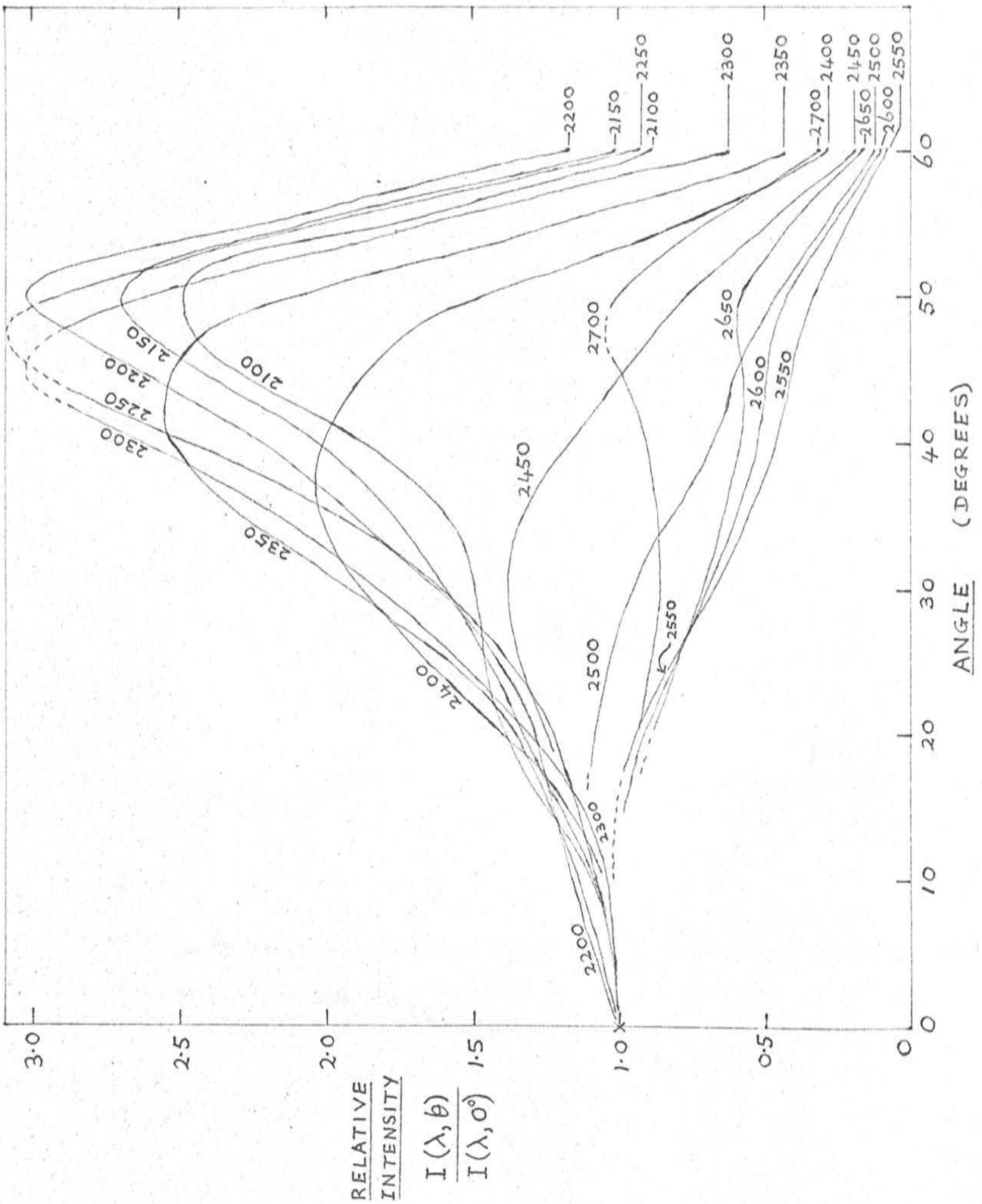

FIGURE 27. Incident Angle dependence - 2500A Filter (2).

(8) Ageing of Salycylate Coating

Measurements have been made to determine any changes in the transmission and re-radiation characteristics of a layer of phosphor over a period of time. A salycylate coating of medium thickness (about one milligram per square centimeter) was applied to a silica glass microslide which was mounted in a cardboard mask. This was set up in a larger screen clamped to the optical bench and irradiated by the Hg-Zn-Cd lamp. Distances from lamp and monochromator were noted. These and other equipment settings were carefully repeated for subsequent measurements on this phosphor.

By traversing the monochromator range from 3000 to 7000 A, the transmitted (and re-radiated) spectrum of the salycylate coating was closely traced in terms of photomultiplier current output. Readings were taken at maxima, minima and stationary points, as well as at closer intervals when necessary. The first such set of readings was taken for the newly prepared coating (actually after 3 hours). Subsequent sets were taken after 1, 4, 8, 25 and 32 days, and given readings normalized with respect to the response at the corresponding wavelength for the fresh coating. Between calibrations, the slide was kept in the dark and away from mechanical disturbance.

The relative intensities (with respect to that of the same wavelength at zero time) were plotted against wavelength for each time. The results were compared with Figure 22 which shows the

relative intensities of the radiation incident upon the salycylate. Up to a period of 8 days from the commencement of the test, the transmitted intensity (which includes any variation in the distribution of the phosphorescence) increases for all wavelengths. This increase with time is also fairly general with still later measurements, although the rate of increase is less. A decrease in relative intensity, however, occurs between about 3250 and 3500 A (8-25 days); and from 4500 to 5000 A (8-25 and 8-32 days). The first of these bands is near the quoted limit of sensitivity (3400 A) and the second within the region of phosphorescence. A notable increase in transmission between 3100 and 3200 A (nearly 2½ times the original after 32 days) is perhaps associated with the very strong incident radiation here.

After one day, transmission is about 1.1 times greater over the whole spectrum; and nearly 1.3 times for lower wavelengths after four days. Thereafter the variation with wavelength is much more pronounced, but a factor of 1.5 is perhaps appropriate for 8 days; 1.6 and 1.75 for 25 and 32 days respectively (up to 4500 A only).

(9) Some Characteristics of a Salycylate coating on an Interference Filter

A phosphor coating similar to that used above was applied to the back of a 2900 A interference filter. A series of spectra was again traced with the photomultiplier to determine angle and incident intensity effects on the phosphor transmission. The

region measured was from 3000 to 5000 A; so, in combination with the 2900 A filter, the response should be largely attributable to the salycylate phosphorescence.

A measurement of angle dependence was first made. The response was traced with filter and phospher normal to the lamp-monochromator beam. This was then repeated, moving the filter at 10° intervals up to 40°, but still monitoring the direct beam. The results are shown in Figure 28, normalised to the response at corresponding wavelengths for 0°.

Figure 29 shows dependence of transmitted radiation (with the filter in normal, 0° position again) upon incident intensity. The response shown is that relative to the value (at a given wavelength) at a distance of 15 cms (reference intensity) in the cases of 4 times (7.5 cms), $\frac{1}{4}$ (30 cms) and $^{1}/16$th (60 cms) of this intensity.

(10) Salycylate Coating Only - Angle and Intensity Dependence

The above measurements were repeated and extended for the case of a salycylate coating alone - that is, with the phosphor placed not on a filter but on a silica microslide. The area irradiated was 1.0" by 0.7", the phosphor thickness and monochromator settings were as before, the distance from phosphor to monochromator slit was 13.0 cms., and the lamp positions were such that its aperture was 7.5, 15, 30, 45 and 60 cms from the glass. Intensity dependence was measured by noting responses for various

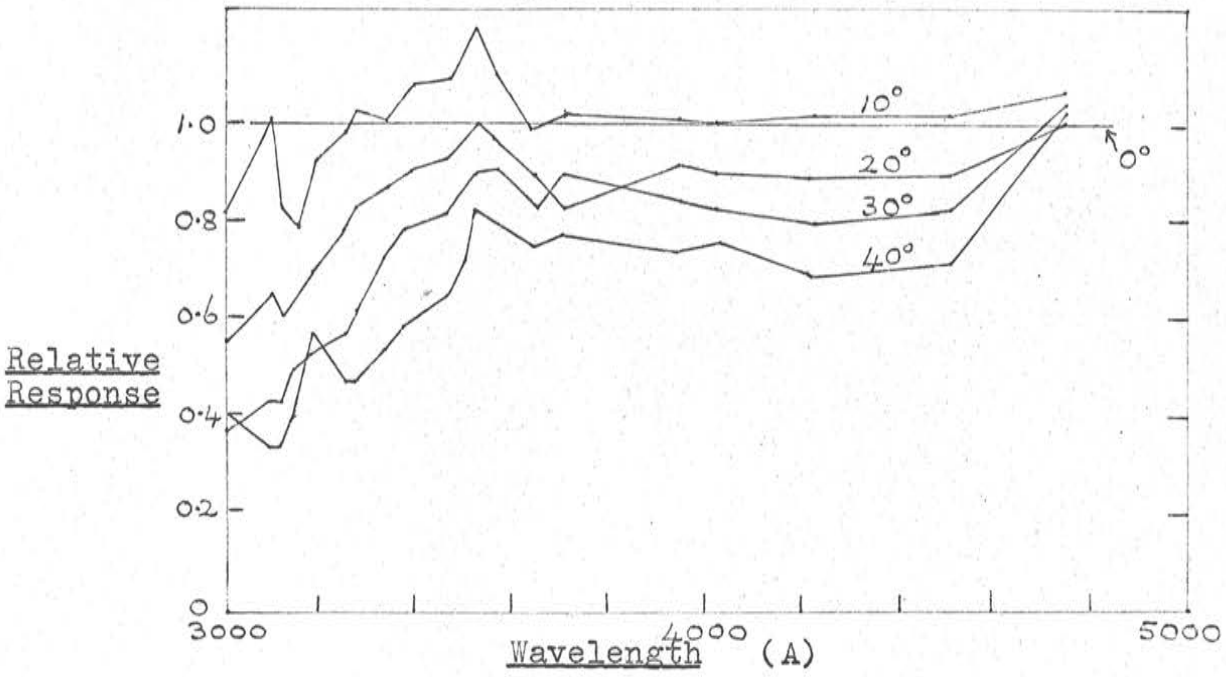

FIGURE 28. Phosphor coating on Filter - Angle dependence.

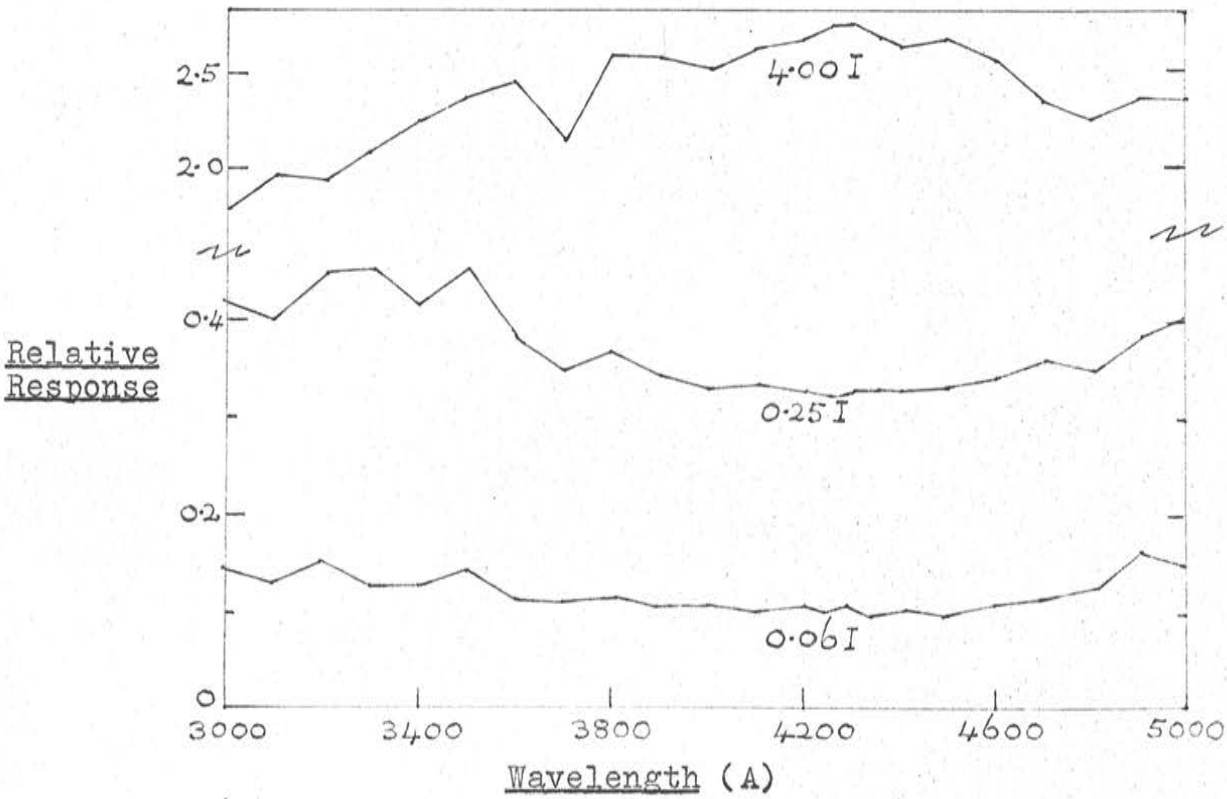

FIGURE 29. Phosphor coating on Filter - Incident Intensity dependence.

wavelengths with the lamp in each of these positions and again using that at 15 cms. as a reference intensity (Figure 30).

At 15 cms., angle dependence was measured as before - the intensity transmitted in a forward direction as the microslide angle θ was increased in 10° steps from 0° (normal to the beam) to 40° (Figure 31). In addition, however, an estimate was here made of the angle dependence of reflected and re-radiated energy. For a given θ (always at d = 15 cms), the monochromator was rotated about the microslide vertical axis and measurements made at different angles φ (as in diagram of Figure 32). The intensities are here given relative to both $\varphi = 0$ and $\theta = 0$ values, and appear to be rapidly reduced for all φ greater than 0°.

For comparison, some of the above angle dependence measurements were repeated with the salycylate removed, leaving the clear silica glass. The effect of reflection of the incident light for different values of θ is shown in Table 6. The scattered light at angles $\varphi > 0°$ which is very small, is also indicated.

TABLE 6

Reflected and Scattered Light from Silica Microslide

Relative Transmitted Intensity
(w.r. value at $\theta = 0$, $\varphi = 0$)

	$\varphi = 0^\circ$		$\varphi = 10^\circ$		$\varphi = 20^\circ$
λ(A)	$\theta = 10^\circ$	$\theta = 30^\circ$	$\theta = 0^\circ$	$\theta = 10^\circ$	$\theta = 20^\circ$
3000	.929	.817	.005	.008	.009
3100	.884	.800	.007	.007	.003
3200	.582	.509	.002	.002	.002
3300	.887	.815	.003	.003	.001
3400	.875	.754	.004	.004	.001
3500	.927	.798	.002	.002	.001
3600	.865	.772	.005	.004	.001
3700	.860	.802	.002	.001	.001
3800	.939	.842	.003	.003	.002
3900	.948	.849	.002	.002	.001
4000	.941	.811	.004	.004	.002
4100	.910	.828	.002	.002	.001
4200	.962	.850	.002	.002	.001
4300	.940	.849	.004	.004	.001
4400	.941	.839	.002	.002	.001
4500	.960	.858	.001	.001	.001
4600	.970	.828	.003	.003	.001
4700	.947	.821	.002	.002	.001
4800	.937	.805	.002	.001	.001
4900	.921	.836	.001	.001	.001
5000	.965	.832	.003	.003	.001

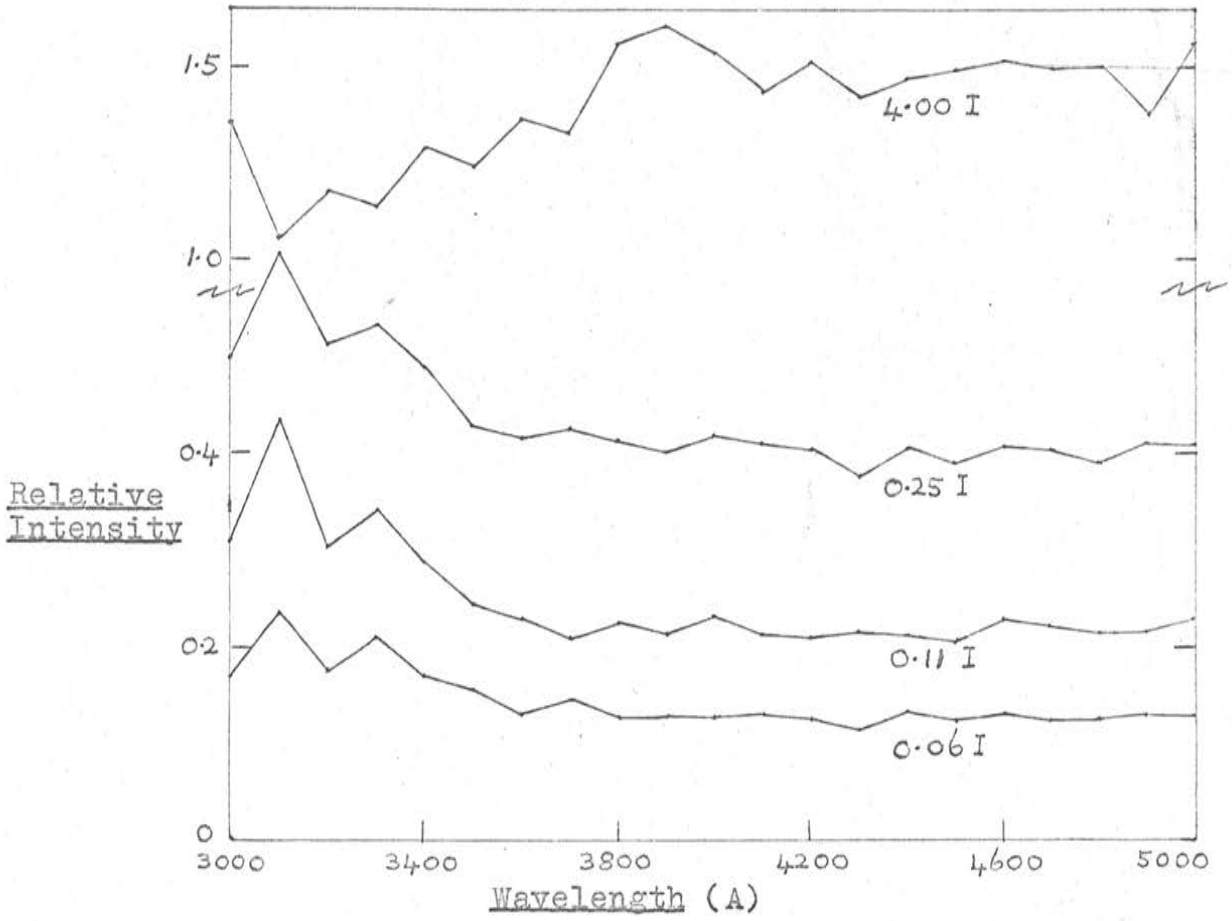

FIGURE 30. Phosphor coating - Incident Intensity dependence.

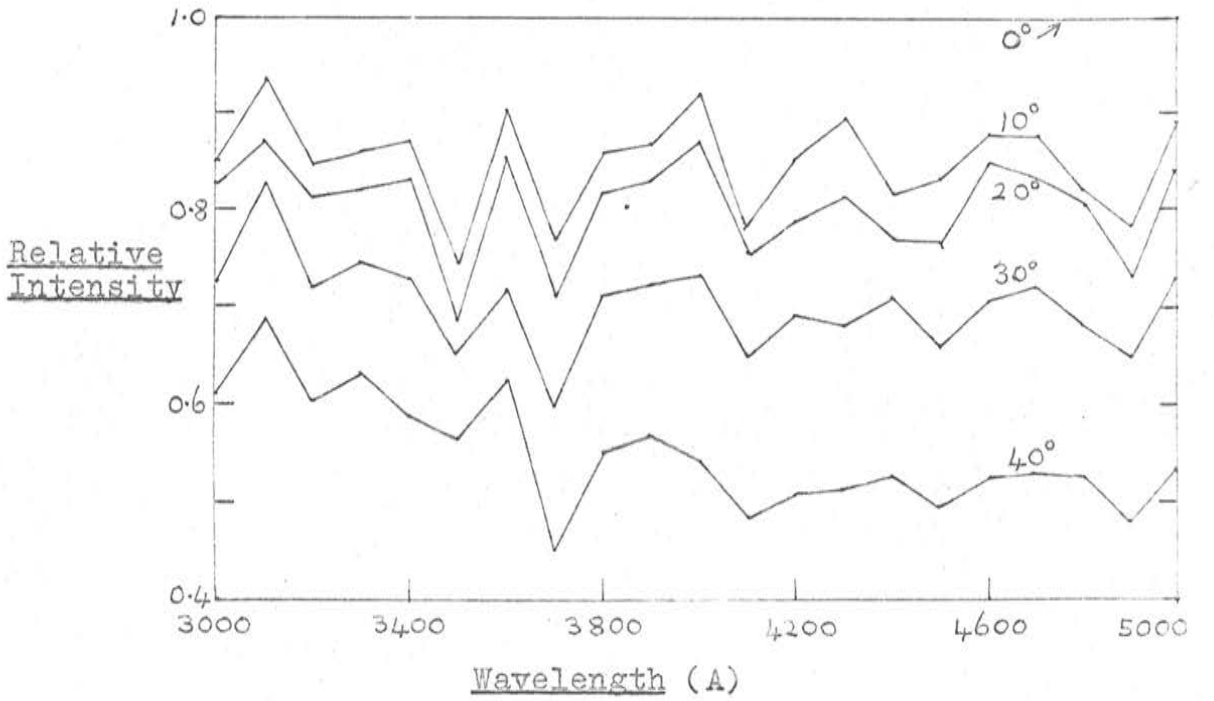

FIGURE 31. Phosphor coating - Angle dependence.

(11) Anode Voltage for Photocell

A new 92 AV photocell was calibrated against the sub-standard tungsten lamp. The object of this measurement was to verify previous culibrations, to calibrate the photocell prior to the heat test of (13), and to ascertain the dependence of current on applied anode voltage.

The standard lamp was set up on the bench with its filament at various distances between 18 and 80 cms. from the photocell sensitive surface. The resulting currents are plotted in Figure 33 for the four series of measurements with applied voltages of 92.5, 70.5, 47 and 23.5 (and with no series resistor). The recommended voltage for this photocell is 90 V, but it is apparent that operation is satisfactory at 45 volts. This is of interest in the present investigations in view of possible space limitations in the rocket installation. A fifth series of measurements at 92.5 V and with a 100K resistor included gave identical results to those obtained before. After the calibrations, the 30-cms. series was repeated, and found to be unaltered.

(12) Effect of Temperature on Interference Filter

A series of tests was carried out to determine the effect of increased temperature on the characteristics of one of the interference filters. It is expected that, mounted close to the rocket skin, filters used in flight will be subjected to high temperatures for a period - although the exact magnitudes are not accurately known.

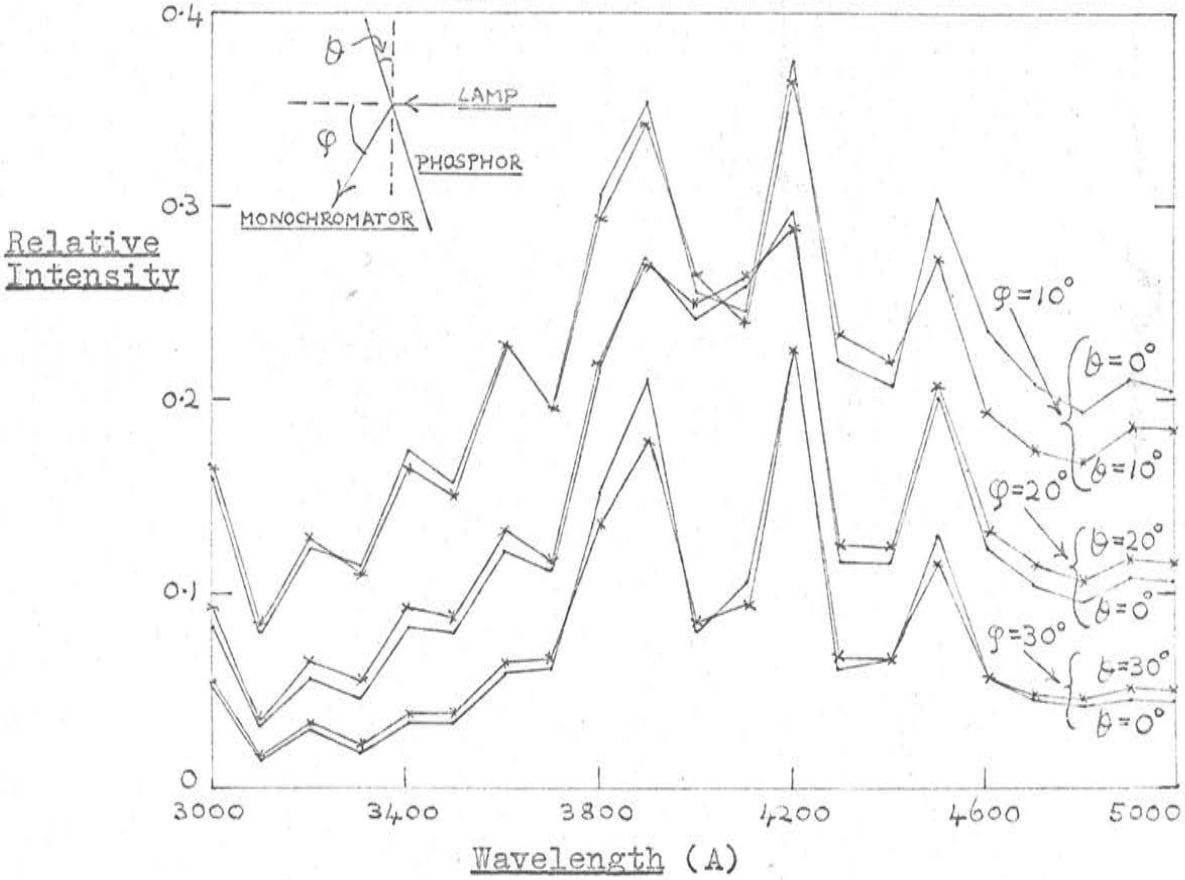

FIGURE 32. Phosphor coating - Angle dependence for Reflection and Re-radiation.

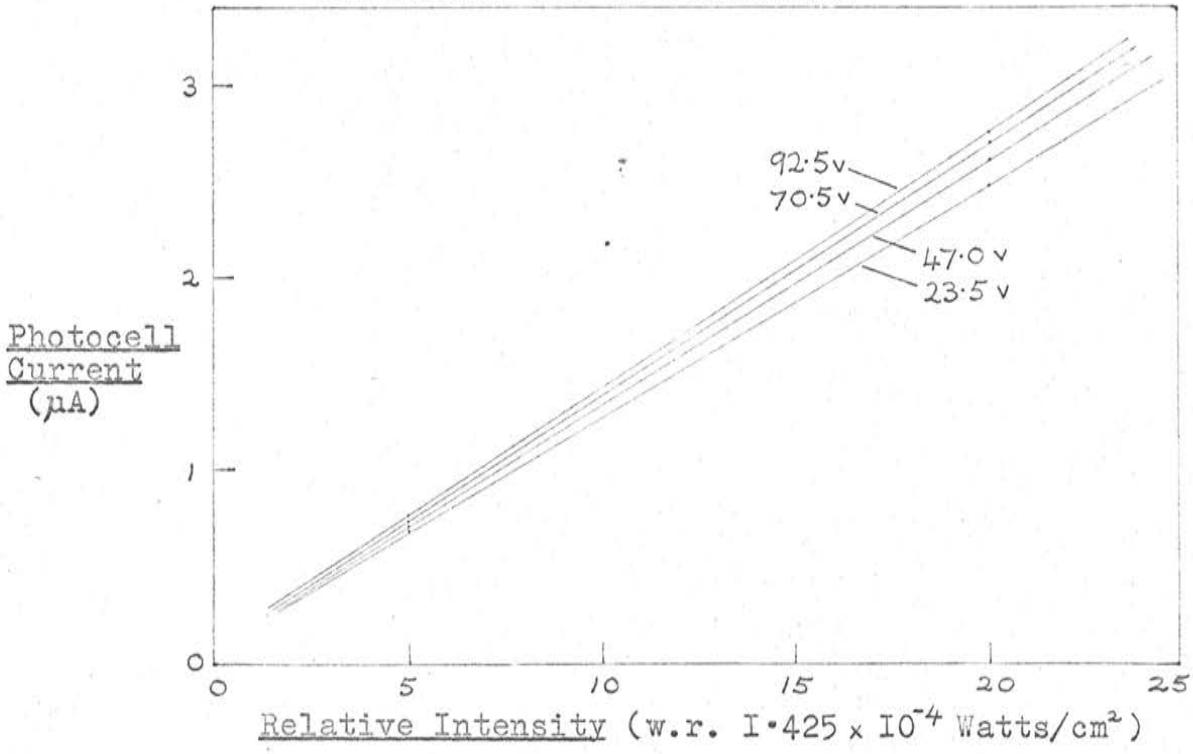

FIGURE 33. Photocell Voltage.

The filter used was No. U755. It was set up on the optical bench, mounted in a larger screen which shielded the monochromator from other stray light from the lamp source. The temperature of the filter was raised by directing a stream of air on to its front surface. This was obtained from a drier placed below and just forward of the filter. The warm air was blown through the coils of a heating element, the current through which was controlled by a variac. In this way the temperature of the filter could be adjusted over a considerable range. The output current from the photomultiplier (with a salycylate window) was monitored for different temperatures; the incident lamp energy remaining unaltered.

The following heat tests were made on the filter:

(1) First the drier was used to provide sustained heating of the filter, steadily increasing its temperature. Additional rapid heating was applied by turning the element on for periods of 15 seconds. Heating to about 45°C resulted in slightly increased transmission at 2900 A; the more severe heating to higher temperatures in a decrease. After 10 minutes from the commencement of the test, the filter was allowed to return to room temperature. The transmission similarly returned to its initial value.

(2) The filter was next subjected to a somewhat longer period of heating, taking its temperature considerably higher and

keeping it above 100°C for five minutes. The early stage of heating is here accompanied by slightly reduced transmission at 2900 A; but it increases markedly with the steep gradient to high temperatures. As the filter returns to room temperature (after 20 minutes), there is at first a still greater transmission (to a peak of 1.3 times the original at 40 minutes). It falls again only very slowly. A permanent change in filter characteristics is confirmed by spectrophotometer calibrations carried out during the course of these heat tests and shown in Figure 34. Curve A is the characteristic before any heating; curve B that after this second heat test. The peak transmission finally fell below its initial value; the peak wavelength increased a little.

(3) During the third heating, calibrations over the whole filter band were made with the monochromator while the filter was held at some constant higher temperature. Results at room temperature (20°C), at 70°C and at 105°C show a progressive but small decrease in transmission with increased temperature; the effect being more apparent over the higher wavelengths. The total time of heating was here about 15 minutes. Curve C of Figure 34 gives the spectrophotometer calibration immediately afterwards. A further reduction in transmission is evident but little peak wavelength variation. However a wavelength displacement is seen in curve D which represents a repeated calibration some days later (but before any further heating of the filter).

(4) Over about five minutes the temperature was raised to 110°C, and maintained there for a further two minutes. On cooling, curve E of Figure 34 resulted, showing further appreciable decrease in transmission.

(5) At this stage it was decided to take the filter through successive temperature cycles as above, and it was expected that progressive further reductions in transmission would occur until the filter failed completely. However, after the next and most severe heating of all - ten minutes at 110°C - curve F shows slightly increased transmission over E.

(13) Effect of Temperature on Photocell

The photocell calibrated in (11) was again set up on the optical bench at a distance of 30 cms. from the tungsten lamp filament which illuminated its whole cathode area. The current through the photocell (with a 92.5 V supply) was monitored as the temperature was raised. A combination of drier and heating element was used again and the temperature immediately in front of the photocell envelope measured. At the time of each reading, a measurement of the "dark current" was also made - that is, the current with the tungsten lamp blacked out. In this way allowance is made for any response to radiation from the heating element. In fact, however, this dark current ranged only from 2.5 mμA (at 49°) to 24 mμA at 101° and in no case did the correction greatly affect the shape of the current curve. The curves of temperature and of current at given times during the 44-minute test are shown in Figure 35. A very

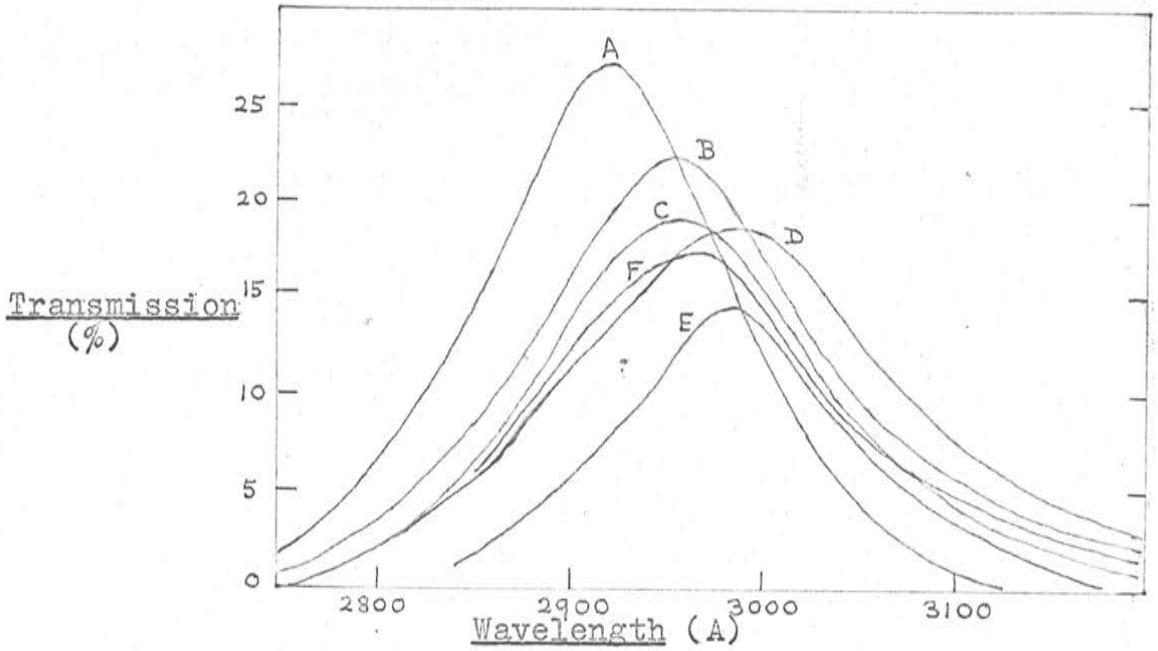

FIGURE 34. Spectrophotometer calibrations during Filter Heat Tests.

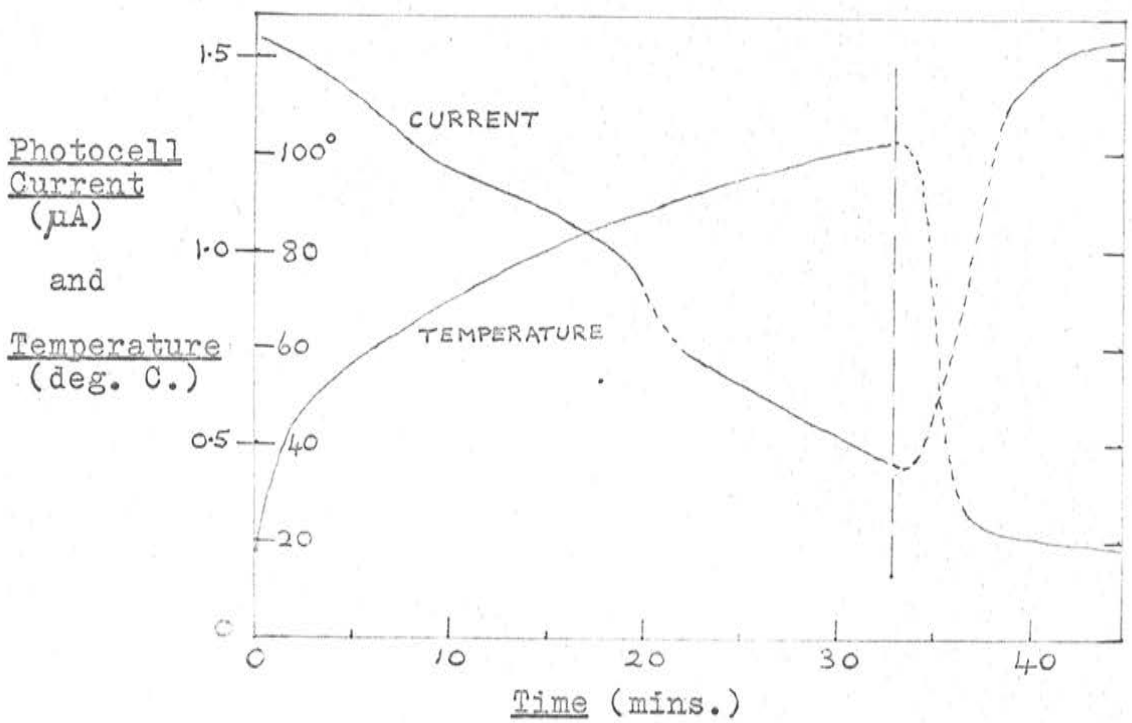

FIGURE 35. Heat Test on Photocell.

pronounced temperature dependence is apparent for the photocell response; which seems, however, to recover with return to normal conditions.

This photocell temperature dependence appears to be the most serious limitation to the accuracy obtainable from the present equipment in rocket flight conditions.

(14) Vibration and Acceleration Tests

Measurements were made on unit F to determine whether the equipment would function satisfactorily in flight after the initial mechanical stress which it will encounter during rocket launching. The unit was first vibrated with a frequency swept from 25 c/sec to 2 Kc/sec at 10 g across each of three mutually perpendicular planes. Subsequently the same unit was subjected to accelerations of 60 g in the direction of its longitudinal axis and of 10 g along the other axes. After each of these tests, the response of the whole assembly to the ultra-violet radiation source and the sensitivity of the photocell alone were both checked. No significant change in these characteristics was observed.

PART D : WAVELENGTH AND HEIGHT DEPENDENCE OF DISSOCIATION RATES IN THE UPPER ATMOSPHERE

Equations (6) and (7) of part A represent the dissociation of molecular oxygen and of ozone which is brought about by the solar radiation incident on the atmosphere. The rates of these reactions, J_2 and J_3 respectively, occur in photochemical relations such as (13) from which the profiles of reacting constituents are determined.

In this part, results are briefly noted of a calculation to find these values as a function of altitude, and to determine also the contributions to the total rates from radiation of various wavelengths. The model atmosphere adopted is shown in Table 7 (Refs. 74 and 102) and for purposes of calculation is divided into the eleven intervals indicated.

A pure oxygen atmosphere was assumed and radiation from 1250 to 3500 A considered. The oxygen cross sections used for the region 1250-1750 A are those given by Watanabe (72); and from 1800 to 2550 A those of Ditchburn (62). Ozone absorption coefficients are those of Tanaka and Inn (103 and 112) for the ranges 1200-2150 A and 3000-3500 A; the values of Vigroux (Figure 3) are used for the remaining wavelengths. Data for the incident solar intensity were taken from Detwiler et al (95) below 2600 A, and from Wilson et al (115) for higher wavelengths.

Calculations were made for 10 A intervals (except where intensity and absorption were sufficiently constant over 50 A). The total value of Kx (cf equ.^{n} (1)), that is the value due to both oxygen and ozone absorption, was first found for each part of the model atmosphere. From these and the appropriate incident intensity the contributions to the total dissociation rates for each wavelength interval were derived. The results for the case of normally incident radiation only are shown in Figures 36 and 37.

Radiation of low wavelengths adds very little to J_3, and even then only at high altitudes. For all altitudes down to about 40 Km. radiation around 2600 A (corresponding to the absorption peak) makes the greatest contribution. At 30 Km. somewhat higher wavelengths (around 3000 A) are the most effective.

In the case of molecular oxygen, the dissociation rate J_2 for heights above 100 Km. is due to absorption in the Schumann-Runge region. The importance of these wavelengths decreases at lower altitudes, until below 80 Km. it is the Herzberg region radiation (and especially wavelengths near 2200 A) which brings about the dissociation. By the time the radiation has penetrated to 40 Km. these wavelengths in turn have also been greatly attenuated, and at still lower altitudes the dissociation rate becomes negligible.

TABLE 7

Model Atmosphere

Height Interval (Km)	(O_2) cms/Km	(O_3) cms/Km	Height Interval (Km)	(O_2) cms/Km	(O_3) cms/Km
140-130	$1.37.10^{-7}$	-	80-70	1.45	$5.49.10^{-6}$
130-120	$2.49.10^{-6}$	-	70-60	4.02	$2.36.10^{-5}$
120-110	$9.06.10^{-5}$	-	60-50	$1.28.10^{1}$	$7.55.10^{-5}$
110-100	$1.17.10^{-2}$	$9.33.10^{-10}$	50-40	$4.76.10^{1}$	$1.07.10^{-3}$
100-90	$4.72.10^{-2}$	$9.56.10^{-9}$	40-30	$1.97.10^{2}$	$1.20.10^{-2}$
90 -80	$3.57.10^{-1}$	$3.60.10^{-7}$			

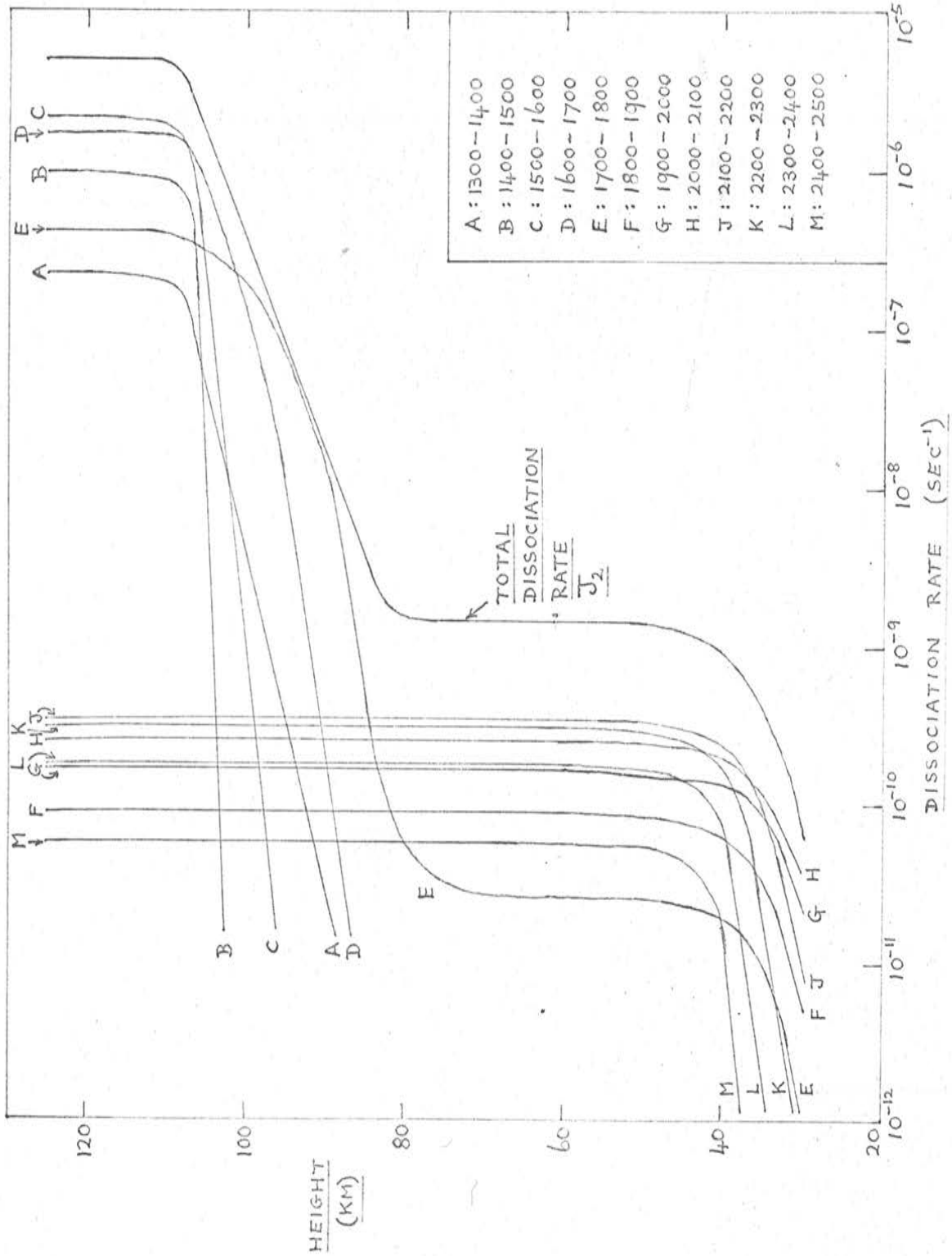

FIGURE 36. Dissociation Rate J_2.

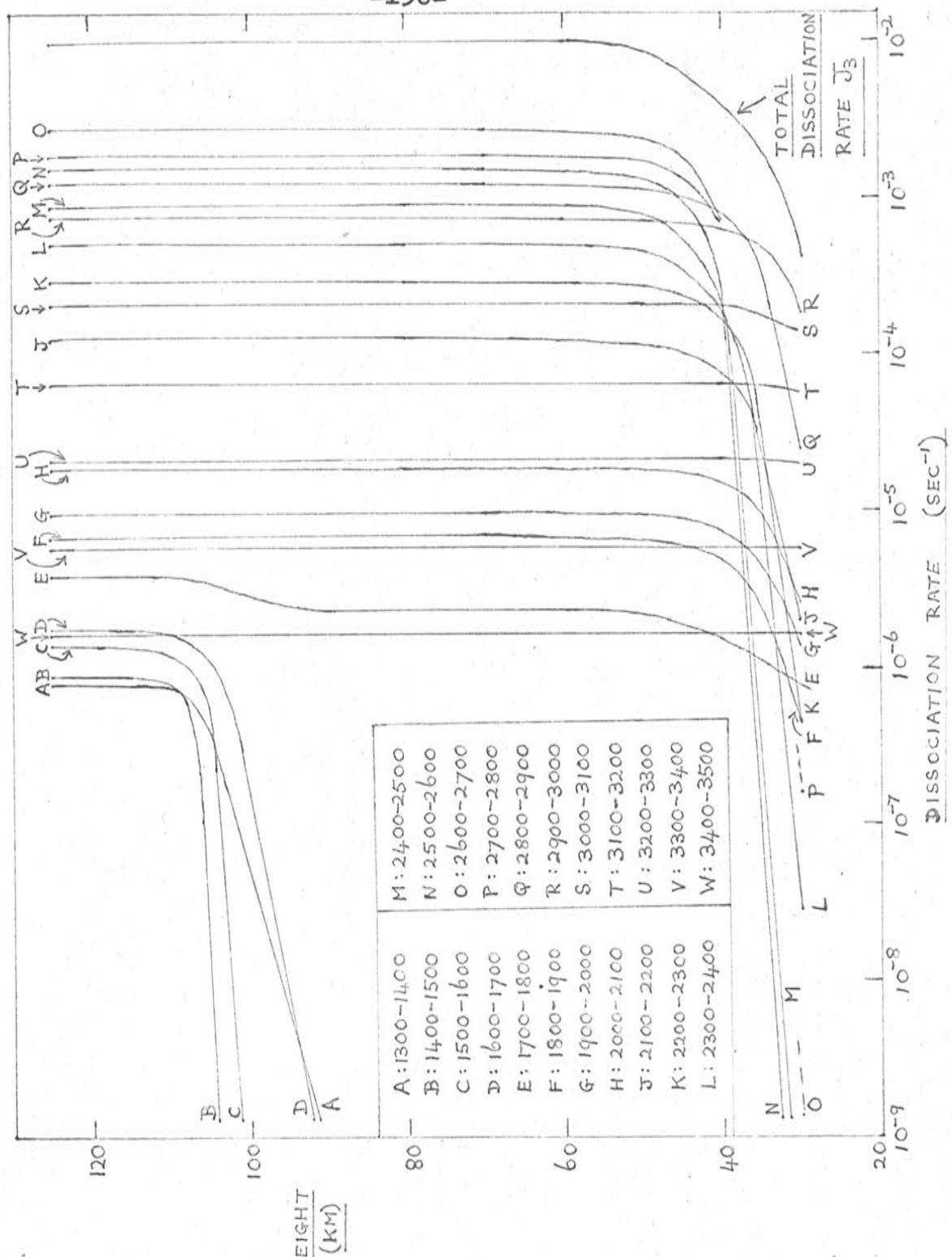

FIGURE 37. Dissociation Rate J_3.

PART E : THE FIRST ROCKET FLIGHT OF THE EQUIPMENT

The first flight of the equipment took place from Woomera at 9.12 a.m. on 6th December, 1963 (trial No. AH 289). The rocket, HAD 301, was launched at an angle of 80.5°. Its initial direction of firing was 313° from true north, but it then went 27° to the right of this line. The rocket reached an altitude of 288,000 feet (87.9 kilometres) at about 142 seconds from time of launch, rolling during this first phase at the very slow rate of about once every 20 seconds. The solar zenith angle was 37° in a direction of 83°. Good telemetry records were obtained throughout the flight.

Figure 38 shows the telemetry record for the ozone experiment from the time the protecting cover was removed (27 seconds) until the rocket breakup at 270 seconds. The upper trace is the record from the monitor unit, the lower from the ozone unit itself. The horizontal time scale is in seconds and the saturation levels correspond to 1.25 volts telemetry output. The calibration unit steps which are periodically switched into the electrometer amplifier of the ozone unit correspond to equal input current steps up to a maximum of $3.6\ 10^{-7}$ amps. It is seen that the ozone amplifier signal reached saturation level each time the sensors were directed towards the sun. This occurs from the time the protecting cover was removed until the end of the rocket flight at

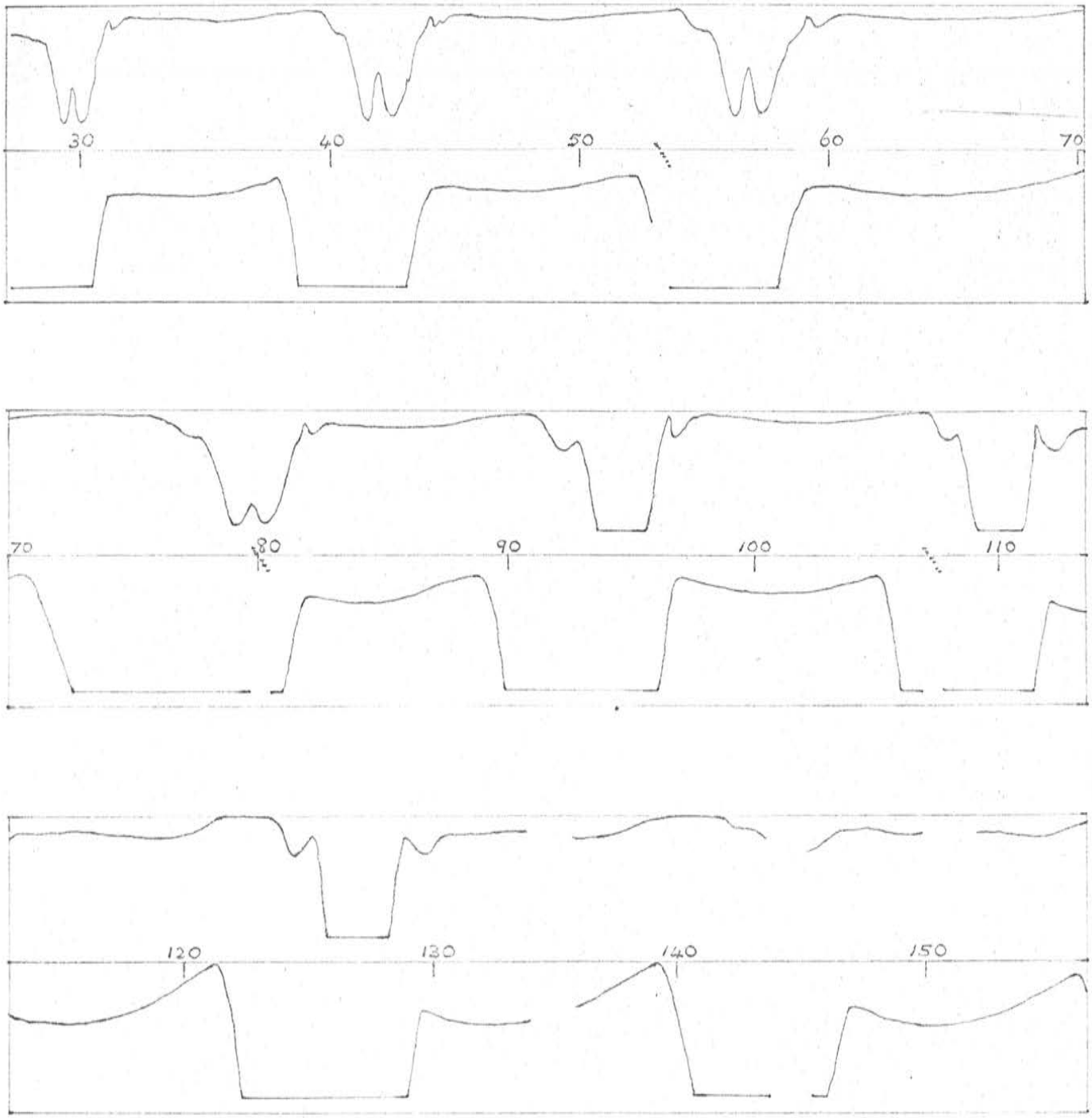

Time in seconds.

FIGURE 38(a). Telemetry Record from Monitor Unit (upper trace) and Ozone Unit (lower).

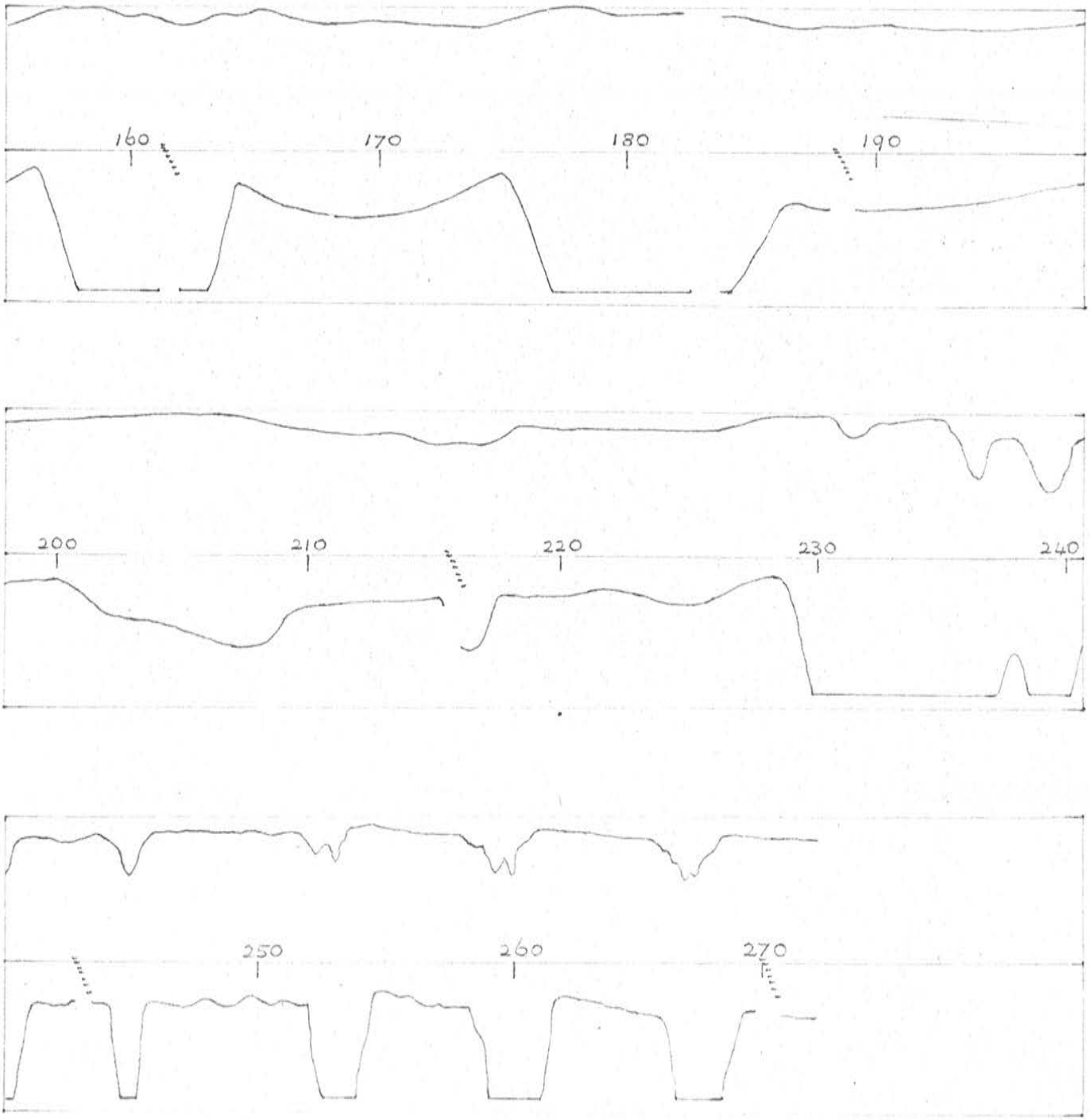

Time in seconds.

FIGURE 38(b). Telemetry Record from Monitor Unit (upper trace) and Ozone Unit (lower).

about 380 secs. Between the peaks of the record, the signal shows secondary peaks occurring when the sensor is facing away from the sun. It is interesting to note that these latter peaks are of the magnitude expected for the main signal and increase to a maximum at the top of the trajectory. The monitor amplifier output is initially large and has a double peak as the rocket rolls. From 90 to 130 seconds, this signal also reaches saturation; thereafter the level is lower and of the order expected.

The unexpectedly high ozone unit signal is present from the beginning of the trace. This corresponds to an altitude of less than 25 kilometres, with almost half of the ozone content of the atmosphere still above the point of observation. Even for normally incident radiation (Figure 4) and allowing for effects of the higher wavelengths of the filter pass-band (Figure 8), virtually no signal at all should be observed here. It is also significant that after rocket breakup (272 secs.) similar saturated signals continue to occur right up to impact. These, certainly, cannot be related to penetration of 2700 A ultraviolet radiation, whatever the initial sensitivity. The electrometer amplifier calibration steps are recorded throughout the whole duration of the flight, indicating correct functioning, although the steps at the beginning are unevenly spaced and are crowded closer together than is the case later in the record. Also, this calibration does not

correspond, in general, with the telemetry calibration. Thermistors in the round indicated a maximum temperature at the photocells of about 60°C. This would have involved a correction factor (Figure 35) but should not have been too great for satisfactory operation. Laboratory measurements (section C 12) also suggested that the filter would stand a considerably higher temperature without any profound change occurring in its transmission characteristics.

It can only be concluded, therefore, that the filters were damaged during the early stage of the flight, either during launch or at the time of the removal of the protecting cover. The drop in the monitor unit signal to a reasonable level (after 130 secs.) while the ozone unit continues to saturate suggests the possibility that damage to the former might have been temporary or of a less severe nature. The difference is certainly not accountable in terms of the small aspect difference between the two units.

The only possibility of analysing the ozone record, as it stands, supposing the saturated peaks to be real signals, was to take measurements on the rapidly rising and falling sides of the response curve. An attempt to obtain meaningful results in this way was made on signals occurring up to a time of 180 seconds, corresponding to a point just beyond the trajectory apogee. The displacement of the saturated peak from the calibration unit zero was measured and the times of reaching this level on both sides of

the response were noted. The amplitude was converted into an apparent photocell current using each of two sets of calibrations. In the first place, the calibration steps nearest to the point of interest on the trace were used; then those later in the record where the steps are uniformly spaced. In each case, the apparent currents were then converted to the corresponding value for normal incidence on the filter, using a factor derived from the pre-flight unit aspect calibration of Figure 23. The appropriate angle between the incident radiation and the face of the filter was found from values of the solar aspect angle and roll rate. This was a small angle because of the restriction on the points which could be used, and so adds further to the inaccuracy of the method. Roll angles up to the time of 120 seconds were taken from the roll telemetry record. Thereafter, values are from a determination of the roll rate from the ozone unit record itself. The latter supposes a constant rate over the whole roll period, but agrees fairly well with the other set of values prior to 120 seconds. Nevertheless, the values are approximate only, especially when applied to the small intervals considered. Even more critical to the derived value of corrected intensity is the aspect information which is obtained from the single sun-slit results.

Except perhaps for the three or four fairly self-consistent readings near the peak, the corrected intensities found by the above procedure are not realistic, with several lower

altitude intensities appreciably greater than that at the peak of the trajectory. Considering the four highest altitude results, a decrease in intensity to 0.8 of the incident value is found between 87.5 and 82.5 kilometres. Using the absorption coefficient for 2700 A (Figure 3), this corresponds to an average ozone density over this range of $0.21\ 10^{-3}$ cms. per kilometre. Excluding the highest altitude point, a curve through the other three gives the following values:

Height (Km.)	Ozone Density (cms./Km.)
83-85	$0.12\ 10^{-3}$
85-87	$0.08\ 10^{-3}$
87-89	$0.04\ 10^{-3}$
Above 89	0.00

These results are of the expected order of magnitude but in view of the considerable doubt in the procedure of analysis and in the various data used, they cannot be regarded as significant. As noted above, it seems in fact far more likely that the saturated signal is not a measure of ultraviolet intensity at all.

Another unexpected feature of these first results is the double peak of the monitor unit record. This effect was not observed during any of the earlier measurements and a first suggestion was that it might have been due to a shadow as the rocket rolled, either from the missile aerials or else from the

anode of the photocell itself. However, a shadow from the nearby telemetry aerials is not a possible cause in view of the orientation of the round during the early part of the flight. Also, the aperture included in the monitor unit is directly above the sensitive area only of the photocell, that is, it is well away from the anode. This could only, therefore, be expected to affect the response at the very extreme solar zenith angles - which are in any case excluded because of the mounting of the photocell. Subsequent laboratory checks did not reproduce the double peaks by such a shadow effect.

Consideration has also been given to the possibility that the double peak is in some way due to a saturation phenomenon analogous to similar known electronic effects. Laboratory measurements since the experiment have been made to determine whether, in fact, continued increase in illumination beyond a certain point would be accompanied by a decrease in photocell current. Increasing illumination resulted, however, in no indication of a double peak but in a monotonic increase in photocell current, even up to one milliamp, which is far in excess of the recommended maximum of five micro-amps. Similar results were obtained when monitor filters were used with the photocell.

As a further check, the aspect responses of Figure 23 were repeated and were extended to other axes. A single peak only was observed in all cases of illumination from 0° to 70°.

It is therefore supposed that the double peak is due to reflection, either from some part of the rocket or from part of a damaged filter assembly. Observations were made of the effect of illuminating the photocell while mounted in the casting for the instrumentation section of the round. However, it was again not possible to reproduce the double peak of the flight record.

It is suggested that future experiments might include some means of recording any break in the filter glass, and of determining at what stage of the flight this occurs. Further consideration must be given also to the temperature dependence of the photocell operation. The replacement of the present photocell by a device directly responsive to the ultraviolet radiation of interest, and the consequent elimination of some of the uncertainties associated with the use of the phosphor, would also be of considerable advantage.

REFERENCES

A. OZONE AND THE ATMOSPHERE

Distribution and measurements
Satellite Photometry and Similar Measurements
Meteorology and Theories of Atmospheric Transport
Radiative Transfer
Variations in Relation to other Geophysical Phenomina
Photochemistry
Tropospheric Ozone
General, and other references.

B. SPECTROSCOPY OF OZONE AND OF OTHER ATMOSPHERIC GASES

C. PHYSICS OF THE ATMOSPHERE - GENERAL

D. CHEMICAL PHYSICS OF OZONE.

E. PHOSPHORS

F. OTHER REFERENCES

* * * * * * *

REFERENCES

(With very general classification according to principal or most relevant topic.)

A. OZONE AND THE ATMOSPHERE

Distribution and Measurements

1. Annals of the International Geophysical Year (Pergamon) Vol. V, Parts I, II, & III (1957).
2. Brewer A.W., et al. Vertical Distribution of Atmospheric Ozone - comparison of different methods : Ann. de Gov., 16, No. 2, 1960.
3. Funk J.P. and Garnham G.L. : Australian Ozone Observations and a suggested 24-month cycle : Tellus, 14, No. 4, Nov. 1962 (pp. 378-382).
4. Johnson F.S. et al : Studies of the Ozone Layer above New Mexico : in "Rocket Exploration of the Upper Atmosphere", ed. Boyd R.L.F. and Seaton M.J. (p.189).
5. Johnson F.S. et al : Direct Measurements of the Vertical Distribution of Atmospheric Ozone to 70 Kilometers Altitude : Jour. Geo. Res. 57, No. 2, June, 1952.
6. Kay R.H. : The Measurement of Ozone Vertical Distribution by a Chemical Method to Heights of 12 Km. from Aircraft : p.208 of "Rocket Exploration of U.A.", op.cit.

7. Kulkarni R.N. : Comparison of Ozone Variations and of its Distribution with Height over middle latitudes of the two hemispheres : R.M.S. Quart. Jour. 88 (1962), pp. 522-534.

8. MacDowall J. : Some Observations at Halley Bay in seismology, glaciology and meteorology : Proc. Roy. Soc., Series A, 256, 1960, pp. 145-197.

9. Mateer C.L. and Godson W.L. : The Vertical Distribution of Atmospheric Ozone over Canadian stations from Umkehr observations : Quart Jour. R.M.S. 86, 1960.

10. Paetzold H.K. : The Mean Vertical Ozone Distribution resulting from the Photochemical Equilibrium, Turbulence and Currents of Air : Jour. Atmos. and Terres. Physics, 3, 1953, pp. 125-131.

11. Paetzold H.K. : New Experimental and Theoretical Investigations on the Atmospheric Ozone Layer : Jour. Atmos. Terres. Physics, 7, 1955, pp. 128-140.

12. Pressman J. : The Latitudinal and Seasonal Variations of the Absorption of Solar Radiation by Ozone : Geophysical Research Papers No. 33, Air Force Cambridge Research Centre, Dec. 1954.

13. Ramanathan K.R. and Kulkarni R.N. : Mean Meridional Distributions of Ozone in Different Seasons Calculated from Umkehr observations and Probable Vertical Transport Mechanisms : Quart. Jour. R.M.S. 86, 1960 (pp. 144 f).

14. Regener E. : Further Investigations of the Ozone Layer : p. 202 of "Rocket Exploration of U.A.".

15. Walton G.F. : Calculation of the Vertical Distribution of Atmospheric Ozone : Jour. Atmos. Terres. Physics, 16, Oct. 1959.

Satellite Photometry and Similar Measurements

16. Frith R. : Measuring the Ozone above the Earth : Discovery, 22, Sept., 1961, pp. 390-1.

17. Pittock A.B. : A Twilight Method of Determining the Vertical Distribution of Ozone : Nature, 190, April, 1961, pp. 426-7.

18. Pittock A.B. : Determinations of the Vertical Distribution of Ozone by Twilight Balloon Photometry : submitted to Jour. Geophy. Res., Feb. 1963.

19. Sekera Z. and Dave J.V. : Determination of the Vertical Distribution of Ozone from the Measurement of Diffusely Reflected Ultra-violet Solar Radiation : Planetary and Space Science, 5, No. 2, June 1961, pp. 122-136.

20. Singer S.F. and Wentworth R.C. : A Method for the Determination of the Vertical Ozone Distribution from a Satellite : Jour. Geophy. Res. 62, No. 2, June 1957, pp. 299-308.

21. Twomey S. : On the Deduction of the Vertical Distribution of Ozone by Ultraviolet Spectral Measurements from a Satellite : Jour. Geophy. Res. 66, No. 7, July 1961, (pp. 2153-2162).

22. Venkateswaren S.V. et al. : Determination of the Vertical Distribution of Ozone by Satellite Photometry : Jour. Geophy. Res., 66, No. 6, June 1961.

Meteorology and Theories of Atmospheric Transport

23. Boville B.W. and Hare F.K. : Total Ozone and Perturbations in the Middle Stratosphere : Quart. Jour. R.M.S., 87, 1961, pp. 490f.

24. Dobson G.M.B. : Meteorology of the Lower Stratosphere : Proc. Roy. Soc. London, 185, p.144.

25. Godson W.L. : Total Ozone and the Middle Stratosphere over Arctic and Sub-arctic Areas in Winter and Spring : Quart. Jour. R.M.S., 86, 1960, pp. 301f.

26. Johansen H. : On the Relation between Meteorological Conditions and Total Amount of Ozone over Tromso : Jour. Atmos. Terres. Physics, special supplement 1957.

27. Murgatroyd R.J. and Singleton F. : Possible Meridional Circulations in the Stratosphere and Mesosphere : Quart. Jour. R.M.S., 87, April 1961.

28. Newell R.E. : Transfer through the Tropopause and within the Stratosphere : Quart. Jour. R.M.S., 89, No. 380, April 1963, pp. 167-204.

29. Ohring G. and Muench H.S. : Relationships between Ozone and Meteorological Parameters in the Lower Stratosphere : Jour. Meteor. 17, 1960, pp. 195f.

30. Reed R.J. : The Role of Vertical Motions in Ozone-Weather Relationships : Jour. Meteor. 7, 1950, pp. 263f.

31. Taba H. : Ozone Observations and their Meteorological Applications : Techn. Note No. 36, World Meteor. Organization,, 1961.

Radiative Transfer

32. Hitschfeld W. and Houghton J.T. : Radiative Transfer in the Lower Stratosphere due to the 9.6 micron band of Ozone : Quart. Jour. R.M.S., 87, 1961, pp. 562f.

33. Murgatroyd R.J. and Goody R.M. : Sources and Sinks of Radiative Energy from 30 to 90 Km. : Quart. Jour. R.M.S., 84, 1958, pp. 325f.

Variations in Relation to other Geophysical Phenomina

34. Adderley E.E. : The Influence of the Moon on Atmospheric Ozone : Jour. Geophy. Res., 68, No. 5, March 1963, pp. 1405-8.

35. Adel A. : The Solar-Terrestrial Parameter "Effective Radiation Temperature of the Ozone Region" and Evidence for Solar Variability with a Period of Ten Weeks : Bull. Am. Met. Soc., 35, 376, 1954.

36. Adel A. and Epstein E.S. : Power Spectrum Analysis of Atmospheric Ozone Parameters : Jour. Meteor., 16, Oct. 1959, pp. 548-555.

37. Ahmed S.J. and Halim A. : Total Atmospheric Ozone and Geomagnetic Activity : Jour. Geophy. Res., 66, No. 10, Oct. 1961, pp. 3213f.

38. Butler S.T. : Atmospheric Tides : Scientific American, Dec. 1962, pp. 49-55.

39. Halim A. : Dependence of Lo on Sunspots for Atmospheric Ozone Measurements : Jour. Atmos. Terres. Physics, 24, April 1962, pp. 303-310.

40. Kofsky I.L. : Effects on the Ozonosphere of the Thermal Flux from Nuclear Detonations : Jour. Geophy. Res. 67, No. 2, Feb. 1962, pp. 739-744.

41. London J. and Haurwitz M.W. : Ozone and Sunspots : Jour. Geophy. Res. 68, No. 3, Feb. 1963, pp. 795-801.

42. Small K.A. and Butler S.T. : The Solar Semidiurnal Atmospheric Oscillation : Jour. Geophy. Res. 66, No. 11, Nov. 1961, pp. 3723-25.

43. Willett H.C. : The Relationship of Total Atmospheric Ozone to the Sunspot Cycle : Jour. Geophy. Res. 67, No. 2, Feb. 1962, pp. 661-670.

Photochemistry

44. Barth C.A. : Nitrogen and Oxygen Atomic Reactions in the Chemosphere : No. 20, pp. 303-326 of "Chemical Reactions in the Lower and Upper Atmosphere", Stanford Research Institute (Interscience).

45. Bates D.R. and Nicolet M. : The Photochemistry of Atmospheric Water Vapour : Jour. Geophy. Res. 55, No. 3, Sept. 1950.

46. Chapman S. : The Photochemistry of Atmospheric Oxygen : Reports on Progress in Physics, Vol. IX, 1942-43, pp. 92-100.

47. Dutsch H.U. : Current Problems of the Photochemical Theory of Atmospheric Ozone : No. 11, pp. 167-180 of "Chemical Reactions in the Lower and Upper Atmosphere", op.cit.

48. Harteck P. and Reeves R.R. : Recent Investigations of Chemical Reactions of Fundamental Importance in the Atmosphere : No. 14, pp. 219-238 of "Chemical Reactions in the Lower and Upper Atmosphere".

49. Paetzold H.K. : The Photochemistry of the Atmospheric Ozone Layer : No. 12, pp. 181-195 of "Chemical Reactions in the Lower and Upper Atmosphere".

Tropospheric Ozone

50. Frenkiel F.N. : Ozone Theory in the Troposphere : Jour. Chem. Physics, 23, No. 2, 1955, p. 2440.

51. Goody R.M. and Roach W.T. : The Determination of Tropospheric Ozone from Infra-Red Emission Spectra : Quart. Jour. R.M.S. 84, 1958, pp. 108-117.

52. Kroening J.L. and Ney E.P. : Atmospheric Ozone : Jour. Geophy. Res., 67, No. 5, May 1962, pp. 1867-1875.

General, and Other References

53. Craig R.A. : The Observations and Photochemistry of Atmospheric Ozone and their Meteorological Significance : Meteorological Monographs, 1, No. 2, Sept. 1950.

54. Epstein E.S. et al : A New Method for the Determination of the Vertical Distribution of Ozone from a Ground Station : Jour. Meteor. 13, No. 4, August 1956, pp. 319-333.

55. Frith R. : Ozone in the Earth's Atmosphere : Contemporary Physics, 3, No. 5, June 1962, pp. 375-381.

56. Hunt B.G. : A Review of the Published Literature on the Ozonosphere : W.R.E. Tech. Note SAD79, June 1961.

57. Junge C.E. : Global Ozone Budget and Exchange between Stratosphere and Troposphere : Tellus, 14, No. 4, Nov. 1962, pp. 363-377.

58. Mitra S.K. : The Upper Atmosphere - Chapter IV "The Ozonosphere" - Calcutta, Asiatic Society, 1952.

59. Paetzold H.K. and Regener E. : Ozon in der Erdatmosphare : Handbuck der Physik, 1957, PH. XLVIII, pp. 370-426.

60. Regener V.H. : The Vertical Flux of Atmospheric Ozone : Jour. Geophy. Res. 62, No. 2, June 1957, pp. 221f.

61. Strong J. : On a New Method of Measuring the Mean Height of the Ozone in the Atmosphere : Jour. Franklin Inst., 231, pp. 121-155.

B. SPECTROSCOPY OF OZONE AND OF OTHER ATMOSPHERIC GASES

62. Ditchburn R.W. and Young P.A. : The Absorption of Molecular Oxygen between 1850 and 2500 A : Jour. Atmos. Terres. Physics, 24, Feb. 1962, pp. 127f.

63. Ditchburn R.W. : Ultraviolet Radiation Absorption Cross-sections : pp. 313f of "Rocket Exploration of Upper Atmosphere", op cit.

64. Herzberg G. : Molecular Spectra and Molecular Structure, van Nostrand, 1947.

65. Hettner G. et al : Die Struktur des Ozon Molekuls und seine Banden im Ultrarot : Zeit. fur Physik, 91, 1934, pp. 372-385.

66. Ny T.Z. and Choong S.P. : L'absorption de la lumiere par l'ozone entre 3050 et 3400 A : Comptes Rendus, 195, 1932, pp. 309-11.

67. Strong J. and Watanabe K. : Pressure Effect on Infra-Red Absorption : Phys. Rev. 57, June 1940, p.1049.

68. Vassey A. : Sur l'absorption atmospherique dans l'ultra-violet : Ann. de Physique 16, 1941, pp. 145-203.

69. Vigroux E. : Mesures absolues des coefficients d'absorption de l'ozone dans la region des bandes de Huggins, a 18° : Comptes Rendus, 234, No. 2, 1952, p. 2351.

70. Vigroux E. : Absorption de l'ozone dans la region des bandes de Huggins. Influence de la temperature". Op. cit. p. 2439.

71. Vigroux E. : Absorption de l'ozone a 18° au-desseous de 3130 A. Op. cit., p. 2529.

72. Watanabe K. : Ultraviolet Absorption Processes in the Upper Atmosphere : Advances in Geophysics, 5, 1958, pp. 153-221.

C. PHYSICS OF THE ATMOSPHERE - GENERAL

73. Hulburt E.O. : Physics of the Upper Atmosphere : Meteorological Monographs, 3, No. 17, July 1957, pp. 160-181.

74. Kuiper G.P. (ed.) : The Earth as a Planet : especially Chapter 12 : Bates D.R. : The Physics of the Upper Atmosphere.
Chapter 13 : Nicolet M. : Dynamic Effects in the High Atmosphere.

75. Nawrocki P.J. and Papa R. : Atmospheric Processes : Prentice Hall, 1963.

76. Ratcliffe J.A. (ed.) : Physics of the Upper Atmosphere : Academic Press, 1960 : especially
Chapter 2 : Nicolet M. : The Properties and Constitution of the Upper Atmosphere.
Chapter 4 : Friedman H. : The Sun's Ionizing Radiations.

D. CHEMICAL PHYSICS OF OZONE

77. Benson W. and Axworthy A.A. : Mechanism of the Gas Phase Thermal Decomposition of Ozone : Jour. Chem. Phys. 26, No. 6, June 1957, pp. 1718-1726.

78. Benson S.W. : On the Existence of Energy Chains in Ozone Decomposition : Jour. Chem. Phys. 33, No. 1, 1960, p. 939.

79. Bunker D.L. : Monte Carlo Calculation of Triatomic Dissociation Rates I. N_2O and O_3 : Jour. Chem. Phys., 37, No. 2, July 1962, pp. 393-403.

80. Ford H.W. et al : Rate Constants at Low Concentrations. I : Rate of Reaction of Ozone with Nitrogen Dioxide : Jour. Chem. Physics, 26, No. 5, May 1957, p. 1336.

81. Ford H.W. et al : Rate Constants at Low Concentrations. II : Reaction between Nitric Oxide and Ozone in Air at Room Temperature : Op. cit. p. 1337.

82. Gill E.K. and Laidler K.J. : The Vibration and Decomposition of the Ozone Molecule : Trans. Faraday Society, 55, No. 1, 1959, pp. 753-759.

83. Phillips L.F. and Schiff H.I. : Mass Spectrometric Studies of Atomic Reactions. III : Reactions of Hydrogen Atoms with Nitrogen Dioxide and with Ozone : Jour. Chem. Physics, 37, No. 6, Sept. 1962, pp. 1233-38.

84. Schumacher H.J. : Mechanism of Ozone Decomposition : Jour. Chem. Physics, 33, No. 1, 1960, p. 938.

E. PHOSPHORS

85. Chevallier A and Duboulez P. : Sur l'application de la fluorescence aux mesures photometriques dans l'ultraviolet : Acadamie des Sciences, Comptes Rendus 194, 1932, p. 174.

86. Dejardin G. and Schwegler R. : Repartition de l'energie dans les spectres continus ultraviolets de la molecule d'hydrogene et --- : Revue d'Optique 13, 1934, p. 313.

87. Hammann J.F. : Zeit. Angew. Physik, 10, p. 187, 1958.

88. Johnson F.S. et al : Fluorescent Sensitized Photomultipliers for Heterochromatic Photometry in the Ultraviolet : Jour. Optical Soc. Am., 41, 1951, p. 702.

89. Krokowski E. : Zur Frage der Fluoreszenzausbeute von Natrium - Salicylat im UV-und Rontgengebiet : Die Naturwissenschaften 45, 1958, p. 509.

90. Smith A.M. : Investigations of Photoconductivity and Photoemission in Lead Sulphide in the Vacuum Ultraviolet : Thesis (Uni. Rochester), April 1961.

91. Thovert J. and J.F. : Utilisation des cellules photoelectriques a enveloppe de verre pour les recherches sur les rayonnements de tres courtes longueurs d'ondes : Comptes Rendus, 191, 1930, p. 731.

92. Watanabe K. and Inn E.C.Y. : Intensity Measurements in the Vacuum Ultraviolet : Jour. Optical Soc. Am., 43, 1953, p. 32.

F. OTHER REFERENCES

93. Adderley E.E. and Bowen E.G. : Lunar Component in Precipitation Data : Science 137, p. 749, 1962.

94. Childs C.B. : Broad-Band Ultraviolet Filters : Jour. Optical. Soc. Am., 51, No. 8, pp. 895-897, August 1961.

95. Detwiler C.R. et al : The Intensity Distribution in the Ultraviolet Solar Spectrum : Ann. de Geophy. 17 (3), pp. 263-272, July 1961.

96. Dobson C.M.B. : Note on the Measurement of Ozone in the Atmosphere : Quart. Jour. R.M.S. 89, No. 381, pp. 409-411, July 1963.

97. Dunkleman L. et al : Middle Ultraviolet Photoelectric Detection Techniques : Goddard Space Flight Centre publication.

98. Elasser W.M. : Atmospheric Radiation Tables : Meteorological Monographs 4, No. 23, August 1960.

99. E.M.I. Electronics Division : An Explanatory Note on the Photomultiplier.

100. Glossary of Meteorology : Amer. Meteor. Society, 1959.

101. Griffith H.L. et al : Power Spectrum Analysis over Large Ranges of Frequency : Jour. Meteor. 13, pp. 279-282, June 1956.

102. Hesstvedt E. : On the Determination of Characteristic Times in a Pure Oxygen Atmosphere : Tellus XV 1963 (1), pp. 82-88.

103. Inn E.C.Y. and Tanaka Y. : Absorption Coefficient of Ozone in the Ultraviolet and Visible Regions : Jour. Optical Soc. Am., 43, No. 10, p. 870, October 1953.

104. Junge C.E. : Atmospheric Chemistry : No. 4, Advances in Geophysics, p. 3. (re aerosols.)

105. Junge C.E. et al : Stratospheric Aerosols : Jour. Meteor., February 1961, pp. 81-108.

106. Lowan A.N. and Blanch G. : Tables of Planck's Radiation and Photon Functions : Jour. Optical Soc. Am. 30, February 1940, pp. 70-81.

107. Philips pamphlet : Light Sensitive Devices.

108. Rollefson G.K. and Burton M. : Photochemistry and the Mechanism of Chemical Reactions : Prentice Hall, 1942.

109. Sant A.J. and Leta A.J. : Calculation of Candlepower and Colour Temperature of Tungsten Lamps : Jour. of the S.M.P.T.E., 65, Dec. 1956.

110. Sidgwick J.B. : Amateur Astronomer's Handbook - Section 7 : Metal-on-Glass Films, pp. 114f.

111. Slater N.B. : Theory of Unimolecular Reactions : Cornell 1959.

112. Tanaka Y. et al : Absorption Coefficients of Gases in the Vacuum Ultraviolet. Part IV, Ozone : Jour. Chem. Physics 21, No. 10, October 1953.

113. Taylor and Taylor : Elementary Physical Chemistry - Chapter 15 : Chemical Kinetics.

114. Walshaw C.D. : Infra-Red Radiation in the Atmosphere : Science Progress, 47, 1959, pp. 67-69.

115. Wilson N.L. et al : A Revised Analysis of the Solar Spectrum from 2990 to 2635 A : Astrophy. Jour. 119, 1954, pp. 590-612.